Abstract

Luthy, Kyle Anthony. The Development of Textile Based Acoustic Sensing Arrays for Sound Source Acquisition. (Under the direction of Dr. Edward Grant.)

This research project dealt primarily with the production of an electronic textiles (e-textiles) demonstrator. The goal of electronic textiles is to integrate textiles technology and electronics to create large area conformal surfaces with embedded electronics. Here, the e-textiles demonstrator serves as an acoustic array for sound source localization and tracking. To create portable acoustic arrays on a flexible textile substrate, an understanding of textile designs and textile processes was obtained. This research resulted in the fabrication of woven substrates with conducting lines and embedded microphone windscreens. Similarly, an understanding of the design and manufacture of flexible substrates for electronics had to be gained in order to produce miniature electronic circuits that will flex when embedded in a textile substrate. The acoustic array technology developed includes microphone arrays with their associated software for data capture and analysis, a multiplexer circuit on a flexible Kapton substrate, and a UC-Berkeley mote-based technology for use with a custom miniature microphone amplification system.

Ultimately, these arrays are used to demonstrate sound localization by triangulation as well as via the spatial filtering technique of beamforming. Experiments were performed to compare different array sizes and geometries in both simulation and real world practice for a variety of target frequencies. Mote performance in the role of beamforming is compared to simulation as well as a commercially available system. Although not as ideal as in simulation, the results achieved are comparable to those of the professional system tested against.

The Development of Textile Based Acoustic Sensing Arrays for Sound Source Acquisition

by
Kyle Anthony Luthy

A thesis submitted to the Graduate Faculty of
North Carolina State University
in partial fulfillment of the
requirements for the Degree of
Master of Science

COMPUTER ENGINEERING

Raleigh

2003

APPROVED BY:

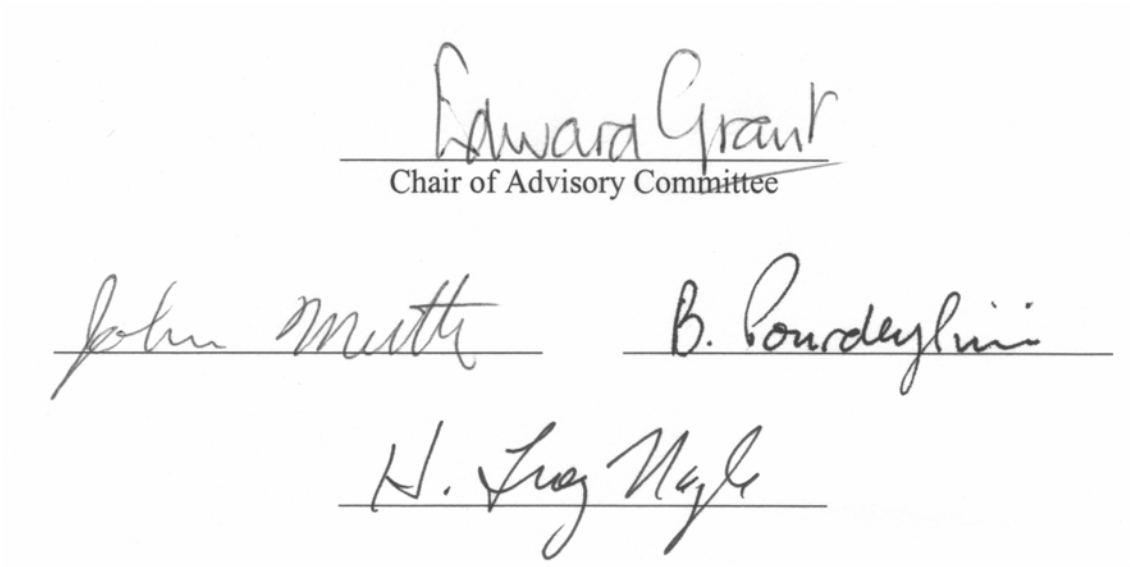

Biography

Kyle Anthony Luthy was born January 6, 1978 in Omaha, Nebraska. Shortly thereafter his family moved to Baton Rouge, Louisiana where he eventually would attend Louisiana State University (LSU). While enrolled at LSU, Kyle was an active member of Theta Xi Fraternity, IEEE, Habitat for Humanity, Eta Kappa Nu, and Golden Key. In May of 2001 he was inferred Bachelor's degrees in Electrical Engineering, Computer Engineering, and Computer Science. His interest in robotics then led him to North Carolina State University to pursue a Master's degree in Computer Engineering. At NCSU he is affiliated with the Center for Robotics and Intelligent Machines under the direction of Dr. Edward Grant. His work has focused on mobile robotic systems, acoustic sensing, electronic textiles, and distributed sensor systems.

Acknowledgements

It is appropriate that I first recognize Dr. Edward Grant, my advisor and director of the Center for Robotics and Intelligent Machines. I thank him for his support and confidence in my abilities. I would like to also thank my committee members, Dr. John Muth, Dr. Benham Pourdeyhimi, and Dr. Troy Nagle, for their ideas concerning this thesis as well as providing direction for future research.

I would have accomplished little without the assistance of all of the members of the CRIM. It's a rare opportunity to be able to work with such a talented group. It is safe to say that I have learned more from working with this group of individuals than I could have in any classroom. I would particularly like to recognize the contributions of Chris Braly and Leonardo Mattos from the CRIM and Anuj Dhawan from the College of Textiles for their assistance.

It is also important to note the contributions of my family, while not directly involved with the content of this thesis, they are ultimately responsible for its foundation. I would like to thank my mother for her patience, encouragement, and good cooking; my father for his unwillingness to let me accept things without asking why, and my sister for the shining example she has set for me.

Table of Contents

List of Figures

List of Tables

Chapter 1 – Introduction

Distributed sensor systems can provide a tremendous amount of information regarding one's environment. Whether embedded in a building or strewn across miles of countryside, they can tell us the temperature gradient, determine the chemical composition of the air, detect seismic activity, or simply listen to the surrounding environment to provide sound localization. The more sensors of a similar type deployed in a given area, the higher quality the data collected is in terms of resolution and redundancy. To further improve on data quality, it is often desirable to have sensing systems arranged in arrays where geometry can be utilized to maximize performance. An example would be an even sensor distribution over a field to map moisture content. If the distribution is uneven (irregular) then more information will be gathered about one particular area than another.

This thesis is dedicated in particular to acoustic sensor arrays. Such arrays are useful for spatial filtering of sound data, also referred to as beamforming. In other words, they facilitate directional listening without the use of parabolic microphones. Array geometry has an effect on the detectable frequency of the system such that sensor elements should be spaced apart by $\lambda/2$ where λ is the wavelength of the lowest frequency sought. This thesis addresses the use of an individual array; one single element in what in the future will be a distributed system. This is useful since although each array in a distributed system will provide a relative direction to a sound source, they cannot effectively provide distance (unless the sound source has been identified and its acoustic properties are well

characterized). Using directional information gathered from multiple arrays the distance to the sound source can be triangulated.

The use of textiles as a substrate for sensor arrays is also examined to provide them with flexibility and portability. The ability to fold a large area array is particularly useful to a soldier deploying distributed sensor systems in the field, as it is less cumbersome than would be a rigid substrate. This allows for the deployment of larger arrays to improve performance. Textiles are also relatively light which is important as a soldier can already be carrying upwards of 100lbs of personal equipment [1]. Since the sensor elements are already laid out, the soldier does not have to measure and place each individual element upon deployment, as is the current mode of deploying an acoustic array. The focus here is on rapid deployment and portability. Embedding such systems in textiles also allows for their non-intrusive inclusion in tents, parachutes, and truck coverings. This can likewise be applied in buildings, through embedding sensor arrays in rugs or drapes in a dwelling or workplace. Sensor arrays can be rolled out during construction and embedded into walls to enhance conference room acoustics, in bridges to measure stress levels, as well as any number of homeland security applications.

1.1 Military Motivation for the Use of Distributed Sensing

Historically, the military powers of the world have adopted the use of defense barriers to deter invading armies. By far the most effective of such barriers was the Morice Line constructed in 1957 by the French to protect their colonial interests in Algeria from Algerian nationalists. This fortification spanned 460km along the Tunisian border and 750km along the Moroccan. Mine fields and barbed wire surrounded a wall whose core consisted of an

eight foot, 5000 volt electric fence. The line was manned by 80,000 French troops and patrolled aerially. Algerian nationalist infiltration was effectively countered [2].

Encouraged by such successes, the United States attempted a similar barrier in Vietnam. The McNamara Line was to expand along the demilitarized zone between North and South Vietnam as well as the Laotian border. Along with the traditional barbed wire and mines, acoustic and chemical sensors were also to be deployed. Although the McNamara Line is considered a failure and was never completed, the sensor technologies implemented proved to be beneficial. Seismic and acoustic sensors were utilized in the defense of Khe Sanh where "the sensors indicated when the enemy were massing for attacks against the base, allowing the concentrated deployment of US aerial and artillery bombardment which countered the attack…defenders at Khe Sanh did not face their enemy across a broad, linear front; rather, they were almost surrounded by them. The fighting there showed that sensor technology worked in 360-degree applications [2]". Such sensors were further activated for operations along the Ho Chi Minh trail after which only an estimated 20 percent of vehicles reached their objective [2] [3].

Within the last 20 years there has been a push towards improving US implementation of the electronic barrier concept. The rapid deployability of the US military once a target has been electronically acquired drastically reduces the need for manpower along the protected border. Also, determining patterns of troop and equipment movement allows for better localization of mines and physical barriers [3]. Not only is this cheaper, but it also reduces the post war impact of munitions left on the battlefield. According to the 2000 Land Mine Monitor Report, there are approximately 1.3 million mines still in place in Algeria. Along the now defunct Morice Line mines are suspected to be located in densities as great as 1 per

meter [4]. While a wall may impede insurgent forces, once in place and mines are laid, counter-invasion plans will also be restricted.

Furthermore, in the past few years there has been a substantial push within the US armed forces towards what is termed the Objective Force Warrior. The premise behind this project is to use technology to increase the effectiveness of individual soldiers. This is largely accomplished by inundating soldiers with information gained from various sensors, providing them with a more comprehensive view of the battlefield [5]. Sensor arrays can provide target information as well as detect the use and density of biological agents.

1.2 Goals of Thesis

The objectives of this thesis are

- Describe the development of a large area textile based triangulation array.
- Develop a beamforming array sensor system based on UC Berkeley's mote.
- Examine flexible circuitry implemented on a Kapton substrate.
- Develop a miniature variable gain data acquisition system for the mote.
- Demonstrate beamforming for sound source localization.

1.3 Thesis Outline

- Chapter 2 - A literature review highlighting current research and applications of electronic textile technologies and acoustic arrays.
- Chapter 3 - A detailed examination of the design and implementation of a 10' x 3' microphone array for sound impulse location through triangulation based on time of flight measurement as well as the implementation and testing of a personal

computer based beamforming system. This includes different wiring techniques, the characterization of woven windscreens, and the development of the associated electronics.

- Chapter 4 – The development of a mote based beamforming array. This includes information regarding the Berkeley mote, the determination of the array geometry, the design and implementation of a flexible data acquisition circuit, the design and implementation of a variable gain data acquisition circuit, software development, and experimentation evaluating performance.
- Chapter 5 - Conclusions and future work.
- Appendix A - Circuit schematics, board layouts, and material listings for developed circuitry.
- Appendix B – Code listing of software associated with the arrays.

Chapter 2 – Literature Review

This chapter investigates many of the recent technological advances and current research interests in the fields of electronic textiles and acoustic arrays. This review provides a wide view of these areas and is not restricted to information pertinent to the content of this thesis.

2.1 Electronic Textiles

Electronic textiles are created in an effort to incorporate computer technology into a medium with which we are already familiar and to do so in a non-intrusive manner. "Textile look and feel must not be impaired by new functions, which means that technology must be small, light-weight and smooth. Mechanical stress must not lead to failure, washing and cleaning must be possible." – Siglinde Zisler [6]. Such requirements have created many challenges for researchers who have answered with imaginative innovations, bringing these goals closer to fruition.

To obtain seamless integration, technologies are required from various disciplines, including textiles, materials, and electronics. Textile engineers and materials scientists have developed several methods for integrating conductors into textile substrates. Optical fibers, metallic or composite fibers, and yarns coated with conductive polymers can be woven or embroidered into the fabric to create transmission lines or circuit layouts [7] [8] [9]. Conductors can also be included in the manufacture of non-woven textiles such as in flocking, a process in which fibers are applied to an adhesive surface. This process is used in

making electric blankets. Conductive inks and dyes can also be used to introduce conductors to a textile [7].

To be better suited for inclusion in textiles, electronic components need to be either smaller than or as flexible as the fabric in which they are embedded. Current minimization trends in electronics have produced much in the areas of both micro and nanometer (nano) scale devices which are well suited for seamless inclusion in textile substrates. Others utilize special fibers sewn in a particular configuration to create the desired device. Such a component is demonstrated by the SOFTSwitch (figure 2.1). The SOFTSwitch uses conductive materials and a quantum tunneling composite to allow resistance to change with pressure [10] [11]. Fitting with the theme of sensing arrays, this technology can be applied to pressure mapping; a useful feature for medical applications.

Figure 2.1 A Flexible PDA keyboard utilizing SOFTSwitch technology [10].

Power consumption must also be minimal to avoid the need for large battery packs. To help solve this problem, Infineon has developed a thermogenerator which utilizes body heat to generate electricity. Currently, enough energy is produced to power either a digital watch or a pulse meter [12]. Another approach is the development of flexible solar cells

based on light harvesting dyes [13]. Flexible battery technology is currently available from Power Paper Ltd. whose thin batteries are printed onto the desired substrate [14].

The current focus of electronic textile application both commercially and in research is on wearable devices. There are many commercially available items in which electronic devices have been embedded [12] such as Infineon's mp3 player jacket (figure 2.2) [11], Northface's MET5 heated jacket [15], and the Polartec electric blanket [16]. The development of such products fuels the current trend of smaller, more robust electronic components.

Figure 2.2 Infineon's MP3 Jacket can be washed and ironed.

Research "wearables" typically focus on health and military applications rather than fashion and entertainment. The Georgia Institute of Technology (Georgia Tech) Smart Shirt for example, is a T-shirt into which various sensors are woven to monitor several vital signs (figure 2.3) [17]. Likewise, researchers at Wollongong University in Australia utilize yarns coated with inherently conducting polymers (ICP) which they imbed into their Knee Sleeve to help train athletes, improving form and preventing injuries to the anterior cruciate ligament

[18]. Other research focuses on embedded actuators [19] [20], electrically controlled camouflage [21], and wearable displays [22].

Figure 2.3 Georgia Tech's Smart Shirt is used to monitor the wearer's vital signs.

Many of the aforementioned technologies are funded by the Natick Soldier Center as a part of their Objective Force Warrior initiative [5]. This program strives to provide the soldier with all pertinent information about their environment as well as defend them from harm by including advances such as adaptive camouflage, automatic tourniquets, and vital sign monitoring directly into their uniform. DARPA has also funded electronic textile projects not involving wearable systems. This includes research on controllable parafoils and large area acoustic arrays for vehicle detection which has been performed concurrently at North Carolina State University [13] [23] and Virginia Tech [24]. This work is discussed in further detail in chapter 3 of this thesis.

2.2 Acoustic Arrays

Since the 60's, the United States military has been looking to mimic the successes of passive sonar technologies on land in order to improve the localization and tracking of military units. Throughout the 1980's and early 1990's, sensor systems such as REMBASS (Remote Battlefield Sensor System) [25] and later IREMBASS (Improved REMBASS) were developed. More recently, the United State's Army Research Lab and several NATO nations have focused on Unattended Ground Sensors (UGS) which are smaller than the REMBASS systems and are more easily deployed [26]. These systems typically comprise a variety of sensors in addition to acoustic sensors including seismic, chemical, and biological. The Army Research Lab (ARL) is actively examining acoustic arrays for addition into such systems since although current systems are useful for providing a large amount of information, they cannot reproduce the spatial discrimination of an acoustic array. Consequently, the ARL is responsible for a large amount of literature on acoustic array processing techniques [27][28][29]. DRDC Valcartier, a Canadian defense contractor, is responsible for the development of free standing and vehicle mounted acoustic arrays [30]. One such system is GUARDIAN (figure 2.4) which is used for sniper localization.

Figure 2.4 GUARDIAN sniper detection system.

Mounting arrays on vehicles can be particularly challenging, not only because the system is moving, but vehicles are often inherently noisy [31]. This is likewise a challenge when including such arrays on robotic platforms. Arrays are incorporated into robots which are used for surveillance, search and rescue, and target localization and tracking [32][33][34].

With advances in computing power and electronic minimization, acoustic arrays have been applied to various tasks involving speech processing [35]. This is rather difficult as human speech encompasses a rather large range of frequencies. Work with array geometries [35] and processing techniques [36][37][38] has aided in the development of products that approve acoustics in conference rooms [39][40] or aid the hearing impaired such as the microphone array necklace shown in figure 2.5 [41].

Figure 2.5 Acoustic array necklace for the hearing impaired.

Chapter 3 – 1st Generation System Designs

This chapter examines the development of the first generation acoustic array constructed on a textile substrate. This system was designed and implemented as part of a DARPA funded project and has been the subject of several papers [23][8]. The final design is shown in figure 3.1.

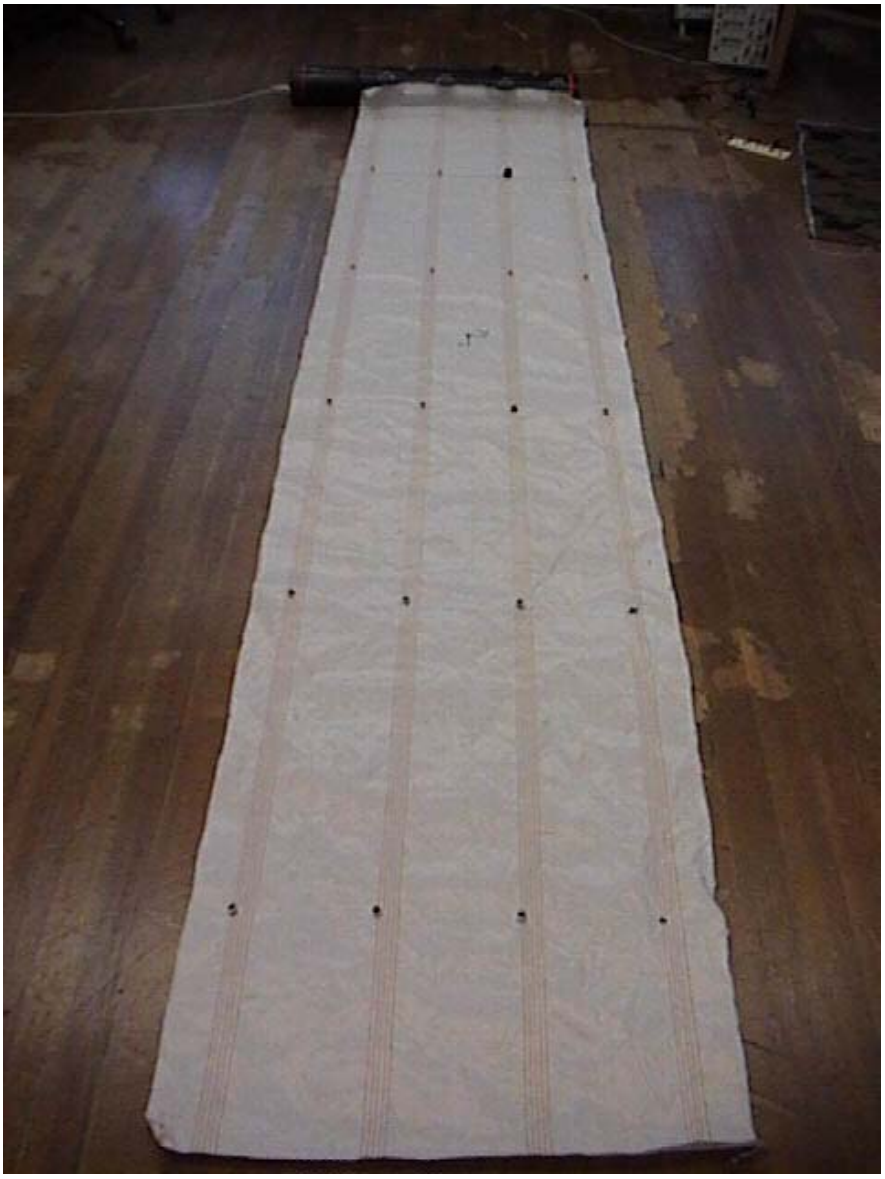

Figure 3.1 The 1st generation 10ft, 20 element, textile based acoustic array.

3.1 Textile Considerations

The textile requirements for this project vary considerably from those associated with typical fashion directed electronic textiles. Durability is more important than style since there are no comfort issues involved with the associated wiring and embedded electronics.

3.1.1 Designing a Substrate for E-Textile Usage

The textile substrate for the array was chosen to be polyester. Polyester is a popular fabric for military applications as it is lightweight (approximately 16g/m^2), strong, has good abrasion resistance, displays uniform characteristics, and is resistant to moisture and other environmental conditions [42]. It is also a fairly simple material to dye in order to provide camouflage in the visible spectrum. Larger area arrays would also need to consider reflectance in the near infrared wavelengths (.7-2um) due to the high infrared reflectance typical of vegetation. Pigment printing techniques for polyester utilizing azoic colorants or isoindolinone residues to reduce NIR reflectance have been developed [42].

A camouflage array was woven on a Jacquard loom and is shown in figure 3.2. This array also has pockets woven into it of various densities. These pockets not only conceal the microphone elements, they also serve as windscreens. This does however have an adverse effect on electronic interfacing in that the wires are not easily accessible. To test the effectiveness of the woven windscreens, their performance is compared to that of a microphone with no windscreen and one with a WindTech™ lavalier windscreen. Using a compressed air source the microphones were simply grouped closely together and they were blown upon. The wind speed was regulated by measuring with an anemometer and sustained approximately at 275 ft/min. The results are shown below in the oscilloscope screen shot of figure 3.3.

Figure 3.2 Camouflage array with woven windscreens. 1 is an unprotected mic, 2 has a lavalier windscreen, 3 is a loosely woven windscreen, and 4 is a tight woven windscreen.

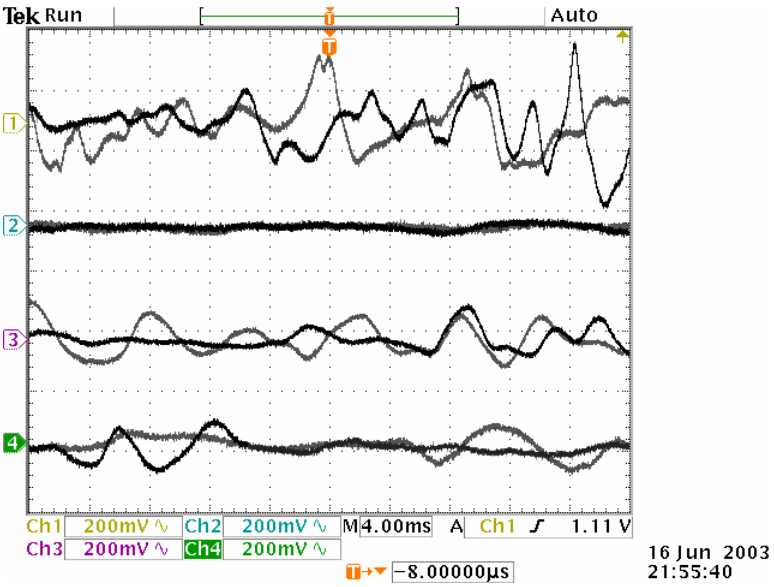

Figure 3.3 Oscilloscope screen shot demonstrating the performance of the windscreen usage of figure 3.1. Channel 1 has no windscreen, channel 2 has a lavalier windscreen, 3 is loosely woven, and 4 is tightly woven. (Gain of 100)

As can be seen, the microphone with the lavalier windscreen outperforms the others. As expected, the unprotected microphone yielded the worst performance. The tightly woven windscreen performed slightly better than did the loosely woven. This test was performed several times with comparable results. The sound acceptance of the microphones was also tested since a windscreen is not effective if it degrades the signal it is intending to pick up. At various frequencies between 20Hz and 500Hz, no appreciable differences in microphone performance were detected.

3.1.2 Wiring

The wiring necessary for the array depends on the complexity of the circuitry which is to reside on the fabric. The preliminary design had each microphone and its associated amplifier collocated on the fabric. This type of node requires individual power, ground, and signal lines. The resulting wiring grid is shown in the 4-element prototype pictured in figure 3.4. The spacing of the wires was chosen to be commensurate with the findings of [9] to reduce crosstalk. All of the wires utilized were stranded to improve flexibility and consisted of bare copper, insulated copper, and twisted pair wires. These wires are all of 36 gauge or smaller in order to pass through the reed of the loom that was available. The twisted pair is particularly important as it carries the resulting signal to some processing station. While not critical in this small design, when scaled upwards, the twisted pair serves to protect signal integrity over large distances. Further, it is important to note the need of interconnections between wires in this design. Interconnects in this array were solder welded but several other methods of forming such interconnects exist [9].

Figure 3.4 Textile array containing both microphones and amplifiers on fabric.

The second and final design removed the amplification from the on fabric node. With this reduced circuit complexity, the necessity for interconnects and wires woven in the weft are removed. Only the twisted pair wires remain as is demonstrated in the finished product of figure 3.1.

3.1.3 Interfacing

Forming external connections to the woven wires requires special consideration. Weaving can be done to facilitate the attachment of node elements by allowing the wire to float at the attachment points (figure 3.5). Also a co-axial snap connector was developed for external device connection (figure 3.6). Not only does such a connection allow for the easy replacement of an element, it also reduces stresses on the wire and distributes them to the fabric.

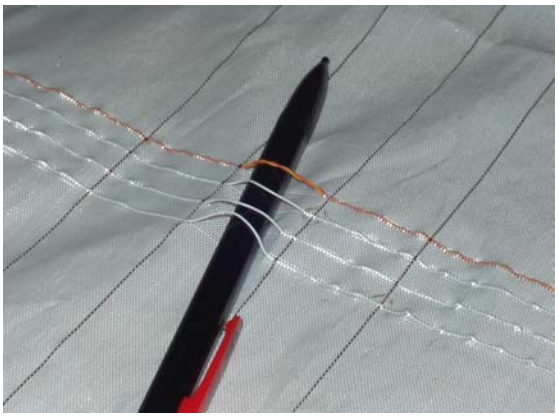

Figure 3.5 Floats woven for device attachment.

Figure 3.6 Coaxial snap connector for microphone attachment.

3.2 Microphones and Amplifiers

To perform well the microphones incorporated into the array must be both small and have an acceptable signal to noise ratio over all audible frequencies. The Emkay WP-3502 microphone shown in figure 3.7 meets the requirements and is small enough that it could probably be woven into the array itself. However, due to cost considerations, the Panasonic WM52B microphone of figure 3.8 was chosen. While larger than the Emkay microphone, it still has a respectable signal to noise ratio of more than 60dB with consistent response over the required frequency band (figure 3.9).

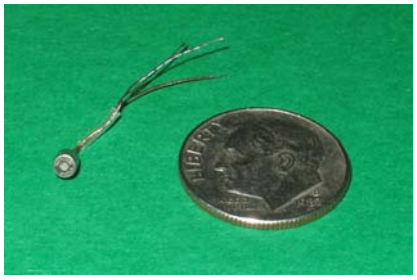

Figure 3.7 Emkay microphone WP-3502.

Figure 3.8 Panasonic microphone WM52B.

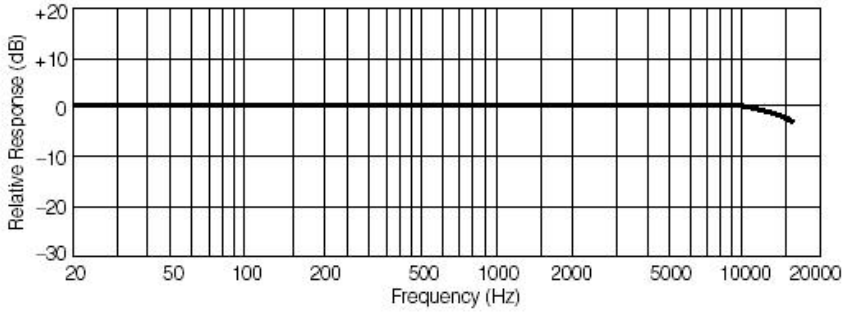

Figure 3.9 Frequency response of the Panasonic WM52B microphone.

In conjunction with the Panasonic microphones, a non-inverting amplifier is used with a gain of 100. The circuit is based on the standard 741 op-amp and the diagram is shown in figure 3.10. The circuit is run off of a 5V supply and is therefore biased to 2.5V to take advantage of the available voltage range. This was done to reduce the amount of woven wires necessary if the nodes contain the amplifiers.

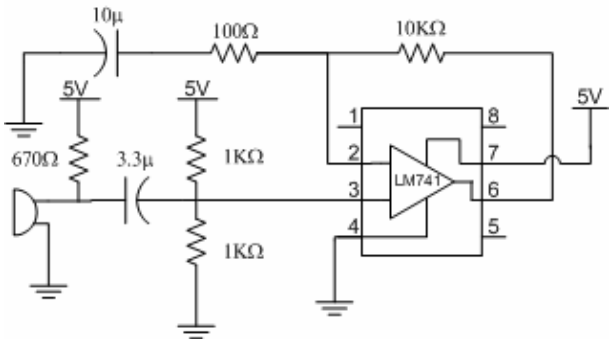

Figure 3.10 Microphone and non-inverting amplifier with gain of 100.

3.3 Beamforming

Beamforming is a method of spatially filtering acoustic signals. This is accomplished via constructive and destructive interference as the detected signals are delayed to listen in a particular direction. These time delays are determined by figuring the time differences from each microphone to a reference point given a particular listening direction. This is demonstrated for the two microphone array of figure 3.11. In table 3.1, the waveforms are shown delayed as well as combined for time delays necessary to listen at 0°, 90°, and 180° for a sound source of 100Hz located at 0°. At 0°, when the appropriate delays are applied, the signals are coincident such that when summed, a large magnitude is realized. At 90°, they are out of phase and the resulting combined signal has a smaller amplitude than when listening at 0°. At 180°, there is considerable destructive interference yielding a small amplitude result. If this process is continued for all 360°, then the polar plot of figure 3.12 is realized. See [38] for a more in depth examination of the time delay method of beamforming.

The remainder of this section outlines the hardware and software necessary to perform beamforming as outlined above with this system. The hardware focuses on data acquisition while the software is responsible for acquisition, processing, and visualization.

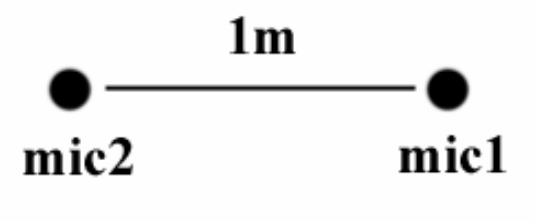

Figure 3.11 Array configuration from which the results of figure 3.12 and table 3.1 are taken.

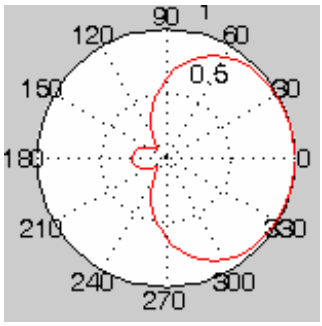

Figure 3.12 The beam pattern realized if a 100Hz source is placed at 0 degrees with respect to the array of figure 3.11.

Table 3.1 The delayed and summed signals for the array of figure 3.11 at different listening angles.

Listening Angle	Delayed Signals	Summed Signals
0°	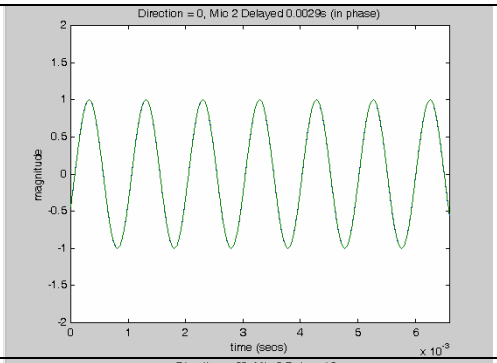	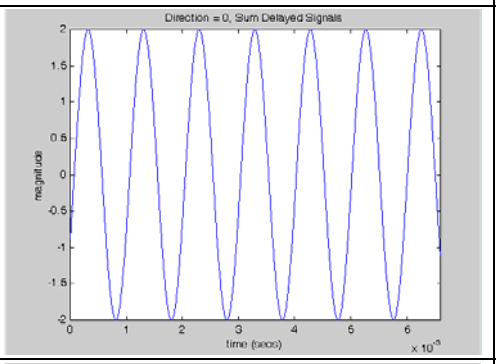
90°	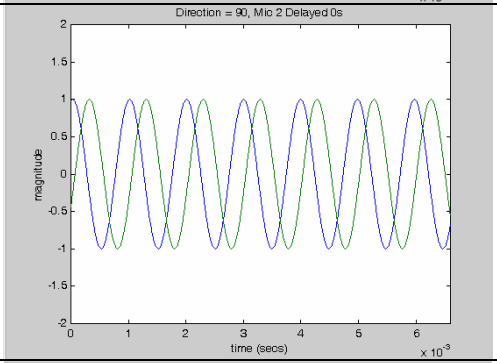	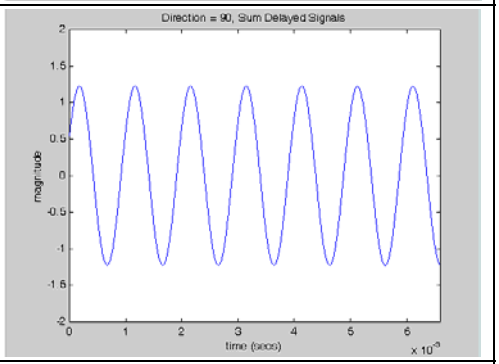
180°	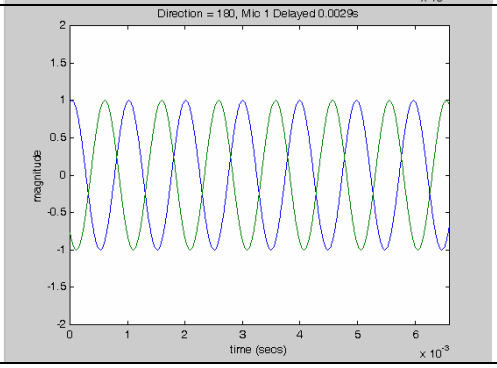	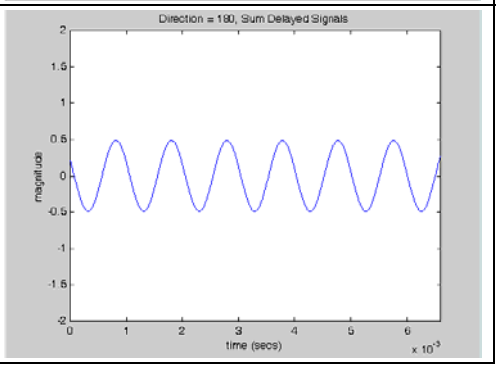

3.3.1 Hardware

An off the shelf solution was used to acquire and process data for beamforming. The data acquisition hardware used is the Hoontech DSP24, which is an audio mixer consisting of 8 mono inputs, sampling at a maximum rate of 96kHz with 24bit resolution. Multiple DSP24s can be installed on the same computer, providing up to 40 input channels. The hardware setup used is demonstrated in figure 3.13.

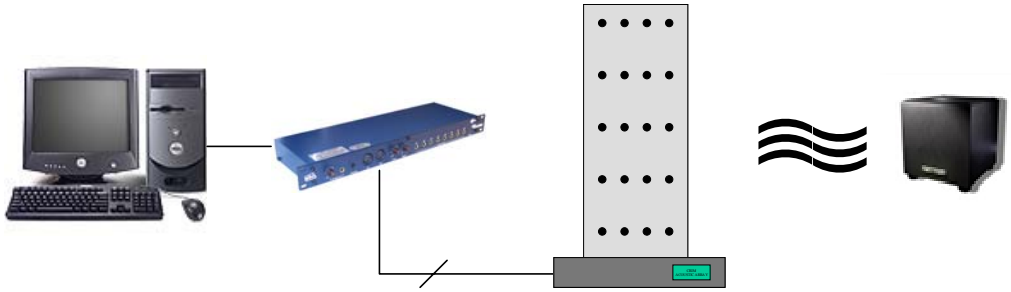

Figure 3.13 Hardware flow of the computer based beamforming system featuring the Hoontech DSP24

3.3.2 Software

Cool Edit Pro is the off-the-shelf software used to collect data from the DSP24. Cool Edit provides excellent control over the DSP24's features allowing for easy data acquisition of all available channels. The data acquired can be converted into several different audio formats. Cool Edit also allows for analysis of the frequency spectrum of the recorded signals which is useful for identifying noisy channels on the array.

The beamforming software for this project was custom designed by Leonardo Mattos and programmed in Matlab [33] based on the methods outlined in [38]. First, a reference point is chosen. The time it takes for sound to travel from every microphone on the array to the reference point can be calculated for every possible angle of the sound source relative to the array. Knowing these times, the recorded sound from each element can be delayed to line up with the reference point for the various angles. If the source is in a particular direction,

when these signals are aligned, they will display constructive interference. If it isn't however, it will be destructive. From the analysis at every possible azimuth and elevation angle, both a 2-D and 3-D beam pattern are created. Figure 3.14 shows a flowchart of this process. This software can also plot a short history of the perceived location in a waterfall plot.

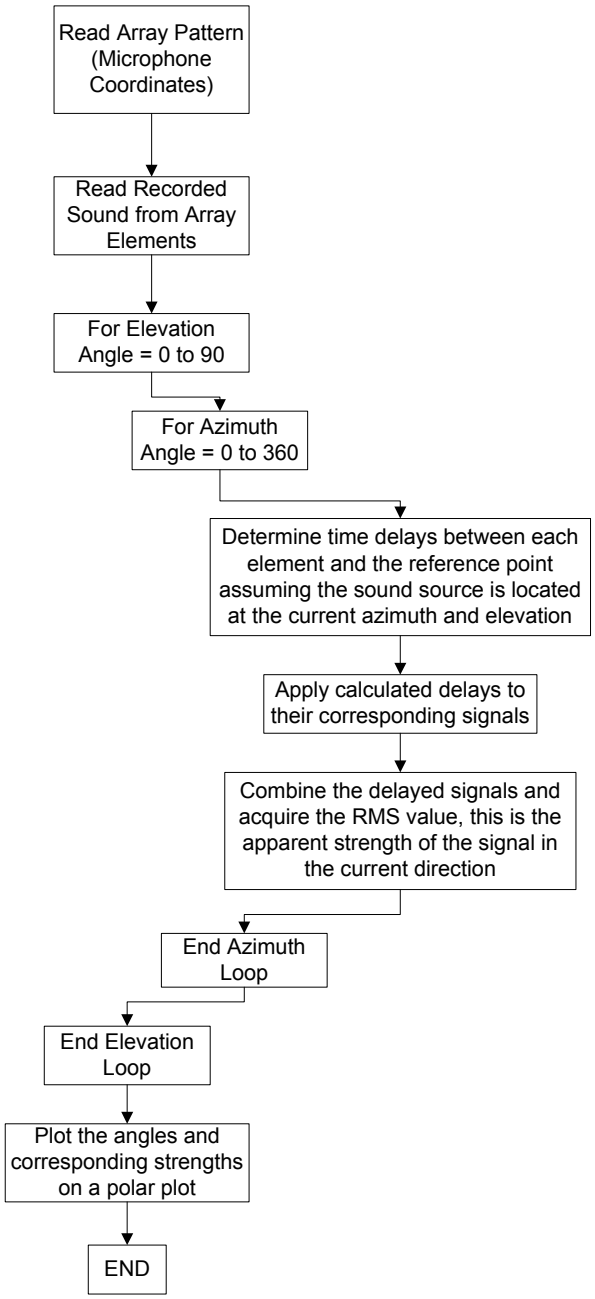

Figure 3.14 Flowchart for the beamforming software.

3.3.3 Beamforming Experimentation

Beamforming experimentation using the Matlab software was performed on the 2x2 array of figure 3.4, the configuration of which is depicted in figure 3.15. The first experiment was performed using a 1kHz tone located 1.5m from the center of the array at an azimuth of 90 degrees and an elevation of 0 degrees. The simulated result for this setup is shown in figure 3.16 which demonstrates both the 3 dimensional and 2 dimensional result. This is then compared to the real world result of figure 3.17.

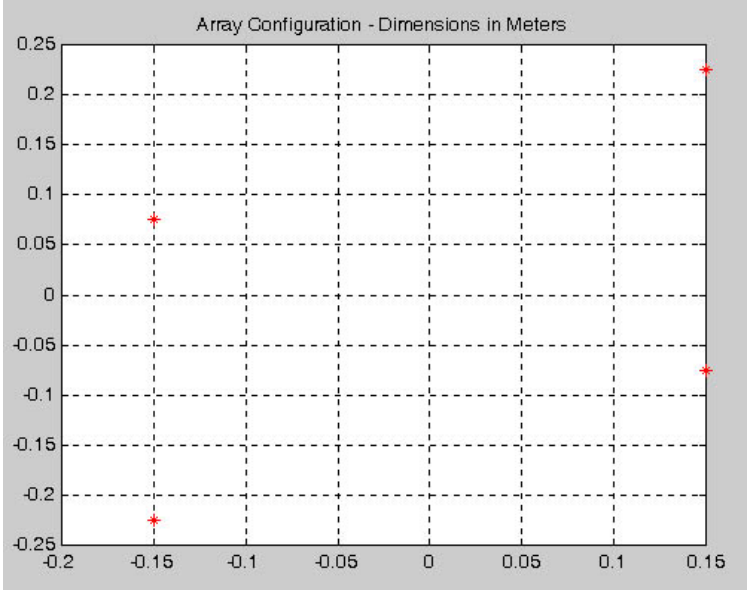

Figure 3.15 Configuration of the 4 element array.

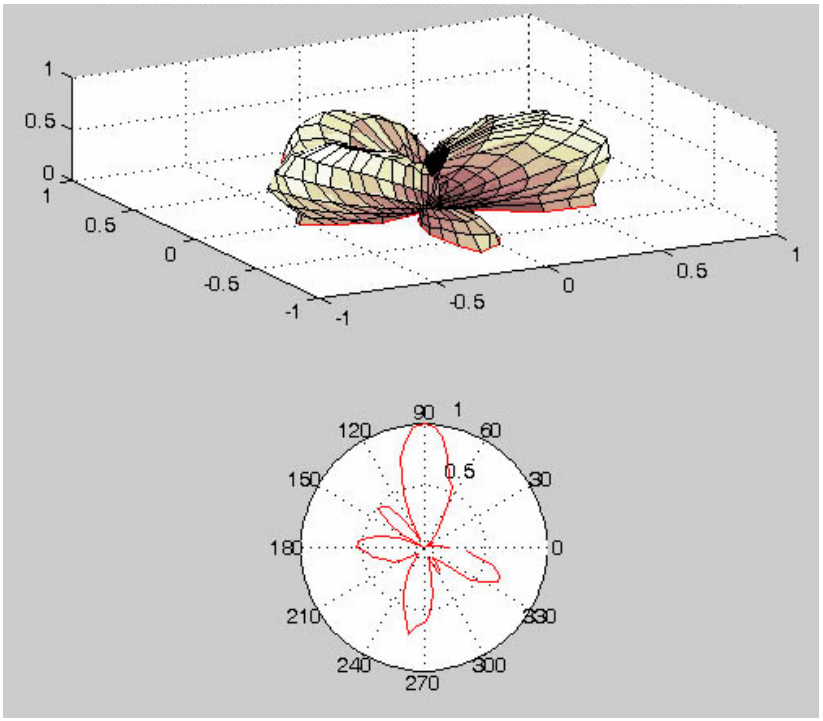

Figure 3.16 Simulated beamforming on 1KHz source at 90 degrees azimuth and no elevation. The result matches the actual location.

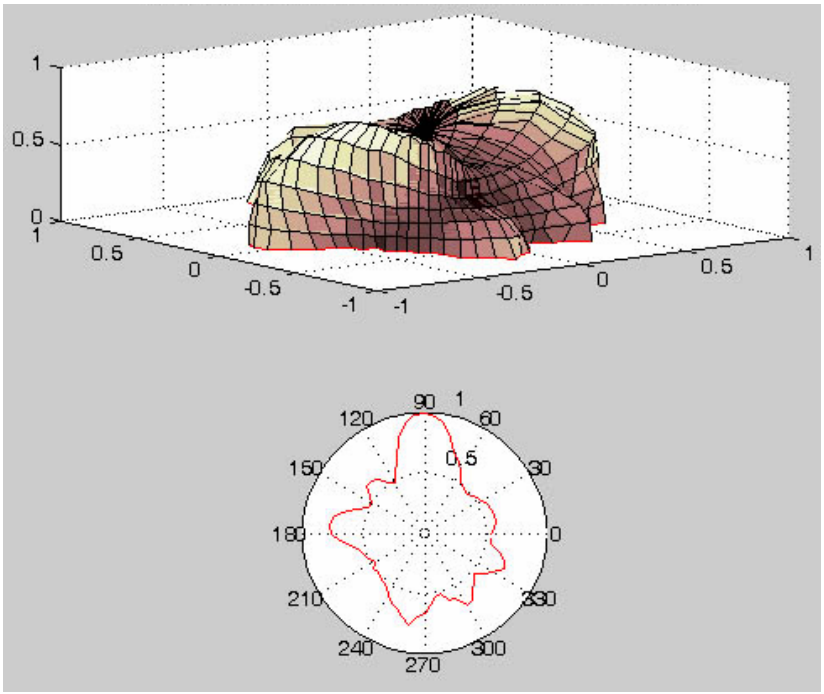

Figure 3.17 Real world beamforming on 1KHz source at 90 degrees azimuth and no elevation. The sound source is detected at an azimuth of 90 degrees and an elevation of 10 degrees.

The real world beam pattern maintains a form that is similar to the simulated result but is obviously noisier, indicative of a less pure tone from the sound source. Realizing that the testing environment was less than ideal it was surmised that other noise introduced by several computers, air conditioning, and outside foot and road traffic could be responsible for this result. Examining the frequency spectrum of one of the recorded signals shown in figure 3.18 shows that there is a considerable amount of noise lower than the desired 1KHz signal.

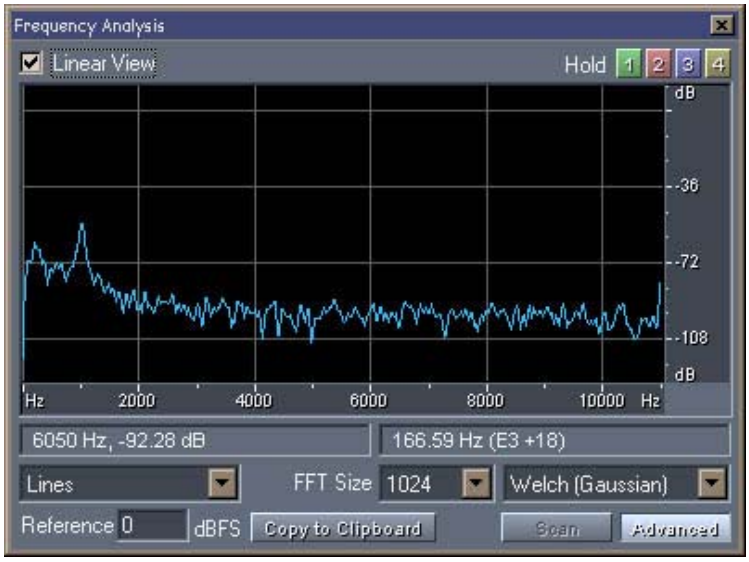

Figure 3.18 Frequency spectrum of one of the signals contributing to the beam pattern of figure 3.14.

A band-pass filter was introduced in software ranging from 800Hz to 1200Hz to compensate for the excess noise. As demonstrated in figure 3.19, this produced the desired result, cleaning up the beam pattern and yielding one more commensurate with the simulated result. This also removed the elevation discrepancy.

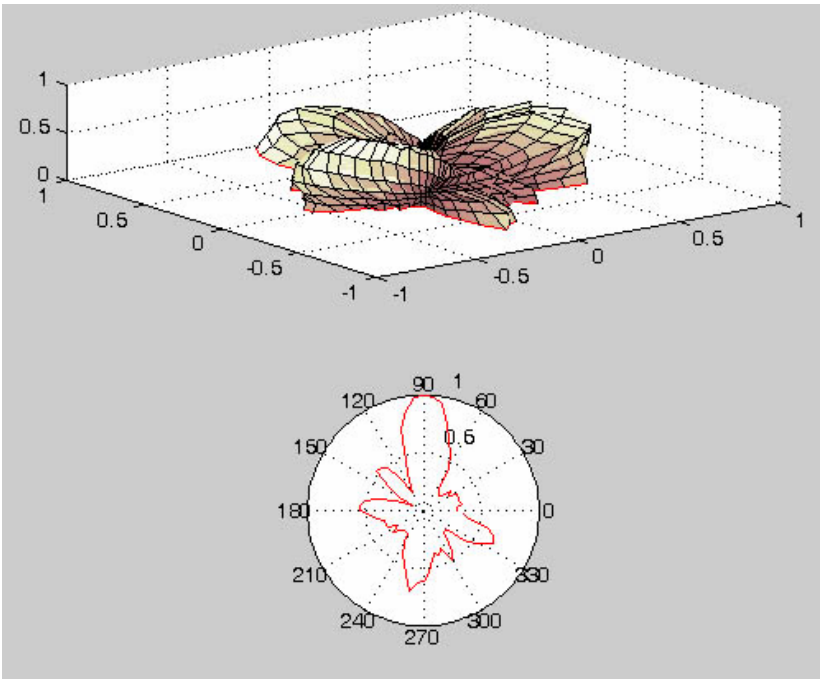

Figure 3.19 Real world result after introducing a software filter. Sound source is at 90 degrees azimuth and no elevation. The sound source is detected correctly.

The next simulation is introduced to examine the effect of sound source elevation on the accuracy of the listening pattern. To do this, the same 1kHz source was used but placed at an azimuth of 90 degrees and elevation of 25 degrees. The resulting beam pattern is shown in figure 3.20. The detected source is located at an azimuth of 200 degrees and elevation of 50 degrees, a substantial deviation. Increasing the height of two elements diagonal to one another yields a non-planar array. Beamforming with the same source at the same position with this configuration produces the pattern of figure 3.21. The two-dimensional plot of the beam pattern is misleading as it is a projection of the three-dimensional plot onto a plane with 0 degrees elevation. The 3 dimensional plot has been oriented to correspond with its two dimensional counterpart. The darker red in this image is indicative of a stronger certainty of sound source location.

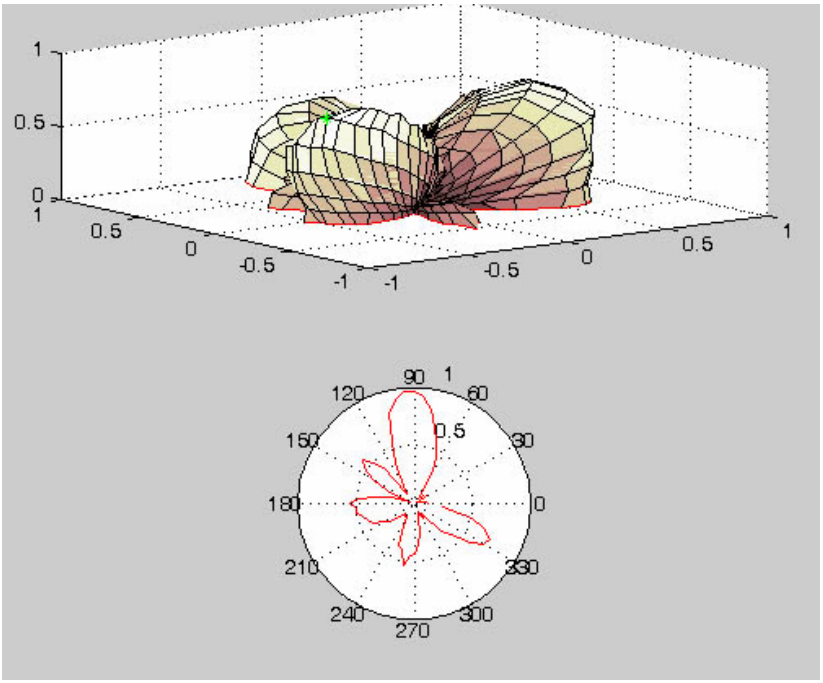

Figure 3.20 Simulation with sound source located at 90 degrees azimuth and 25 degrees elevation. Detected at an azimuth of 200 degrees and elevation of 50 degrees.

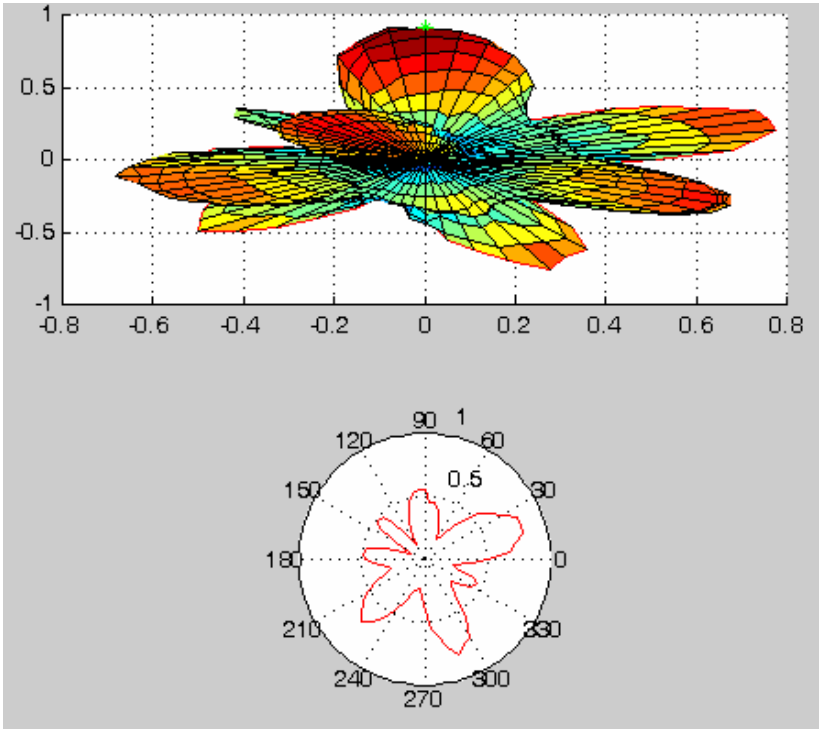

Figure 3.21 Listening pattern using a three dimensional array. Source location and detected location are identical at 90 degrees azimuth and 25 degrees elevation.

3.4 Triangulation

A stand-alone demonstrator was developed to triangulate the position of a sound source. This requires considerably less processing power than beamforming and can potentially supply distance information as well as direction. The geometrical basis of triangulation is demonstrated in figure 3.22.

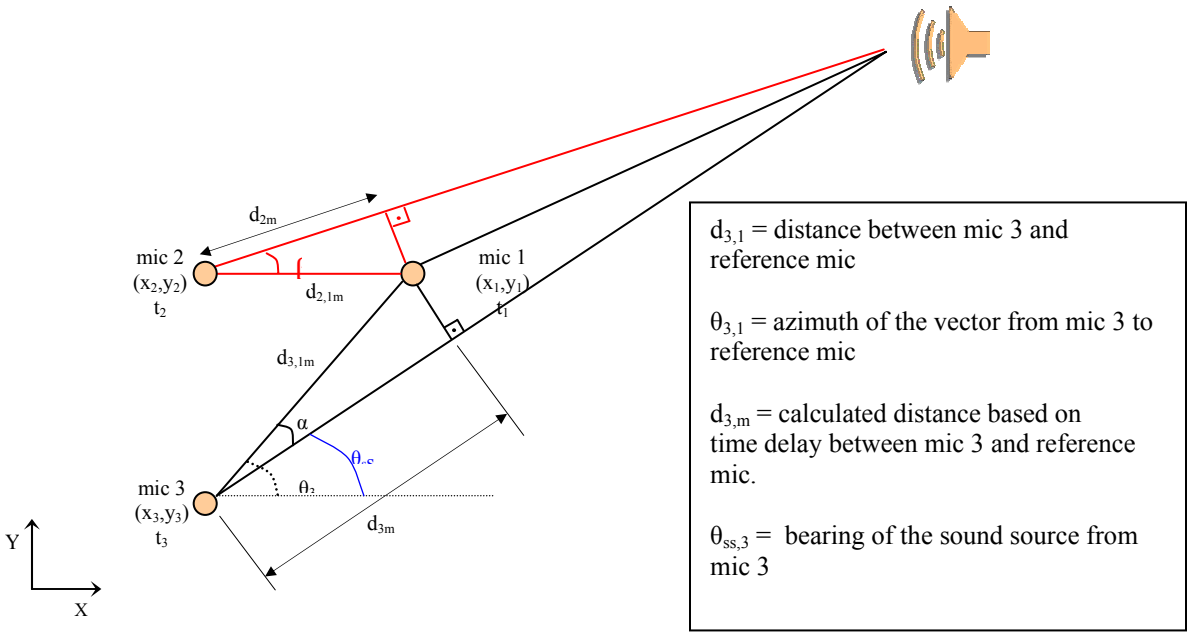

Figure 3.22 Geometrical basis for triangulation based on time of flight between microphones.

3.4.1 Hardware

The prototype was developed to be a single soldier deployable system. Keeping that in mind, all of the electronics developed were contained inside of a 3½ft blueprint tube about which the array itself could be wound. The tube has an LCD display which outputs the azimuth of the sound source. It also has a serial interface port through which data can be recorded or the system can be reprogrammed.

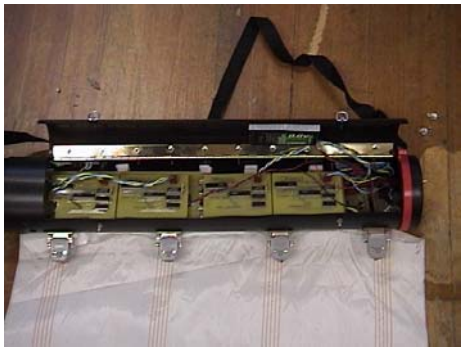

Figure 3.23 Triangulation electronics housed in a blueprint tube.

The electronics were custom designed to record time delays between microphone elements as a sound impulse propagates across the array. The first microphone to experience the impulse starts an internal counter. As every microphone hears the sound they latch the current counter value which is representative of a time delay. A BasicX microprocessor retrieves this information after all of the microphones have signaled that they have received the sound. The implemented system is shown in figure 3.23 and a block diagram of this process is shown in figure 3.24.

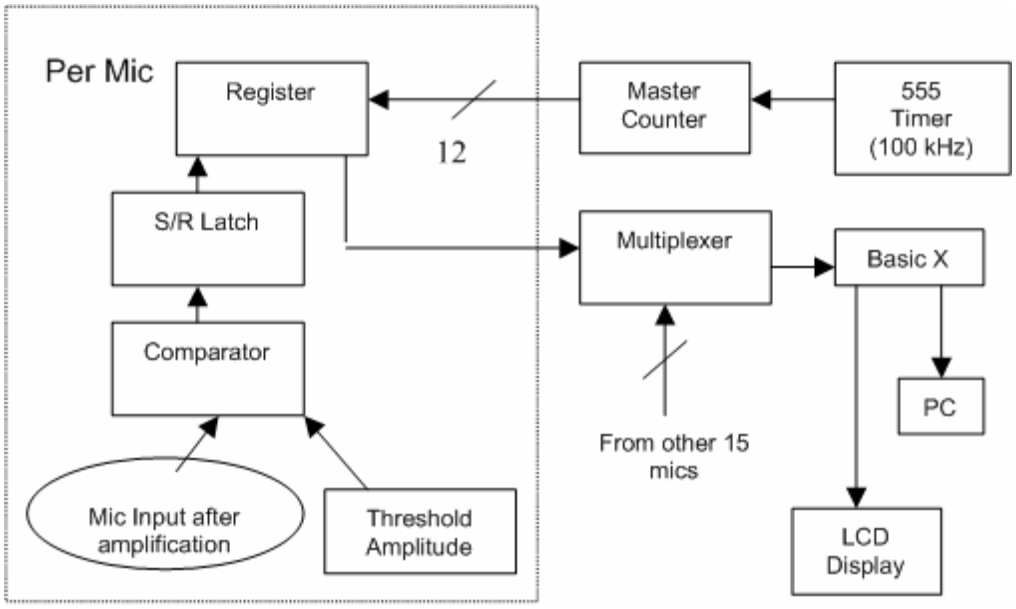

Figure 3.24 Block diagram of circuitry used to measure time delays for triangulation

3.4.2 Software

After collecting the counter data and converting it to times based on the speed of sound, the triangulation method outlined in [43] is applied. This approach uses only four of the available elements to solve the system of equations shown in figure 3.25. The four corner microphones are chosen as they are the furthest apart and will provide the largest baseline for triangulation. Error-checking code was also developed due to occasional aberrations in the data collected. This code essentially checks the data received from these 4 microphones and determines whether or not they physically make sense. If not, a neighbor of the erroneous element is chosen and the calculation is performed.

$$\begin{bmatrix} 2x_1 - 2x_2 & 2y_1 - 2y_2 & -2c\Delta T_{12} \\ 2x_1 - 2x_3 & 2y_1 - 2y_3 & -2c\Delta T_{13} \\ 2x_1 - 2x_4 & 2y_1 - 2y_4 & -2c\Delta T_{14} \end{bmatrix} * \begin{bmatrix} u \\ v \\ d \end{bmatrix} = \begin{bmatrix} c^2\Delta T_{12}^2 + x_1^2 + y_1^2 - x_2^2 - y_2^2 \\ c^2\Delta T_{13}^2 + x_1^2 + y_1^2 - x_3^2 - y_3^2 \\ c^2\Delta T_{14}^2 + x_1^2 + y_1^2 - x_4^2 - y_4^2 \end{bmatrix}$$

Figure 3.25 Solving this system of equations yields u (x coordinate of sound source), v (y coordinate of sound source), and d (distance to sound source) where ΔT refers to the time difference between the microphones designated in the subscripts [43].

3.4.3 Experimentation

To evaluate the performance of the array a sound impulse was generated at various angles with respect to the center of the array. As long as the impulse was generated at or near 0 degrees elevation, the results achieved were agreeable to the actual location. Some error is introduced which can be attributed to the resolution of the counters utilized in the timing circuitry of the array. If the resolution of the timer is increased, the array should yield more precise results. Much like the beamforming experimentation, this array is not amenable to elevated sound sources. This is commensurate with the findings of [43].

Chapter 4 – System Design

This chapter focuses on the development of the phase II acoustic array system shown in figure 4.1. This array inherits the polyester substrate and microphones from the previous array. The areas of concentration are the development of the electrical systems investigated, the decisions behind the array geometry, the software involved, and an evaluation of the system's performance.

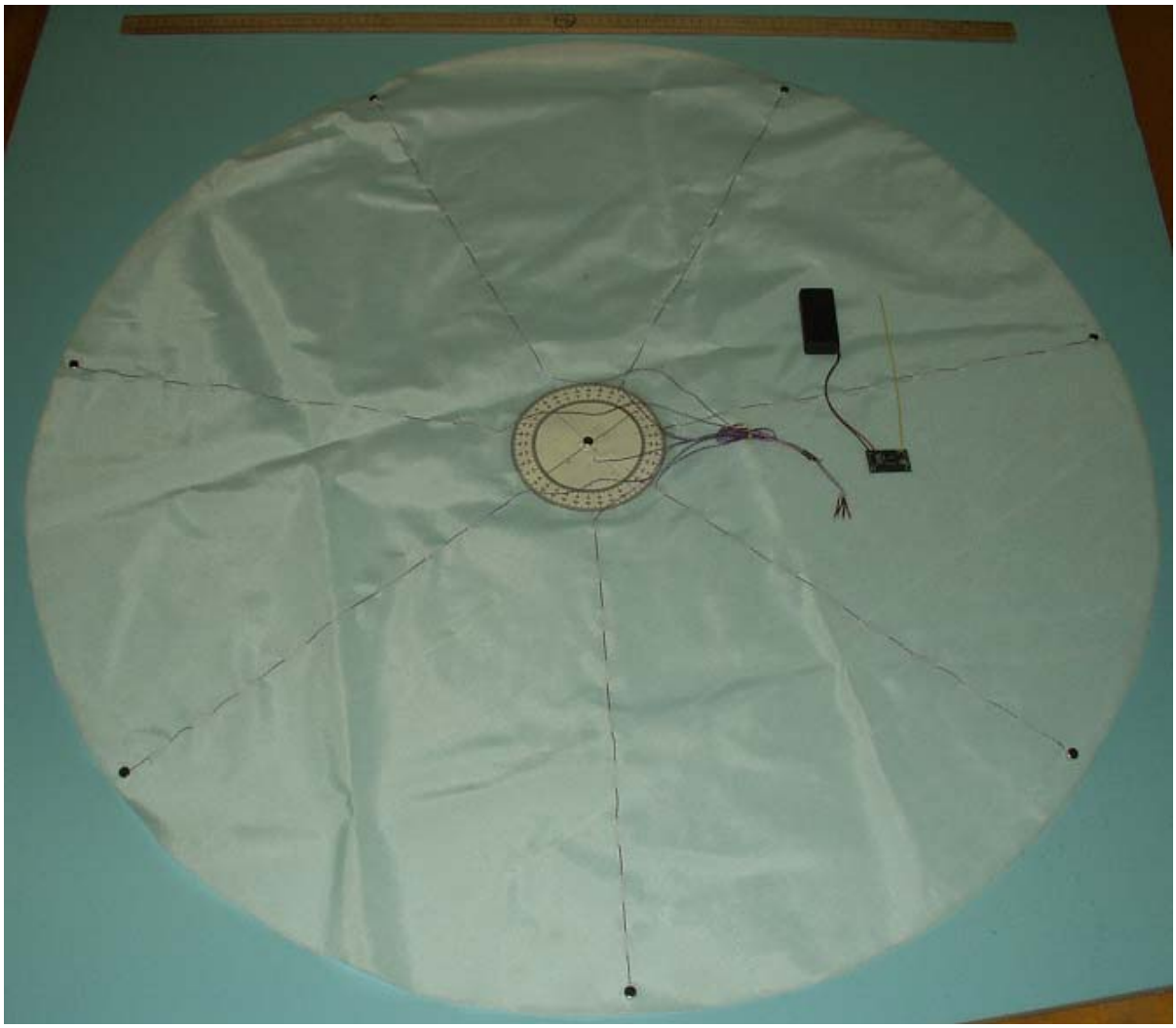

Figure 4.1 The mote based acoustic sensing system.

4.1 Electrical Considerations

The electrical aspects of this system are divided into two areas. The first area to consider is the Mote which is the processing and communications unit of the array. The second area concerns both the sensors and any signal preprocessing that may be necessary. This could be a broad topic ranging over several different sensor types, but for the purposes of this thesis will be limited to the collection, amplification, and filtering of acoustic signals.

4.1.1 The Berkeley Mote Concept

Developed by Jason Hill at the University of California at Berkeley, the mote is a fully functional microprocessor board centered on the Atmel 90LS8035 microprocessor [44]. This is a 4MHz processor with 32 I/O lines of which 8 can be used as 10-bit analog to digital converters. It also contains a programmable UART, 512 bytes of SRAM, 512 bytes of EEPROM, and 8Kb of flash for program storage. The mote is further accentuated with 256Kb of external EEPROM and a 916.5MHz transceiver from RF Monolithics. The entire device measures only 1.5'' x 1'' and is shown in figure 4.2. The mote can function for several weeks off of two AA batteries if run conservatively. The size and RF capabilities of the mote are particularly attractive for its inclusion in this system. Since the mote is small it will minimally affect the flexibility of the host substrate, while the RF transceiver makes it suitable for distributed sensor applications.

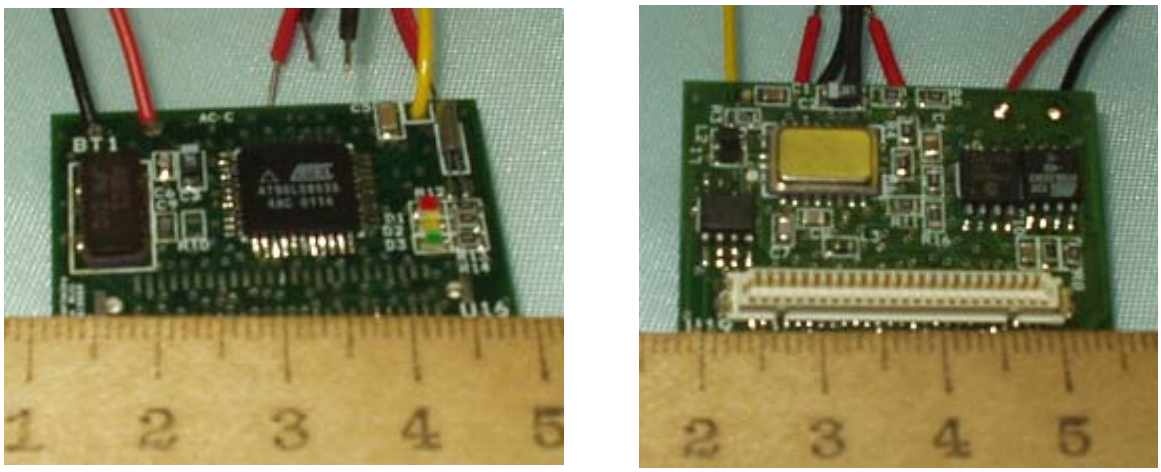

Figure 4.2 The Rene mote developed by Jason Hill at UC Berkeley. Top (left), bottom (right)

The mote just described is one of the early generations of mote referred to as the Rene mote, others being the WES mote and the Mica2 mote, with the latter being the most functional. The Rene was chosen as it is more powerful than the WES and physically smaller than the Mica. Initial simulations also suggested that the Rene would be suitable for beamforming. The Rene mote is shown in figure 4.2 and development information for the Rene mote can be found in Appendix A.1. Sensor boards have also been developed including light, temperature, and single channel sound.

Berkeley researchers have also developed software tools for use with the Mote. TinyOS was developed to allow easy interaction with the components of the mote providing a platform which can be programmed with a language that is essentially a cross between C and Java. Also available are TinyDB, which is an SQL database configured to run on the mote and Bombilla which is a TinyOS virtual machine.

4.1.2 Data Acquisition Circuitry

Two different data acquisition circuits were developed for use with the mote. The first of the proposed systems was designed as a flexible circuit so as to not interfere with flexibility when included in the textile array. The second system was designed to overcome shortcomings of the flexible circuit while providing an additional variable gain stage.

4.1.2.1 Flexible Multiplexing Circuit

The first tenet of electronic textiles is that they must maintain the flexibility of their textile substrate. While electronic components are inherently rigid, advances in component manufacturing have drastically reduced their size such that they would add little to the rigidity of a textile system. The problem then is how to provide the appropriate footprint to connect these components to the fabric in question. To address this issue, a circuit patch was designed on a Kapton film (developed by Dupont) and then sewn into the target fabric. The circuit was etched in the Biomedical Microsensors Laboratory (BMMSL) at NCSU and is shown in figure 4.3. This circuit is designed to contain a multiplexer, an op-amp, a programmable filter, resistors, capacitors, and connection points for woven wires from the array.

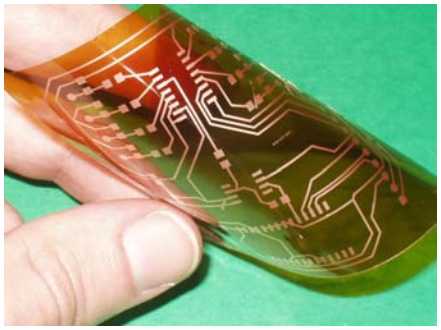

Figure 4.3 Flexible data acquisition circuit on a Kapton substrate.

The circuit design revolves around the programmable filter which is incorporated to provide a means for target discrimination in a noisy environment as well as double as an anti-aliasing filter. It was hoped that by isolating certain frequencies, the array could target specific vehicles based on identifying frequencies, effectively ignoring other vehicles. The filter chosen is the MAX263 featuring dual second-order filters, 4 operating modes (band pass, low pass, high pass, and all pass), 128 possible digitally selected Q values depending on mode, and a digitally programmable center frequency. It is desirable for all microphones to use the same device since the filter is relatively expensive and occupies a large amount of circuit real estate. The microphones were therefore multiplexed using a 74HC4051 analog mux/demux. This arrangement requires the use of only one of the available analog to digital converters available on the mote for all eight microphones. To further decrease component count, the acoustic signals are amplified after the multiplexer. The amplifier is the same 741 op-amp as utilized in the first generation array but is oriented in an inverting configuration with a gain of 100. The inverting scheme requires fewer external components and reduces the possibility of undesirable filtering by removing extraneous capacitors. The circuit diagram and associated bill of materials can be found in Appendix A.4.

Tests on the completed circuit identified a few adverse speed limitations of the system. The fastest possible sampling time of the mote's analog to digital converters in the design used is 154kHz. To simulate simultaneous sampling, all 8 microphones must be sampled as fast as possible per time step. At 154kHz, each group of eight can sample at a frequency of 19250Hz. As such however, the time the first microphone is sampled is closer to the time of the sampling of the last microphone in the previous group than it is to samples 3-8 in its own group. If the group sampling rate is halved to 9625Hz, based on the Nyquist

criterion the maximum frequency which can be sampled is 4812.5Hz. To achieve any reasonable results however, the target frequency range should be considerably lower. It would likewise be best to have a larger sampling time between groupings of eight. The small frequency window left is still suitable for beamforming as most frequencies of military interest are below 200Hz. This will not however allow the full potential of the filter to be realized, as it is not a high enough order filter to discriminate among frequencies in this range. Furthermore, when prototyped, the multiplexer was switched at low speeds and the chosen signal was passed through both the op-amp and filter, and then analyzed. However, at high speeds, switching the multiplexer switches the input to the filter. Since the filter is used primarily as a low pass filter and the input is switched at high frequencies, the input is essentially nullified.

The multiplexer also has issues with high frequencies. When switching the select lines on the multiplexer, a small amount of noise is introduced in the output signal. Amplifying the signals after the multiplexer thereby amplifies the switching noise. Since the microphone signals have very little amplitude, they are indistinguishable in the amplifier output. To determine the extent of noise introduced in the signal by the 74LS4051, the least significant bit of the multiplexer's select lines was clocked using a function generator while the other two were grounded. Only microphone 0 was connected to the circuit so the microphone output should appear only on the low cycle of the lsb clock. The initial test frequency is 75.69kHz, mimicking the desired switching frequency which is commensurate with the fastest ADC frequency. Figure 4.4 shows universal acceptance of the signal with significant noise added. The test is then run at half the desired rate, or about 37.23kHz,

yielding figure 4.5. Appearance of the signal during the positive cycle of the select clock has been diminished but noise is still quite significant throughout.

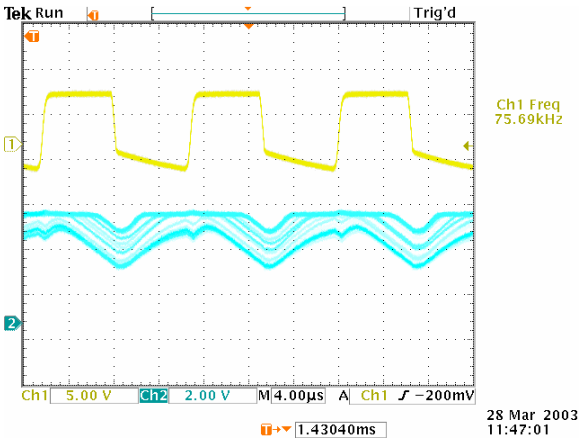

Figure 4.4 Multiplexer crossover of signals occurs at high frequencies. Top - clock, Bottom - output.

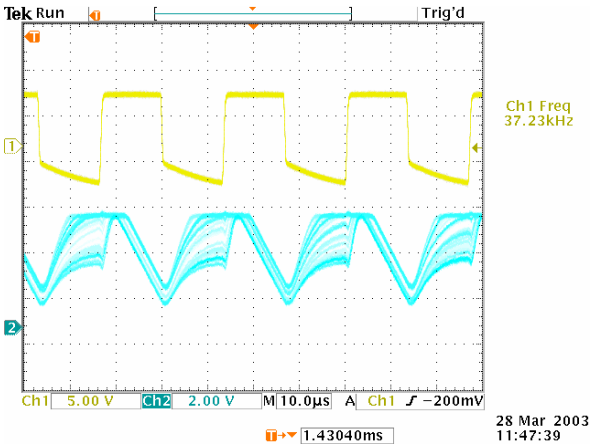

Figure 4.5 Multiplexer noise reduces with lower frequency but is still prevalent. Top - clock, Bottom - output.

Another drawback of this design is that it requires a 5V power supply. The mote, designed to be a low power device, has only a 3V supply. All of the components on the mote can happily accept a 5V supply, but that would increase the size of an already large battery pack.

Although proven to not be particularly useful, this is a working circuit and its flexibility can be demonstrated. The circuit was populated and sewn into a miniature array as shown in figure 4.6. This system allows the user to specify which microphone to listen to and will allow filtering of the received signal. While the Kapton based circuit can not be crumpled or creased, it is a definite advancement in flexibility when compared to a standard printed circuit board. The images of figure 4.7 show the circuit's flexibility.

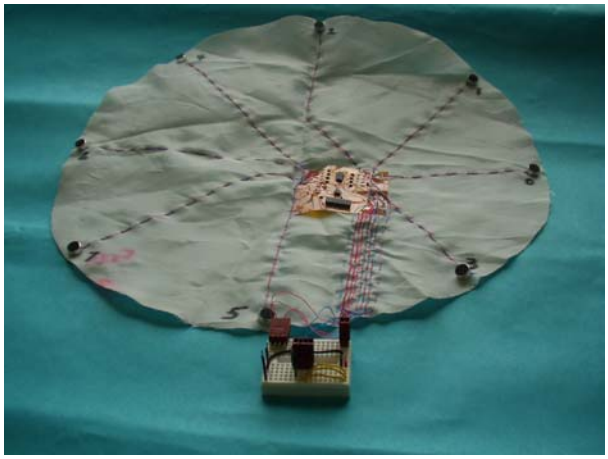

Figure 4.6 Kapton based circuit sewn into a miniature array.

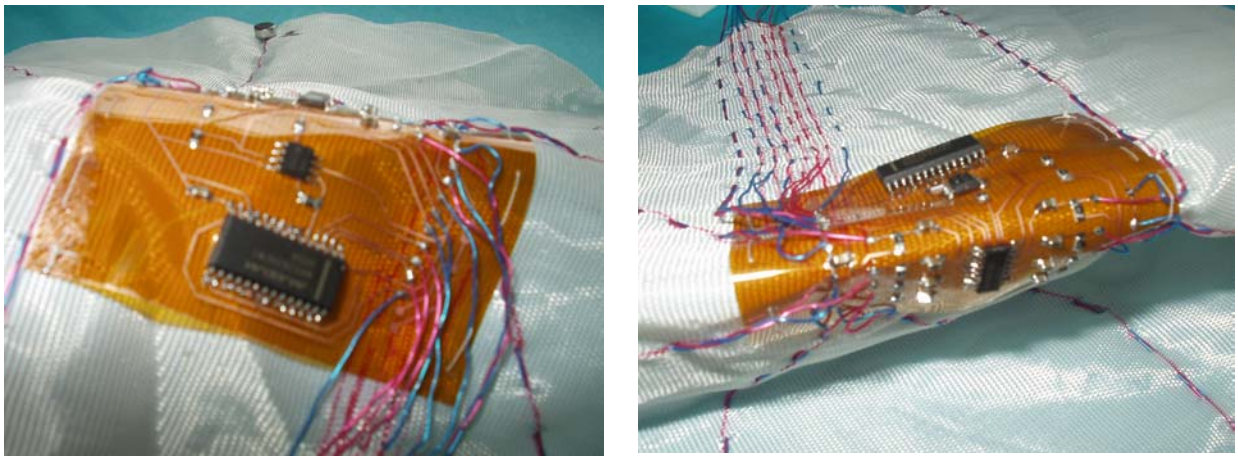

Figure 4.7 Flexibility demonstration of the Kapton based circuit.

4.1.2.2 Intelligent Variable Gain Data Acquisition System

The data acquisition scheme addressed in this section provides advantages for distributed arrays working to track the same target. The amplitude of the received target signal depends on the location of each array with respect to the target sound source. An array close to the source will have a much higher amplitude than one farther away. While both arrays can potentially pick up the signal, it is conceivable that the further array cannot detect

the sound or the closer array could actually saturate. With this in mind, it is desirable to be able to adjust the amplifier gain based on the sound levels the array detects.

The circuit created is shown in figure 4.8 and the circuit diagram can be found in appendix A.5. While this acquisition system does not have the flexibility of its predecessor, its size was minimized to reduce added array rigidity. This board measures approximately 1.4’’x1.8’’ and it is directly pluggable into the mote as well as the array, a re-configurability feature the flexible array did not have. The array is connected via a flat flex cable and a zero insertion force connector on the data acquisition board.

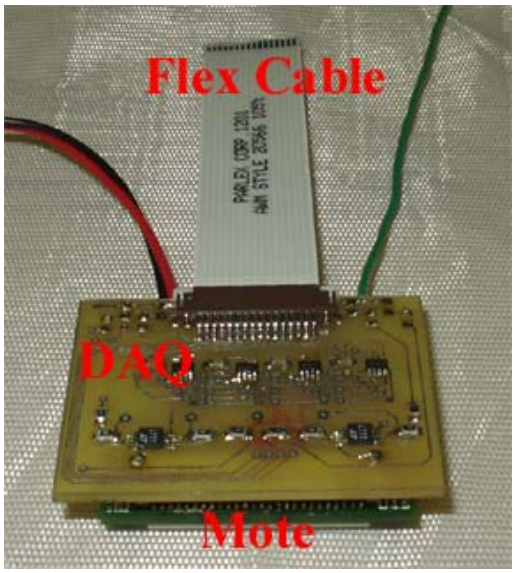

Figure 4.8 The 8 channel variable gain data acquisition circuit.

This circuit’s primary component is the LTC6910-2 from Linear Technologies. This chip is a variable gain op-amp adjustable to gains of 0, 1, 2, 4, 8, 16, 32, and 64 via 3 digital input lines. This chip alone cannot provide adequate gain for sampling of the microphone signal, so the incoming signal is first sent to a non-inverting op-amp with a static gain of 100. The LT1807, also from Linear Technologies, was chosen for this task as it provides rail-to-

rail operation not provided by the standard 741 op-amp used in the previous amplifier circuitry.

When determining the gain and the possible variable gains it was important to choose values that would provide high sensitivity without over accentuating ambient noise while at the same time allowing a target to be located within a few meters of the array without it saturating. Unfortunately, an anechoic chamber was not readily available and the following experiments were performed in a typical computer laboratory. To minimize ambient noise, unnecessary computers were powered down, air conditioning was turned off, and the tests were run after business hours to avoid people and outside traffic disturbances. The tests were run utilizing a sound source of 100Hz at 100 decibels (dB). This was chosen as it is the mid-range of the military vehicle frequency range (20-200Hz) with the dB equivalence of a large truck or drill. It is important to note that this is dBA which is frequency dependant and models the sensitivity of the human ear. This is not an appropriate scale for characterization of this array as it has, as previously shown, a rather consistent frequency response across the audible range [45]. The dBC scale is therefore utilized for experimentation as it is independent of frequency. The 100 decibels on the dBA scale has a measured equivalency to 118dBC. Utilizing just the first amplification stage, with a gain of 100, saturation occurs within 5 meters. This is sufficient for localization such that if an array is saturating and the array's position is known, the source position is also known and it can then be targeted.

Initially, two channels of this system were prototyped and tested. The testing showed that there is little noise introduced on the signals. After fabrication however, the circuit demonstrated considerable noise. The signal and power lines on the board are in some cases as thin as and as close to one another as is allowed by the fabrication company in order to

make the board as small as possible. It is surmised that this minimization inadvertently introduced the noise since analog and digital lines run in parallel in close proximity. To decrease the noise, several approaches were taken. First capacitors were added from power to ground at each op-amp but showed little benefit. Filtering capacitors were also added at the output of the op-amp stages also showing no improvement. The coupling capacitor and pull up resistor for the microphone were removed from the pcb and placed directly on the back of the microphone, essentially turning it into a three terminal microphone. The power is therefore run separately from the ground and signal wires which are a twisted pair. This showed promise but still did not yield the desired results. When completed the alterations allowed for acceptable performance on only 4 of the 8 channels whereas initially only 2 were usable.

Although the fabricated circuit is not functional enough to be useful, the circuit design is still viable. The circuit was therefore prototyped on a standard breadboard and interfaced to the acoustic array until a new layout could be fabricated. This prototype only contains the first gain stage (the LT1807) simply for testing purposes (figure 4.9).

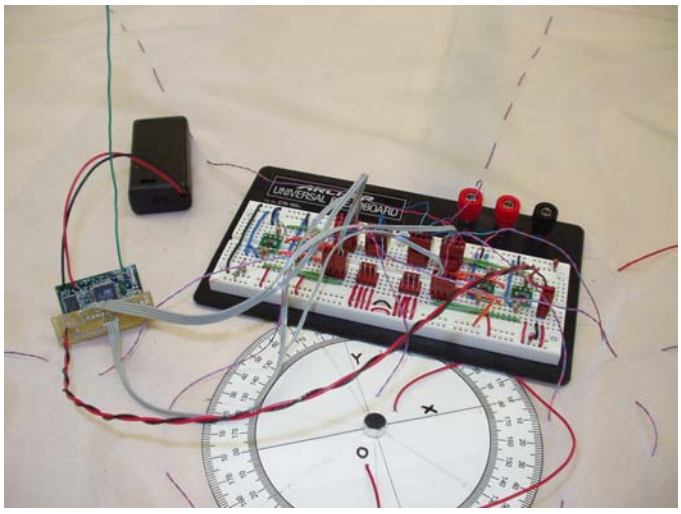

Figure 4.9 Protoboard data acquisition circuit.

4.2 Array Geometry

The second-generation system also attempts to improve performance by altering the microphone geometry. During simulation with the 4 x 5 element array of figure 3.1, whose layout is shown in the plot of figure 4.10, system ambiguity was observed when the sound source was perpendicular to the broad side of the array or at 90 degrees with reference to the array's center. This is shown with the spurious spikes in the leftmost image of figure 4.11. Also shown in this figure is a simulation with the sound source located at 0 degrees. In this orientation, there is one obvious directional beam with only insignificant extraneous beams.

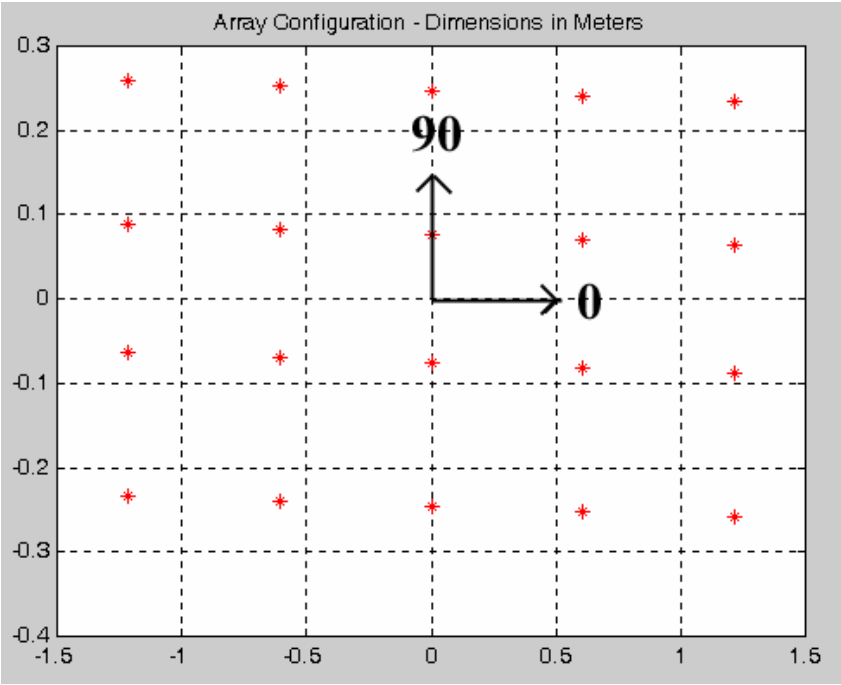

Figure 4.10 4 x 5 element array configuration of the 1st generation array shown in figure 3.1.

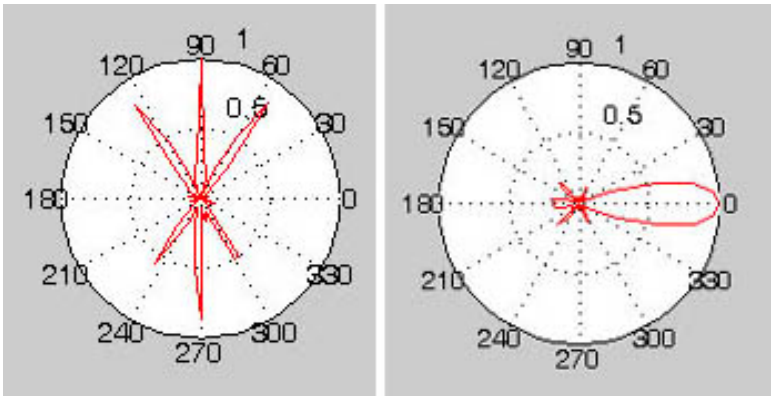

Figure 4.11 Beam Forming Simulations for the Rectangular Array of figure 4.10. Multiple beams are observed with a 1kHz sound source at 90 degrees (left) but are not present when located at 0 degrees (right).

The new array layout attempts to obtain a more consistent beam pattern regardless of the position of the sound source. This would help to eliminate any confusion caused by spurious beams as demonstrated. To accomplish this, the array was laid out in a circular pattern. Furthermore, it was laid out such that there are 7 elements along the perimeter and one in the center (only 8 are used as there are only 8 ADC ports available on the mote). The simulations of figure 4.13 show that the acoustic array geometry as proposed gives more consistent results and is less likely to introduce confusion. Although there are many extraneous spikes in the diagrams, it is important to realize that a longer spike equates to higher confidence, so these particular spikes do not carry as much weight as those in the rectangular simulation at 90 degrees. With the maximum distance between microphones of approximately 1 meter, this array is best suited for frequencies greater than 350Hz. For better performance at lower frequencies a much larger array would be needed. For example, minimal spacing for detection of a 20Hz signal is 17.25m and for 100Hz is 3.45m. These would be more ideal for beam-forming with military targets (characteristically 20-200Hz) but due to space limitations in the development environment this was not feasible.

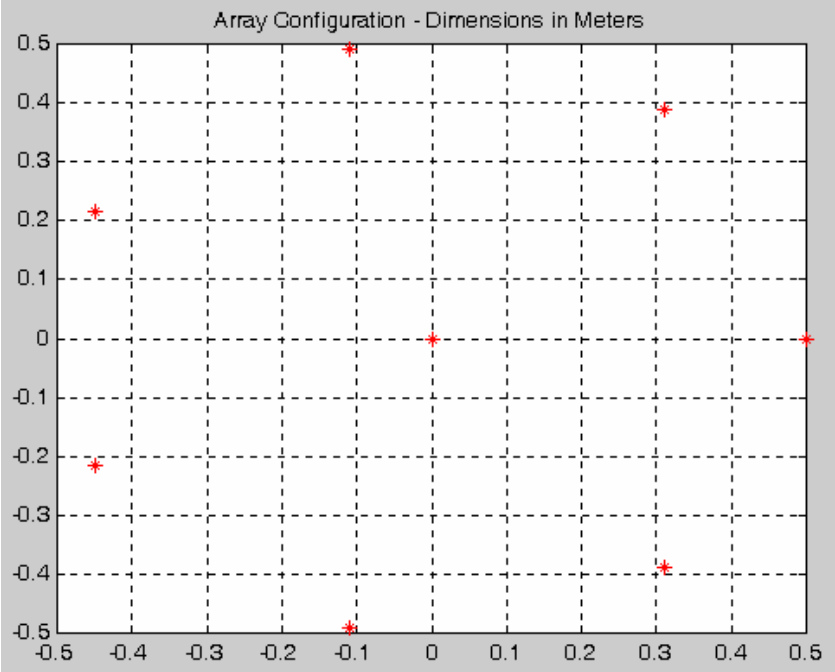

Figure 4.12 8 element array configuration for mote based sensing.

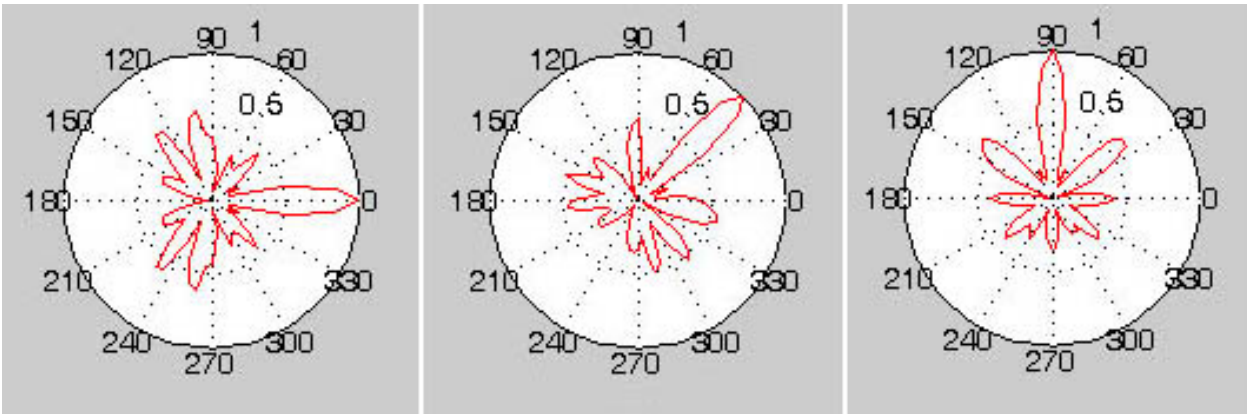

Figure 4.13 Beam Forming Simulations of 8 Element Circular Array at 0, 45, and 90 degrees Respectively given a 1kHz sound source.

4.3 Software

The software involved is responsible for the control of the data acquisition, the communication between motes or base computer, and processing of the data for beamforming. For data acquisition, the program must sample and store data on command

from the base node and then transmit that information back to the base node for processing. This can be done either directly through the serial port or through an intermediary mote which essentially serves to provide RF capabilities to a PC. To facilitate the RF operation, a board was created based on the mote programmer of Appendix A.2 that simply performs RS232 communication. The layout for this board can be found in Appendix A.3. The home computer then must process the information gathered and present it to the user.

4.3.1 Data Acquisition Software

The data acquisition software is largely dependant upon the hardware components available on the mote. Data must not only be sampled and stored at an appropriate frequency, to sample the target acoustic source, but each of the eight channels must be sampled fast enough that the sampling delay between channels can be considered negligible. Due to the stringent timing requirements of this program, it was coded in assembly.

As previously outlined, the mote has three types of memory: 512 bytes of internal SRAM, 512 bytes of internal EEPROM, and 256Kb of external EEPROM. Ideally the external EEPROM would be utilized, as it would allow for a considerable amount of sampling of the target signal. This memory is serial and accessed via the I2C protocol. While this does not require much of the processor's resources, it is regrettably slow with a maximum write time of 5.0ms. While faster, the internal EEPROM is also too slow due to its large write time of 2.5-4.0ms. The SRAM is the only viable solution as it can be written to in two clock cycles (0.5μs) but it is important to note that the data must share its meager 512 bytes with the program stack. Fortunately, the software on the array does not require extensive use of the program stack. Allowing only 16 bytes for the program stack leaves 496

bytes available for data. The analog to digital converter output on the mote has a 10 bit resolution, requiring 2 bytes of storage per sample. This would allow for only 31 samples which is insufficient, so the data is left aligned to ignore the lower 2 bits thereby allowing for 62 samples per microphone.

Ideally, all eight channels would be sampled simultaneously. The mote's ADCs do not sample simultaneously so it is necessary to sample all eight channels as fast as possible to make the timing difference appear negligible. Using the ADC in free running mode and the maximum 2MHz ADC clock (given a 4MHz system clock), samples are taken at approximately 154k samples per second. The eight samples at 154kHz in this example are only taken every 640Hz so a software timer must be introduced to meet this requirement. Timer Counter 0 is set up for this purpose. This timer uses the system clock (4Mhz), prescaled by a factor of 32, or 125kHz (otherwise the count necessary would be larger than 1 byte). At this frequency, if the counter counts to 195 every 1.5625ms for a frequency of 640Hz. After 8 ADC samples, the ADC is disabled. After Timer Counter 0 counts to 195, the counter is reset and the ADC is enabled. The timing associated with the ADC and Timer Counter 0 interrupts is shown in the oscilloscope screen shots of figure 4.14.

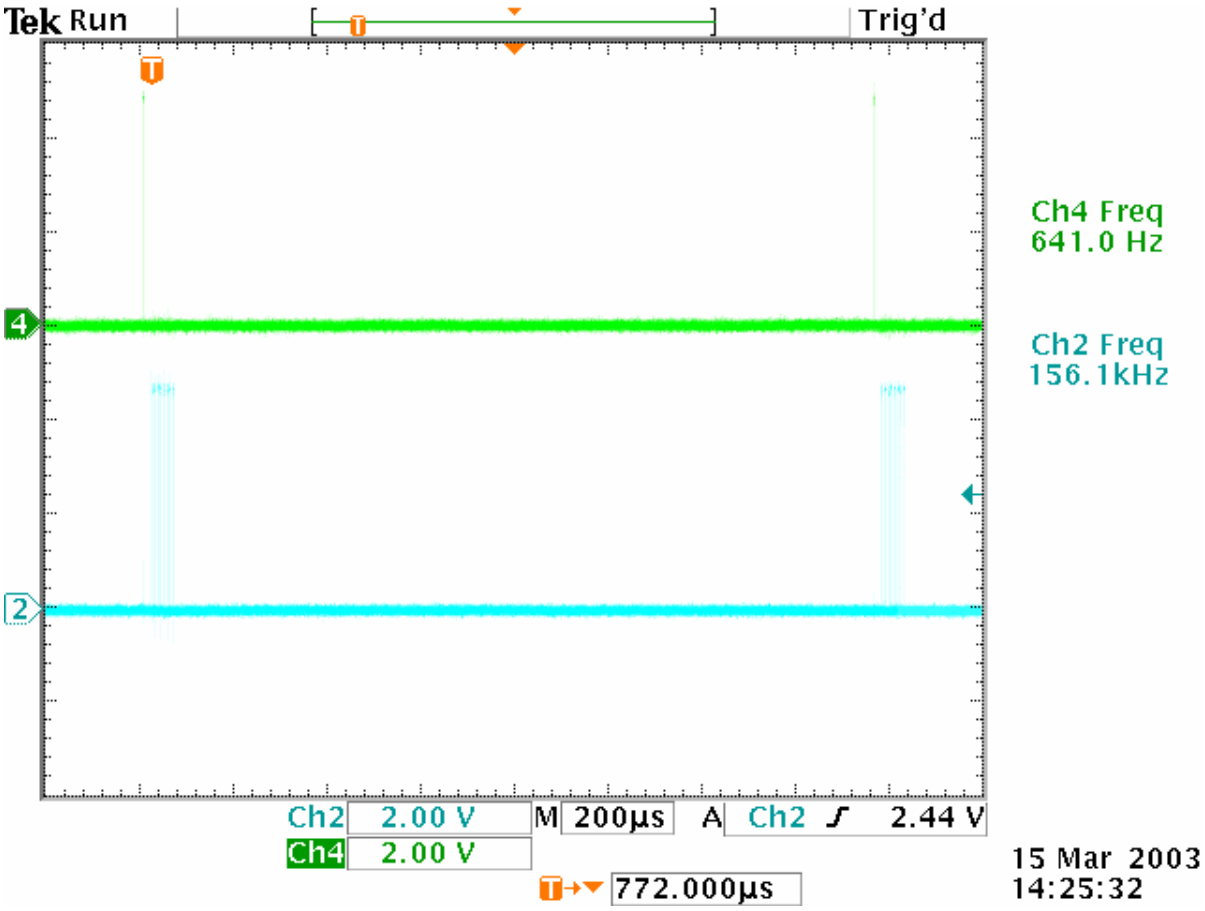

Figure 4.14 Oscilloscope screen shot displaying the sampling frequency used to sample the acoustic source (top) and the sampling time used to sample the 8 microphone elements (bottom).

The main program as shown in the flowchart of figure 4.15 primarily serves to initialize the system for data collection and to communicate with the base station. The program first awaits a start signal from the base computer (or polls the RF receiver) instructing it to begin sampling. Once received, the necessary hardware is initialized and the interrupts are enabled. The ADC and OC2 interrupts perform the sampling operation until the SRAM is full then stop collecting data. Control is returned to the main program which transmits the collected data (either through the UART or the RF transceiver). The program then awaits the next sampling command. The assembly code can be found in Appendix B.1.

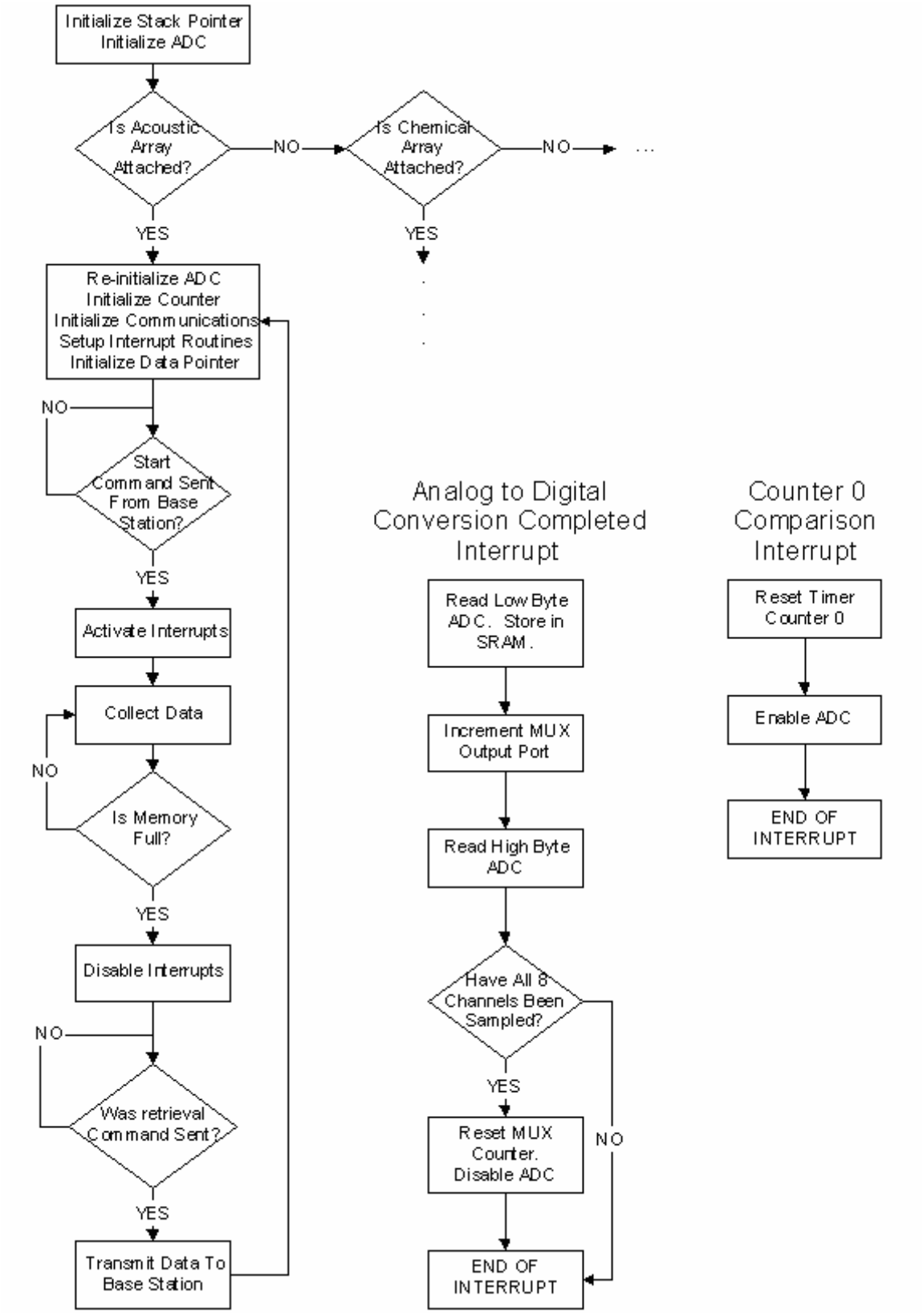

Figure 4.15 Program Flow Chart for a Sensor Array.

4.3.2 Base Station Software

All of the beam-forming and visualization is done on a base computer with which the mote or motes must communicate. The communication is facilitated by a Java program which transmits simple commands through the serial port and accepts the response. When the samples are taken, they are stored sequentially such that adjacent bytes are from different microphones. This data is reorganized in preparation to be run through the Matlab beam-forming software discussed in chapter 3. Java was chosen as it typically portable across many platforms and work is currently underway to include pocket computing systems. In the future the Matlab beam-forming software can also be translated into Java without losing the elaborate visualization capabilities. The code for this program can be found in Appendix B.2.

4.4 Experimentation

The first experiment is performed to determine the sampling rate that will be used for the remaining experiments. The subsequent experiments will compare the performance of the mote based system to simulation as well as the Hoontech system for sound sources of various frequencies as well as real-world multi-frequency sound sources.

4.4.1 Sampling Frequency Experimentation

This first experiment is designed simply to determine the sampling frequency that will be used for data acquisition in the remaining experiments. Typically, the faster the better, but due to the limited memory resources available, the sampling frequency has a great effect on the time over which the samples are taken. How does this affect the quality of a beam resolved from such samples?

The figures of table 4.1 show simulated beam-patterns formed on a 1kHz sound source located 90 degrees with respect to the array. The sampling frequency in each case is 12500Hz, the maximum reliable sampling frequency obtained with the mote. The same simulation is run 3 times, varying only the time over which sampling occurred. First for 1s, then for 0.1s, and finally for 0.005s, which is approximately what can be achieved with the mote at this sampling frequency. The results indicate no appreciable difference in the beam patterns realized for 1s and 0.1s. However when sampling at 0.005s, there is an obvious, although not result altering, degradation in the beam pattern. The same is repeated in table 4.2 changing the sound source to 100Hz with the same general result.

Table 4.1 Beam-patterns with varying sampling times taken of a 1kHz source at a rate of 12.5kHz.

Sampling Time	Resulting Beam-Pattern (Simulation)
1s	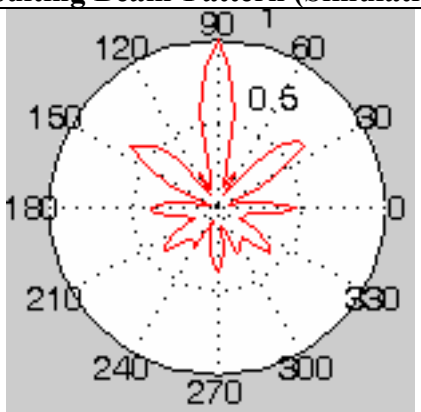
0.1s	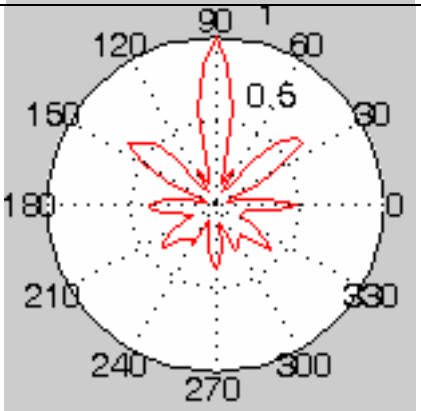
0.005s (mote attainable when sampling at 12500Hz)	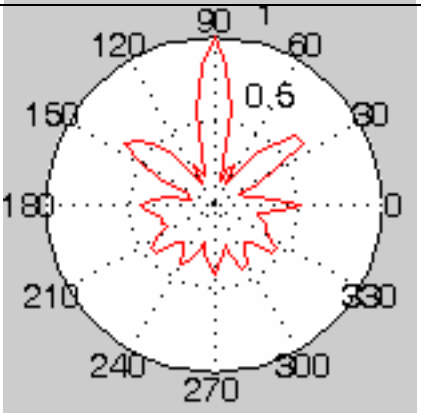

Table 4.2 Beam-patterns with varying sampling times taken of a 100Hz source at a rate of 12.5kHz.

Sampling Time	Resulting Beam-Pattern (simulation)
1s	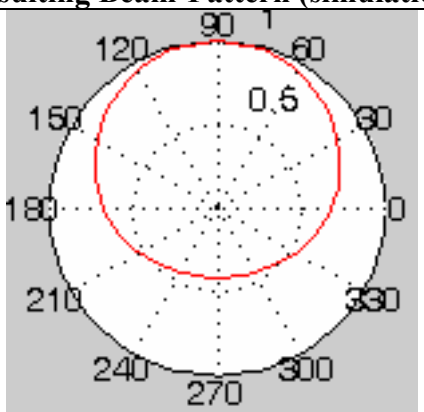
0.1s	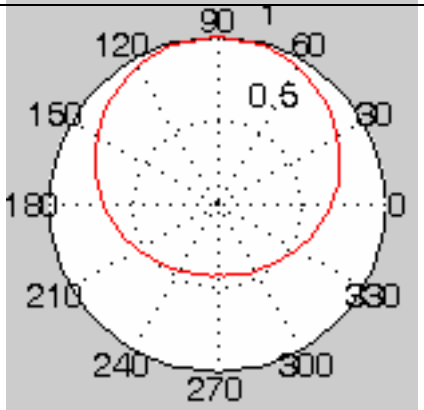
0.005s (mote attainable when sampling at 12500Hz)	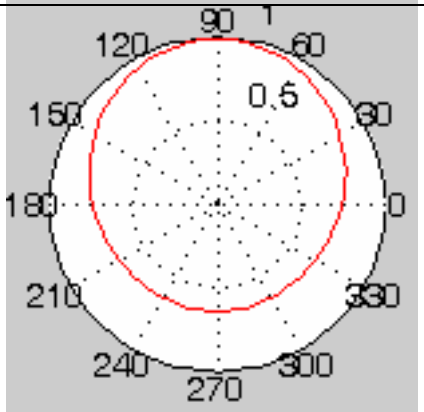

So far results have indicated that 0.005s is not an ideal sampling period. All of the figures of table 4.3 therefore have a sampling period of 0.0124s, which is mote attainable with a sampling frequency of 5000Hz. The topmost figure is run (unrealistically) with a sampling frequency of 12500Hz for comparison with the second figure which is run at 5000Hz. The two are similar with minor changes in quality and shape. The third figure is

run with a sampling frequency of 5000Hz and a source of 1000Hz. This figure appears jagged with respect to the figures of table 4.1 but generally acceptable by comparison.

Table 4.3 Effects of a sampling period of 0.0124s for various sampling and source frequencies.

Conditions (all have sampling time of 0.0124s)	**Resulting Beam Pattern (simulation)**
Sampling frequency of 12500Hz Source frequency of 100Hz	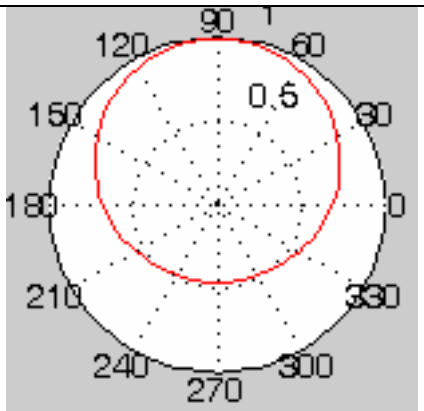
Sampling frequency of 5000Hz Source frequency of 100Hz	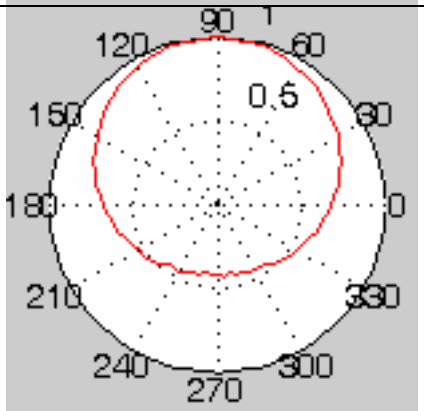
Sampling frequency of 5000Hz Source frequency of 1000Hz	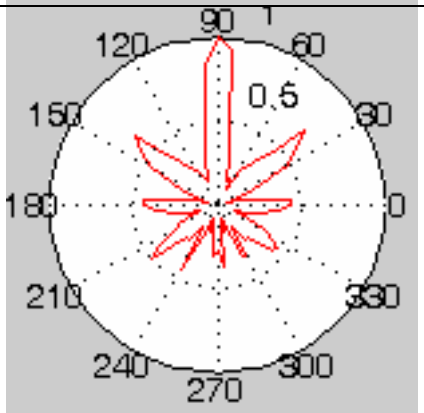

Ultimately, this experiment has shown that the sampling rate of 5KHz performs just as well as a more frequently sampled signal. The advantage of the higher sampling rate

would be that one could sample for a higher range of frequencies (sampling at 12500Hz, one can uniquely sample signals up to 6250Hz).

4.4.2 Sound Source Frequency Experimentation

This experiment compares the actual array's performance to those from simulation. An example comparing simulated signals to sampled signals is shown in figure 4.16. The sampled signals are considerably rougher than that of the simulated signals. This is likely a result of the sound source, background noise, and circuit noise. Furthermore, this experiment was performed in a closed room with no precautions taken to prevent reflections.

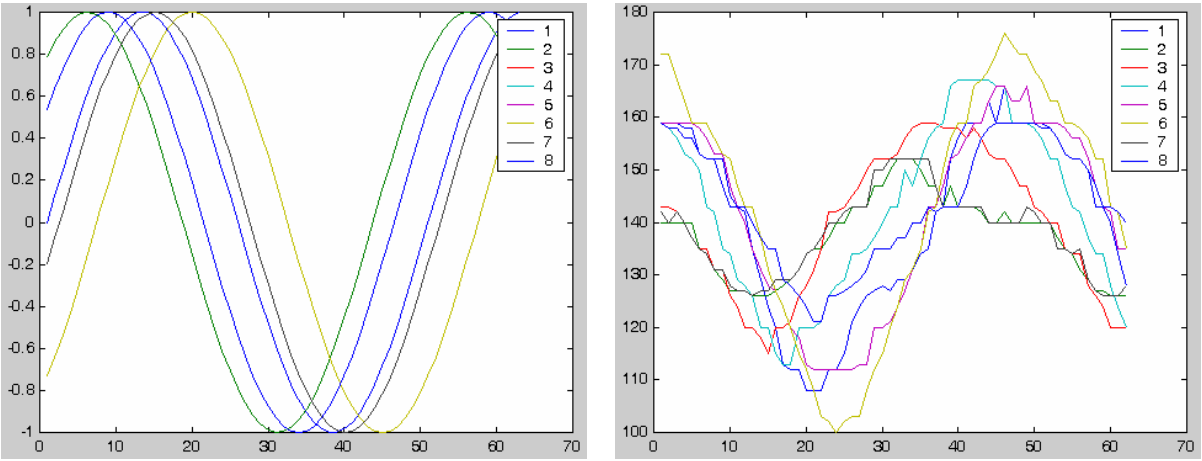

Figure 4.16 Simulated sound recordings (left) and real world sound recordings (right).

This experiment is performed for various frequencies for each of which a beam-pattern is realized at both 0 degrees and 285 degrees. 0 degrees is in line with one of the radially located microphones, whereas 285 degrees lies approximately between two of the radial microphones. Each of the beam-patterns for the actual system were run 5 times to insure repeatability. The results are given in table 4.4.

Table 4.4 Simulated and actual beam-patterns realized from various target frequencies at both 0 and 185 degrees.

Frequency	Position Azimuth/ Elevation	Simulated	Actual (mote)
100Hz	$0^o/0^o$	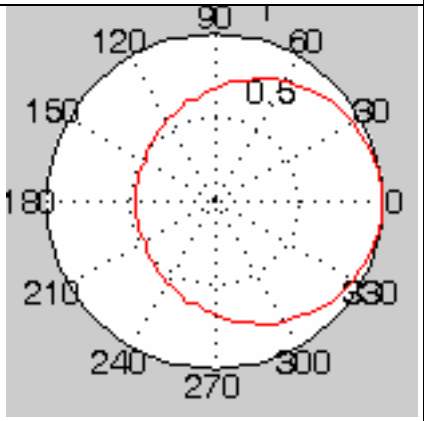 $0^o/20^o$	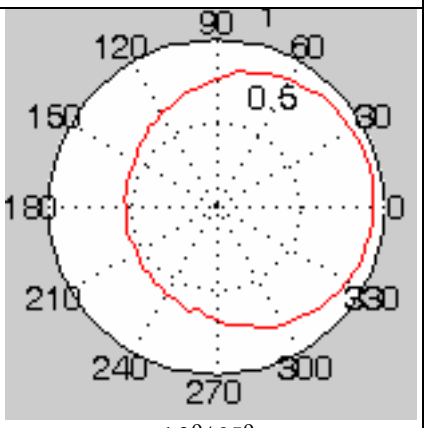 $10^o/65^o$
	$285^o/0^o$	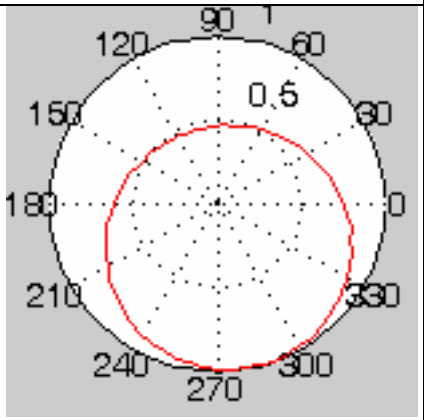 $285^o/35^o$	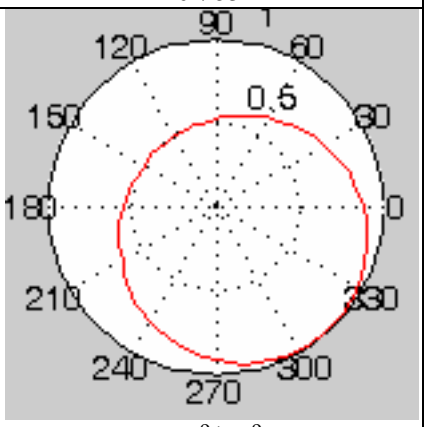 $310^o/35^o$
500Hz	$0^o/0^o$	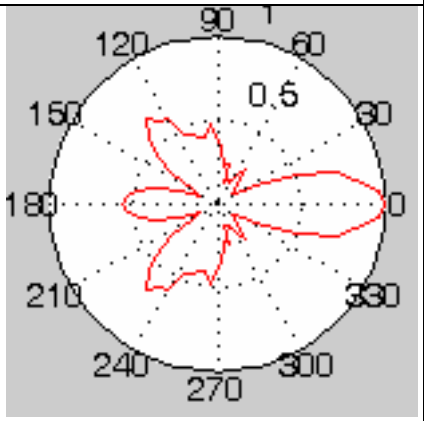 $0^o/0^o$	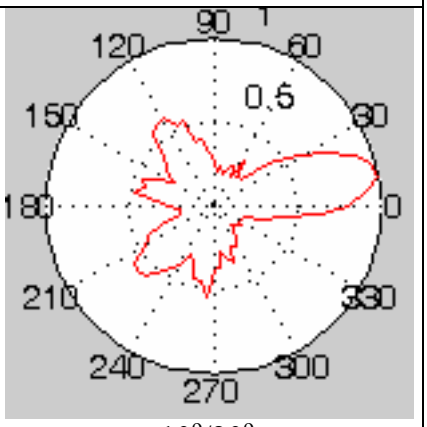 $10^o/20^o$

Table 4.4 (continued)

285°/0°	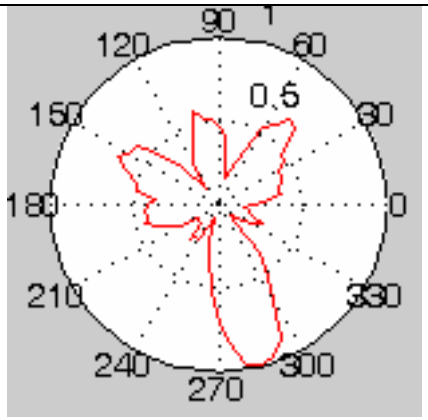 285°/0°	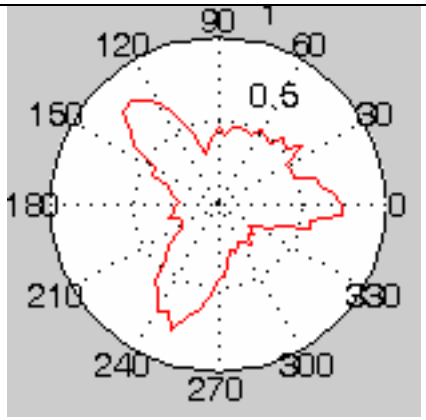 250°/40°
0°/0°	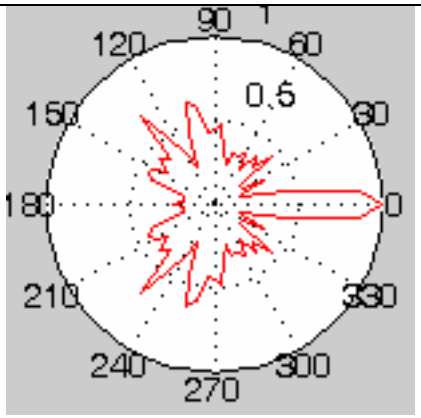 0°/0°	
285°/0°	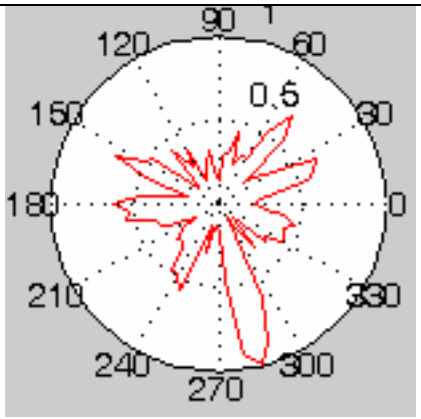 285°/0°	

While the actual beam-pattern shares the same general shape as its simulated counterpart, they do not yield the same results. The actual system performs best at an angle that is in line with a microphone as demonstrated with a typical azimuth error of 10 degrees. Between microphones however, this error can be as great as 35 degrees. Error as great as 45 degrees is realized when examining determined elevation angles. These errors are not surprising given the sampled signal quality from figure 4.16. Another source of error is the application of the far-field assumption. The far-field assumption states that assuming a sound source is far enough away then the wave front can be modeled as a plane. The beam-forming software is based on this assumption and this experiment was performed with the sound source located at a mere 12ft.

The real world results for the 1000Hz sound source have been left out of table 4.4. At this frequency, the mote-based system yielded grossly inconsistent and error prone results. Three examples of these results are shown in table 4.5. The most accurate result is off by an azimuth of 45 degrees whereas the worst is off by 160 degrees. Although previous simulations have demonstrated that this array should perform well at 1KHz with a 5KHz sampling frequency, due to the aforementioned errors with the system and the experiment itself, this is not the case.

Table 4.5 Inconsistent results after sampling a 1KHz source located at 0 degrees.

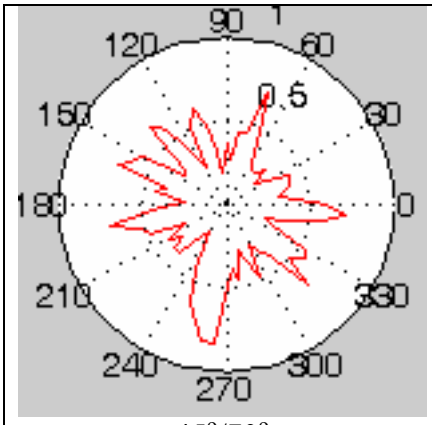	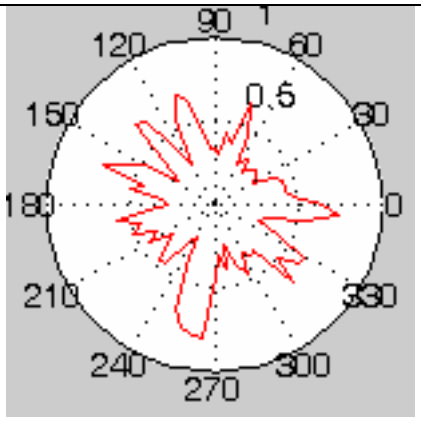	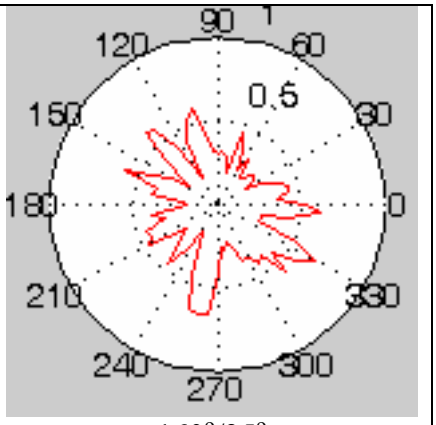
45°/70°	60°/70°	160°/35°

4.4.3 Multi-Frequency Sound Source Experimentation

This experiment attempts to characterize the performance of the array on multi-frequency sound sources. This is accomplished through the use of sound files acquired from the ARL website [46]. The sounds consist of a tank, a truck, a helicopter, a missile, and a gun shot. The frequency spectrum of each of these sounds is shown in figure 4.17. The composite frequencies all lie at or below 500Hz. Table 4.6 shows the beam pattern resulting from beam forming on these sources.

Table 4.6 Beam patterns for various sound sources located at 0 degrees.

Sound	Resulting Beam Pattern (mote)
Tank	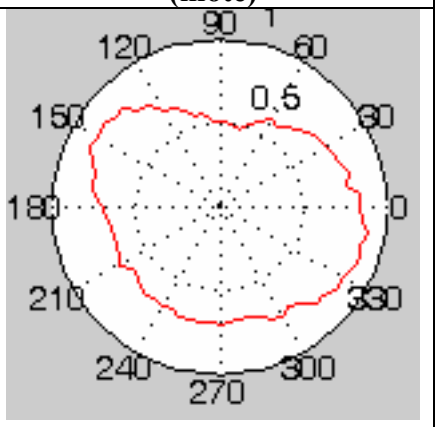 305°/35°
Truck	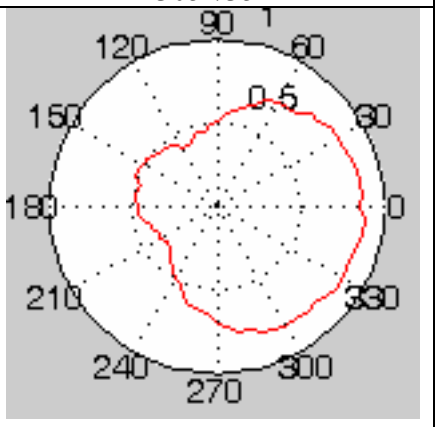 5°/50°
Helicopter	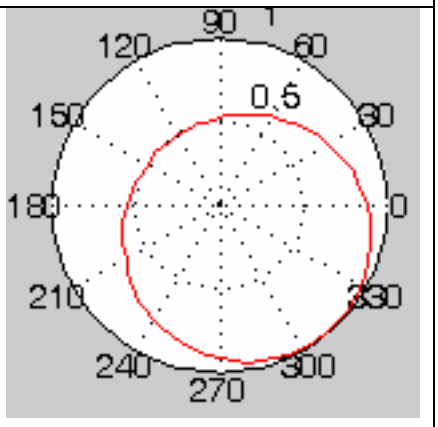 310°/35°

Table 4.6 (continued)

Sound	Resulting Beam Pattern (mote)
Missile	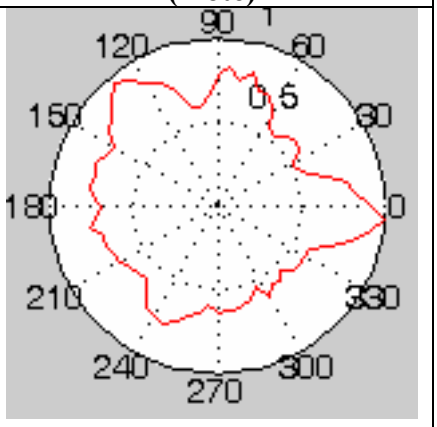 0°/0°
Gun Shot	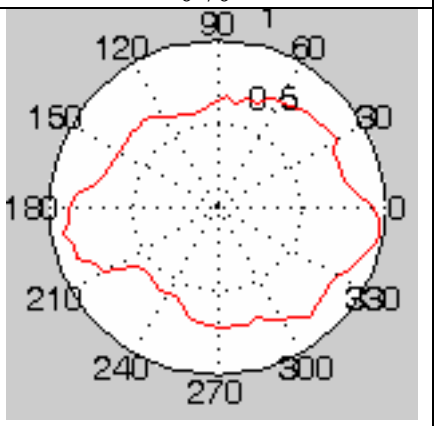 355°/25°

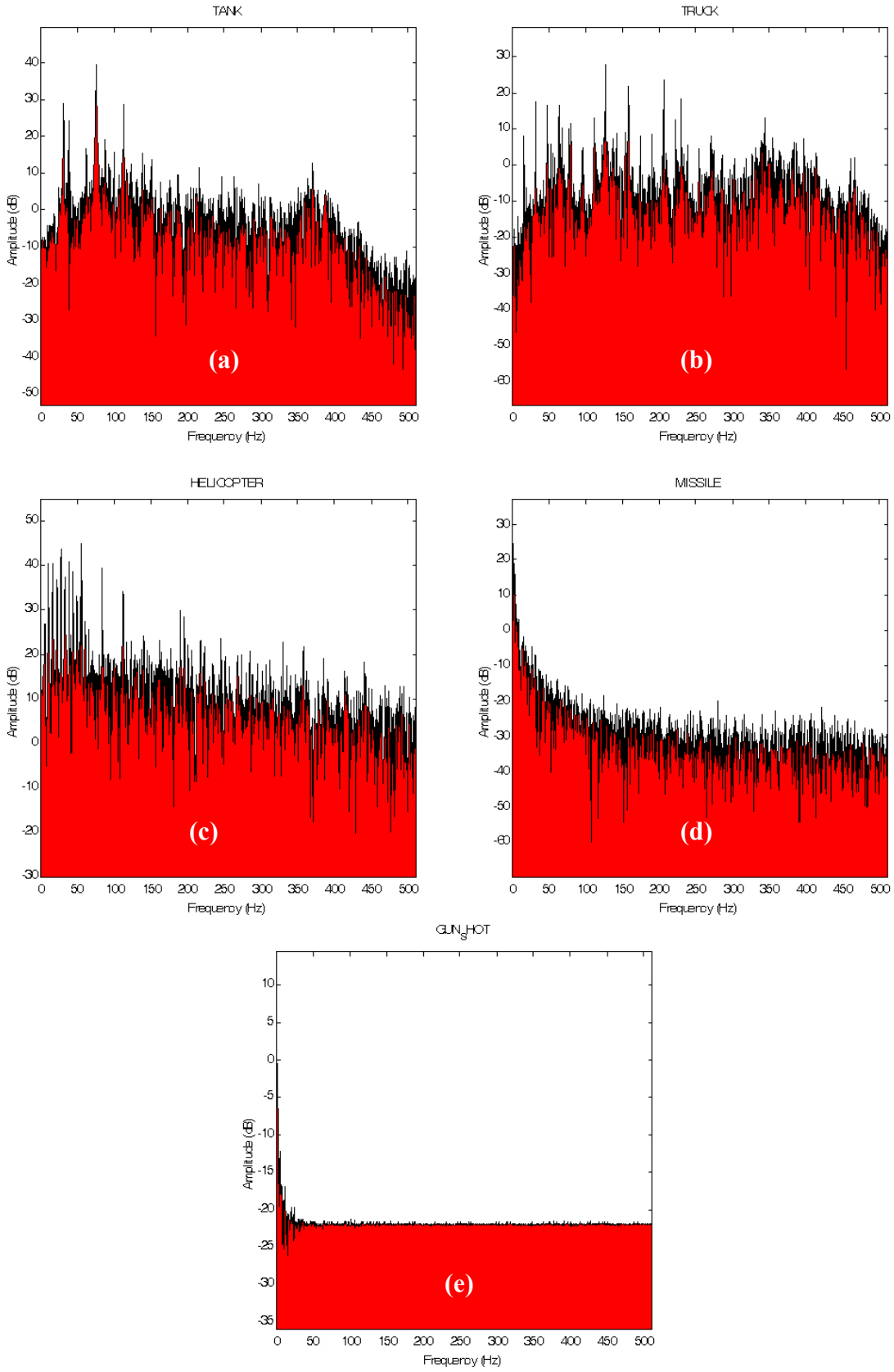

Figure 4.17: Frequency spectra of (a) tank, (b) truck, (c) helicopter, (d) missile, and (e) gun shot [46]

The resulting beam-patterns from these systems performed within reason for the missile and the gun shot. The helicopter and tank performed the worst with azimuth errors of 50 and 55 degrees respectively. The elevation is not of particular interest as it has been previously demonstrated that this method of beamforming performs poorly for determining elevation. This will be further examined in experiment 4 where the performance of this system will be compared to that of the Hoontech system of chapter 3.

It is important to note that each run was performed several times and the best visual result utilized. These are difficult sounds to beam form upon because the sampling time of the mote is so small that not much information can be obtained. These are also poor quality sound files themselves sampled at a low frequency. Furthermore, they represent their object in motion so the sound tends to fade in and out. Essentially, when the sample is taken determines how well the system will perform. This inconsistency due to the changing sound source is shown by the images taken on the truck sound in table 4.7.

Table 4.7 Demonstration of inconsistent beam patterns formed on truck sounds located at 0 degrees.

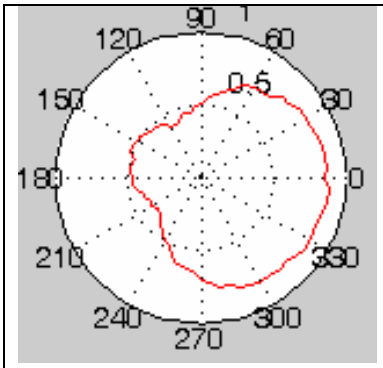	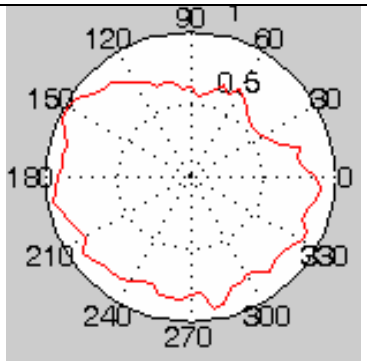	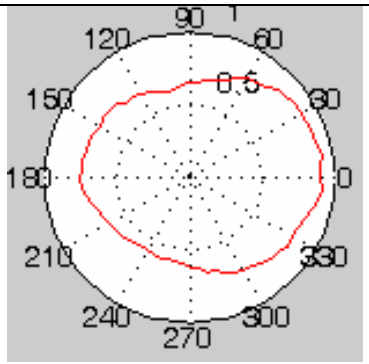
5°/50°	150°/15°	10°/65°

4.4.4 Mote Vs. Hoontech Data Acquisition Experimentation

This experiment compares the performance of the mote based data acquisition with that of the Hoontech system described in chapter 3. The Hoontech system is set to sample at 44100Hz and samples for a period of 1s. An example of the sampled signals of the Hoontech system is shown in figure 4.18. When compared to the sampled waveforms from the mote system in figure 4.16, these are a lot smoother and more closely resemble the ideal. The figures of table 4.8 show the resulting beam-patterns for the various sounds using the Hoontech system.

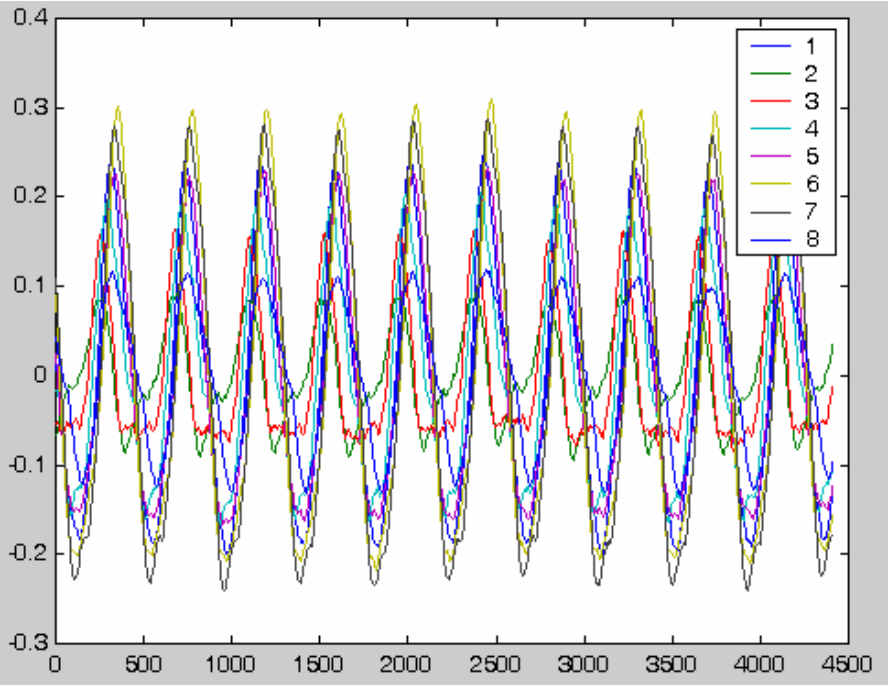

Figure 4.178 Samples of a 100Hz sound source taken at 44100Hz using the Hoontech data acquisition system.

Table 4.8 Beam patterns achieved by sampling at 44100Hz for 1s with the Hoontech system.

Sound	Resulting Beam Pattern (Hoontech)
Tank	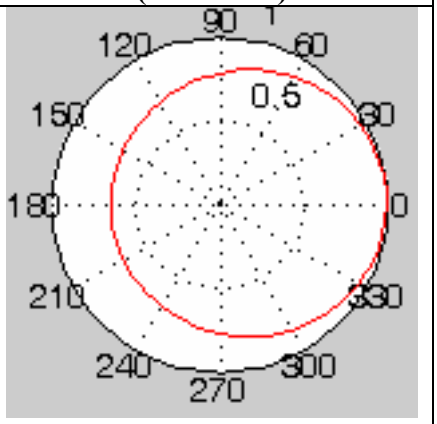 5°/30°
Truck	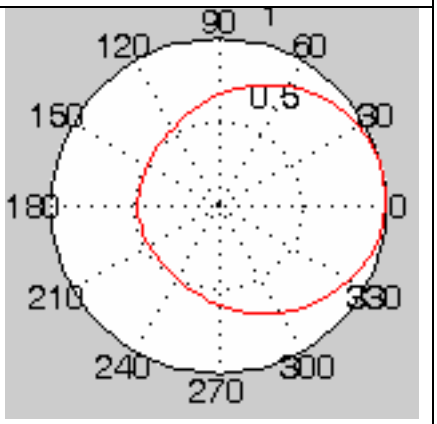 10°/0°
Helicopter	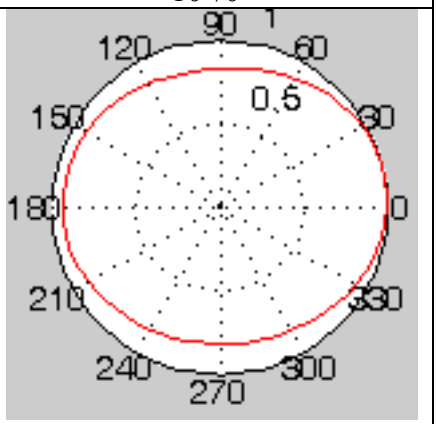 10°/0°

Table 4.8 (continued)

Sound	Resulting Beam Pattern (Hoontech)
Missile	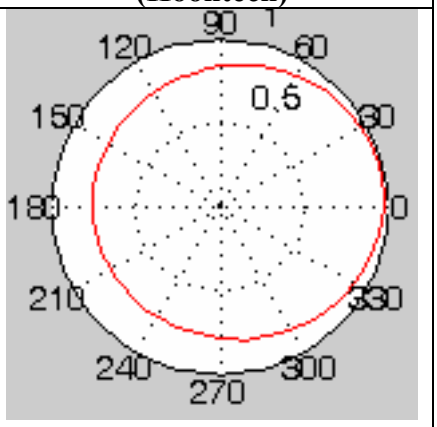 10°/50°
Gun Shot	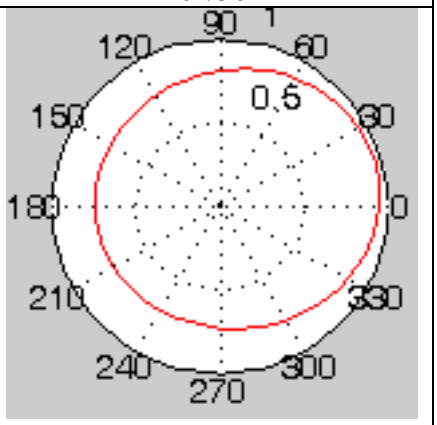 15°/50°

The resulting beam patterns of the Hoontech system outperform those achieved from the mote data acquisition system for the tank, truck, and helicopter. For the missile and gun shot however, the mote is actually more accurate. Considering the difference in both sampling time, sampling frequency, and observed signal quality the mote based system performed surprisingly well.

Chapter 5 – Conclusions and Future Work

5.1 Conclusions

The work presented in this thesis has examined aspects of both electronic textiles and acoustic array systems. This work has culminated in the implementation of several different textile based arrays useful for examining real-world performance of triangulation and beamforming methods.

The development of the textile system has brought about the investigation of wire layout, interconnections, and external interfacing. Wires can be woven in the warp and weft directions to provide several lines to the integrated electronics. It was shown however, that reducing the complexity of the pattern reduces the number of interconnects and can kept the overall size of the array to a minimum. Floats were proven to aid in the attachment of external components, as was a customized co-axial snap connector. Also, while not as effective as commercial windscreens, densely woven pockets did demonstrate resistance to wind noise without adversely affecting the microphone's listening ability.

Electronic systems were developed such that they would not adversely effect the flexibility of the system. A flexible circuit implemented on a Kapton substrate was sewn into the fabric. Due to design error, this circuit did not work as desired. During testing, it was discovered that the analog multiplexer used cannot operate at the high frequencies required for this circuit's operation. Therefore, at slower speeds, this is a functioning circuit and as such was used to demonstrate its flexibility. While not as versatile as the fabric to which it is sewn, it is more desirable than a traditional pcb of comparable size. Yet another system was developed with improved amplification providing variable gain. This circuit functions well

as a prototype, but striving for minimization, noise was introduced on the developed pcb. The prototype system however was more than adequate to interface with the Berkeley mote to collect data for beamforming.

Simulation was used to develop an array with more consistent performance regardless of source azimuth. The acceptable sampling frequency was likewise determined in simulation. It was shown that although it will yield a more accurate sampling of a sound source, due to minimal memory, the fastest sampling frequency is not necessarily the best. Finally, the performance of the mote-based system was compared to the corresponding results from simulation and the Hoontech data acquisition system. Although performance varied substantially in comparison to the simulation, the mote-based system was comparable to the Hoontech system. This was a surprising result as the Hoontech system sampled 1 second of data at a rate of 44100Hz. With a few upgrades, the mote system could be a competitive multi-channel fast data acquisition system.

5.2 Future Work

Based on the aforementioned conclusions there is much work that can be done to improve the themes touched upon in this thesis. The electronic textiles aspect of this project can be expanded to improve the manufacturing of woven systems as well as the inclusion of flexible circuitry. The acoustic array could benefit from a more streamlined geometry, an upgraded microprocessor with additional memory, provisions for self determination of geometry, and algorithms allowing the use of multiple systems working cooperatively to locate and track a target.

5.2.1 Electronic Textiles

Use of a Leno weave for woven electronic textiles may improve the manufacturing of woven systems. The Leno weave, as depicted in figure 5.1, can be used to form a mock twisted pair configuration. The advantage of using this weave is that there is more control over the location of the wires which would be beneficial for the attachment of external electronic components. Previously, floats, as shown in figure 3.5 were utilized, but the twisted pair wire was still twisted making it particularly challenging to automate the attachment of devices. Also, using the Leno weave, only one wire must pass through a reed. In the woven systems created in this thesis, the size of the reed was the limiting factor in the gauge of the wire used. Weaving separately would allow for an effective doubling of the wire gauge used.

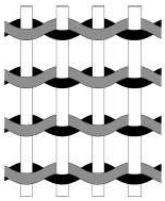

Figure 5.5.1 Demonstration of a Leno weave. [1]

Non-woven textile production methods of electronic textiles could also be examined. If a circuit is created on a substrate of either Kapton or Tyvek it can then be formed into a textile by flocking. The flocking fibers would effectively coat the circuit and its components not only making it look more like a traditional textile, but perhaps adding strength to the circuit without compromising its flexibility.

It is also of interest to further examine the flexible battery products available from Power Paper. As in the case of the array, there is an abundance of dead space where no wires

or components are located. If feasible, this dead space could be the power source for the array through the use of such products, removing the need for large, rigid battery packs.

5.2.2 Distributed Acoustic Array

As demonstrated, the most important improvement for the acoustic array is a microprocessor upgrade. The new Atmega8535 released in the spring of 2003 is a drop in replacement of the currently used AT90LS8535. The processor can run off of a 16MHz clock and provides the ability to left align the 10-bit ADCs. While a definite improvement, this chip does not provide more SRAM. Upgrading to the Mica2 mote (also released spring 2003) which is based upon the Atmega128L would provide 4Kb of internal SRAM. This generation of mote also comes equipped with 4 megabits of external flash. Where the mote is concerned, it would probably also be beneficial to take advantage of TinyOS and related software technologies. For use with the acoustic arrays it is also necessary to lay out the amplifier board once more to reduce noise.

The geometry of the array is important in making the array a more dynamic sensor system. Increasing the diameter of the array should help with its beam-forming abilities at lower frequencies. Furthermore, it would be beneficial to develop a way for the array to determine its own geometry. This could perhaps be done by the strategic inclusion of speakers at various locations. By emitting a particular tone the system should be able to gather enough information to determine its own geometry. Since the array is flexible and could conceivably be deployed folded or lying over debris, this would be a significant attribute to ensure the best possible performance is realized.

Since beamforming cannot provide reliable distance information it would be ideal to use one or more of these arrays cooperatively. Since they each can provide the direction of

the sound source, if their location is known, they can then be used to triangulate the target's position as demonstrated in figure 5.2. Perhaps GPS and a digital compass could be integrated into the mote or the sensor board to facilitate this behavior.

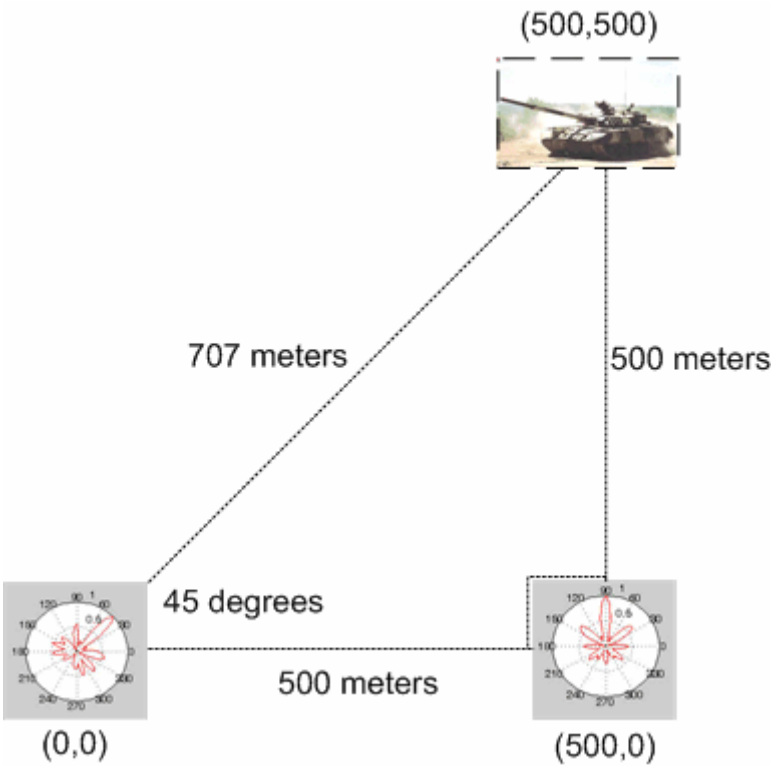

Figure 5.2 Triangulation of sound source position using two acoustic arrays of known position.

Likewise, if the timing is worked out appropriately, multiple arrays can be used to form a single beam for a particular target as shown in the simulation of figure 5.3.

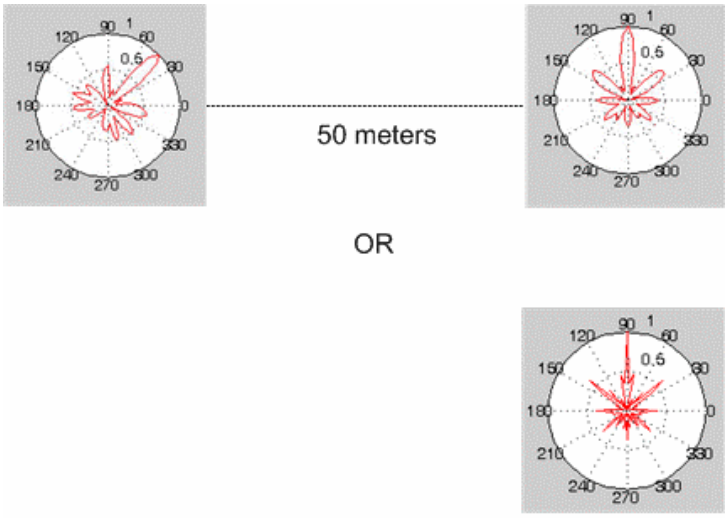

Figure 5.3 Demonstration of beam thinning using information from multiple arrays to form the same beam-pattern.

References

[1] Schorow, Stephanie. "MIT Targets High-Tech Innovations for U.S. Soldiers." SmallTimes. 01/06/2002. Small Times Media LLC. 01/2003. <http://www.smalltimes.com>.

[2] Brush, Peter. "The Story Behind the McNamara Line," *Vietnam* 1996: 18-24.

[3] *Defeating Insurgency on the Border,* GlobalSecurity.org. <http://www.globalsecurity.org/military/library/report/1985/HJR.htm>. Last Accessed 27 June 2003.

[4] Land Mine Monitor Report 2000. Human Rights Watch. <http://www.hrw.org/reports/2000/landmines/LMWeb-28.htm>. Last Accessed 27 June 2003.

[5] Objective Force Warrior. Natick Soldier Center <http://www.natick.army.mil/soldier/WSIT/>. Last accessed 27 June 2003

[6] Zisler, Siglinde. Infineon. <http://www.wearable-electronics.de/intl/>. Last accessed 27 June 2003

[7] Meoli, Dina**, "**Interactive Electronic Textiles: Technologies, Applications, Opportunities, and Market Potential", Masters Thesis Dissertaion under the direction of Dr. Traci May-Plumlee, North Carolina State University, May, 2002.

[8] J.F. Muth, E. Grant, K.A. Luthy, L.S. Mattos, J.C. Braly, A. Dhawan, A.M. Seyam, T.K. Ghosh. "Signal Propagation and Multiplexing Challenges in Electronic Textiles", Materials Research Society. 2002.

[9] A. Dhawan, "*Woven fabric-based electrical circuits*", Masters Thesis, North Carolina State University, (2001).

[10] SoftSwitch website. <http://www.softswitch.co.uk/>. Last accessed 27 June 2003.

[11] Jones, Dianne C. and Leftly, Steven A. "Interactive Fabrics Using SoftSwitch Technology". WRONZ EuraLab Ltd, UK

[12] Backgrounder: Wearable Electronics Fashionable Technology of the Future (Press Release). Infineon. <http://www.wearable-electronics.de/intl/>. Last Accessed 27 June 2003.

[13] L. Samuelson, F. Bruno, J. Kumar, Russell A. Gaudiana , and P. Wormser, Conformal Solar Cells for the Soldier, Proceedings of the International Interactive Textiles for the Warrior Conference, Cambridge, MA, July 9-11, 2002.

[14] Esenberg, Anne, “What’s Next? Batteries Push Paper Into Electronics Age”. Circuits. Section G, Page 9. May 24, 2001.

[15] Northface. <http://www.thenorthface.com>. Last Accessed 27 June 2003.

[16] Biberdorf, Curt. “Active Fabric, Electronics, Optics integrated into clothing shows initial success” The Warrior, January-February 2002.

[17] Moulton, Donalee. “Space Age T-Shirt Senses Vital Signs, Wound Location”, The Medical Post. Volume 34, no. 33, October 6, 1998 page 63.

[18] Steele, Julie, "The Intelligent Knee Sleeve - A Wearable Fabric Biofeedback System for Preventing ACL Injuries", Intelligent Textiles for the Warrior Conference, Boston (2002).

[19] Smela, Elisabeth, "Conjugated Polymer Actuators", Intelligent Textiles for the Warrior Conference, Boston (2002).

[20] Madden, John, "Conducting Polymer Molecular Actuators", Intelligent Textiles for the Warrior Conference, Boston (2002).

[21] Hammond, Paula T., "Optical and Functional Thin Films Using Polyelectrolyte Multilayer Assembly: Potential for Flexible Electrochromic Coatings", Intelligent Textiles for the Warrior Conference, Boston (2002).

[22] Universal Display Corporation. <http://www.universaldisplay.com>. Last Accessed 27 June 2003.

[23] K.A. Luthy, J.C. Braly, L.S. Mattos, E.Grant, J.F. Muth, A.Seyam, A. Dhawan, T.Ghosh, “An Acoustic Array as an example as a large scale electronic fabric”, Electronics on Unconventional Substrates- Electrotextiles and Giant-Area Flexible Circuits, Fall Materials Research Symposium, Boston (2002).

[24] The Virginia Tech E-Textiles Group. <http://www.ccm.ece.vt.edu/e-textiles/>. Last Accessed 27 June 2003.

[25] FM 34-10-1 Tactics, Techniques, and procedures for the Remotely Monitored Battlefield Sensor System (REMBASS), 18, June 1991.

[26] Srour, Nino, "Unattended Ground Sensors A Prospective for Operational Needs and Requirements", Prepared for NATO Land Group 6 on Battlefield Surveillance, Target Acquisition, Night Observation, Countersurveillance and Electronic Warfare, U.S. Army Research Laboratory Sensors and Electronic Devices Directorate, October 1999.

[27] Pham, Tien and Fong, Manfai, "Real-Time Implementation of MUSIC for Wideband Acoustic Detection and Tracking," U.S. Army Research Lab.

[28] Pham, Tien and Sadler, Brian M., "Wideband Acoustic Array Processing to Detect and Track Ground Vehicles," U.S. Army Research Lab.

[29] T. Pham and B. M. Sadler, "Adaptive Wideband Aeroacoustic Array Processing," 8th IEEE Statistical Signal and Array Processing Workshop, pp. 295 – 298, (Corfu, Greece), June 1996.

[30] DRDC Valcartier. < http://www.drev.dnd.ca/>. Last Accessed 27 June 2003.

[31] Braunling, Russell. Gallo, Michael A., "Acoustic Sensor Performance for Vehicle Mounted Arrays," Proceedings of the 1998 SPIE Robotic and Semi-Robotic Ground Vehicle Technology, pp. 29 – 37, (Orlando, Florida), April 1998.

[32] S. H. Young, M. V. Scanion, "Robotic Vehicle Uses Acoustic Array for Detection and Localization in Urban Environments," Proceedings of the 2001 SPIE Unmanned Ground Vehicle Technology III, pp. 147 – 158, (Orlando, USA), April 2001.

[33] Mattos, Leonardo. "The EvBot II: An Enhanced Evolutionary Robotics Platform Equipped with Integrated Sensing for Control." Master's Thesis (2003).

[34] S. H. Young, M. V. Scanion, "Robotic Vehicle Uses Acoustic Sensors for Voice Detection and Diagnostics," Proceedings of the 2000 SPIE Unmanned Ground Vehicle Technology II, pp. 72 – 83, (Orlando, USA), April 2000

[35] Brandstein, M., and Ward, D. eds. *Microphone Arrays*. New York: Springer, 2001.

[36] L. Kleeman and R. Kuc, "An Optimal Sonar Array for Target Localization and Classification," IEEE International Conference on Robotics and Automation, Vol. 4, pp. 3130 – 3135, 1998.

[37] G. C. Carter, "Time Delay Estimation for Passive Sonar Signal Processing," IEEE Transactions on Acoustics, Speech and Signal Processing, vol. ASSP-29, no. 3, pp. 463 – 470, June 1981.

[38] B. D. V. Veen and K. M. Buckley, "Beamforming: A Versatile Approach to Spatial Filtering," IEEE ASSP Magazine, pp. 4 – 24, April 1988.

[39] Acoustic Magic. <http://www.acousticmagic.com/press/>. Last Accessed 27 June 2003.

[40] Steele, Michael. "A Direction Finding – Beam Forming Conference Microphone System". Lexington Center/School for the Deaf.

[41] Widrow, Bernard. "A Microphone Array for Hearing Aids". <http://www-isl.stanford.edu/~widrow/paper.pdf>. Last Accessed 27 June 2003.

[42] Horrocks, A. R., Anand, S. C., eds. Handbook of Technical Textiles. Cambridge, Woodhead Publishing Ltd. 2000.

[43] Walworth, Maurice and Mahajan, Ajay. "3D Position Sensing Using the Difference in the Time-of-Flights from a Wave Source to Various Receivers". ICAR, 1997, Monterey, CA.

[44] TinyOS Project. <http://webs.cs.berkeley.edu/tos/>. Last Accessed 27 June 2003.

[45] HyperPhysics. <http://hyperphysics.phy-astr.gsu.edu/>. Last Accessed 27 June 2003.

[46] Army Research Laboratory. <http://www.arl.army.mil/sedd/acoustics/acoustics.htm>. Last Accessed 27 June 2003.

Appendices

Appendix A

Circuit Diagrams, Material Listings, and Printed Circuit Board Layouts

A.1 Mote

A.1.1 Circuit Schematic

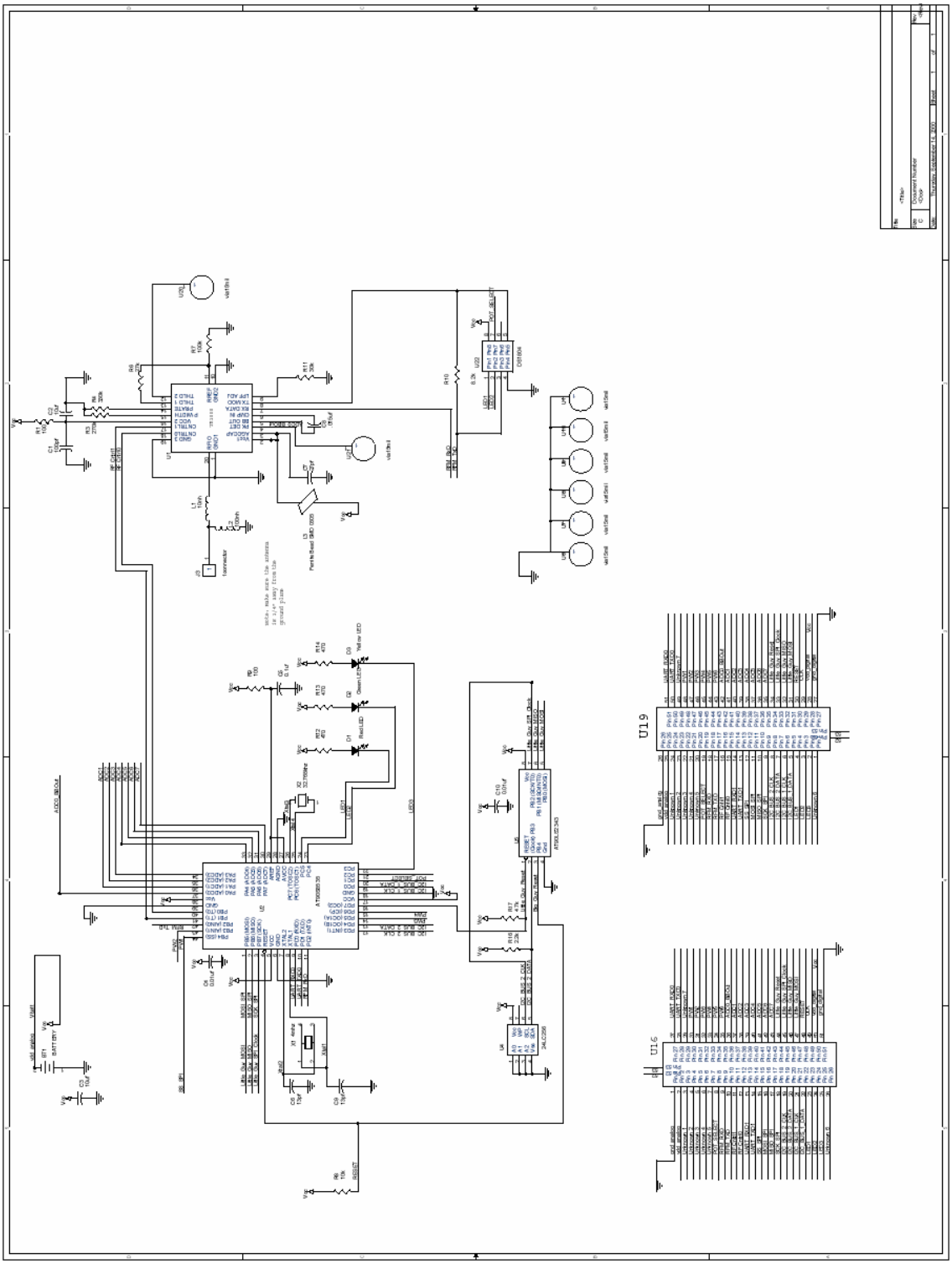

Figure A.1-1 Schematic for the Rene mote designed by Jason Hill of UC Berkeley.

A.1.2 Printed Circuit Board Layout

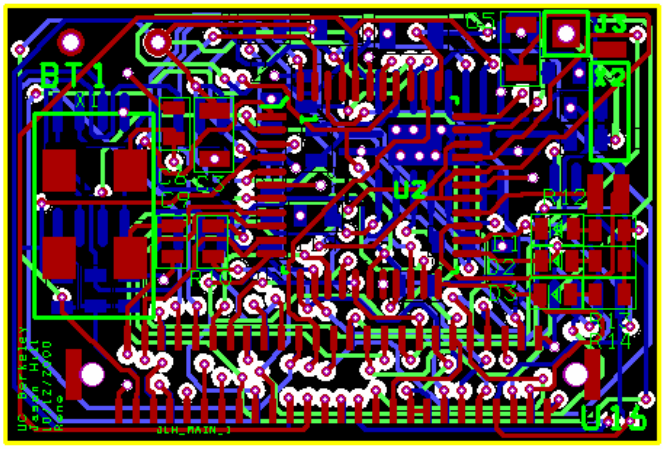

Figure A.1-2 Composite of all PCB layers for the Rene mote designed by Jason Hill at UC Berkeley.

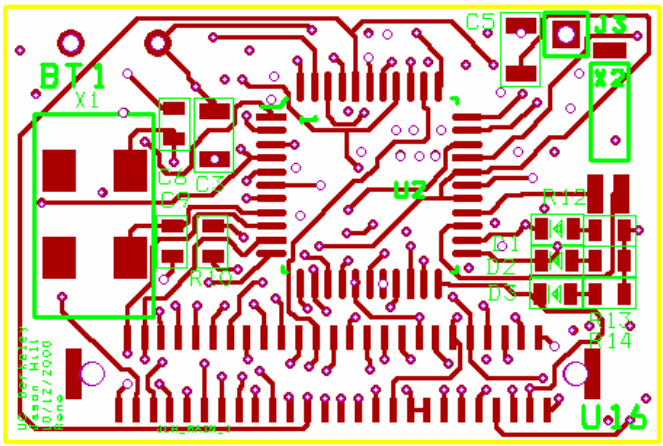

Figure A.1-3 Top PCB layer of the Rene mote.

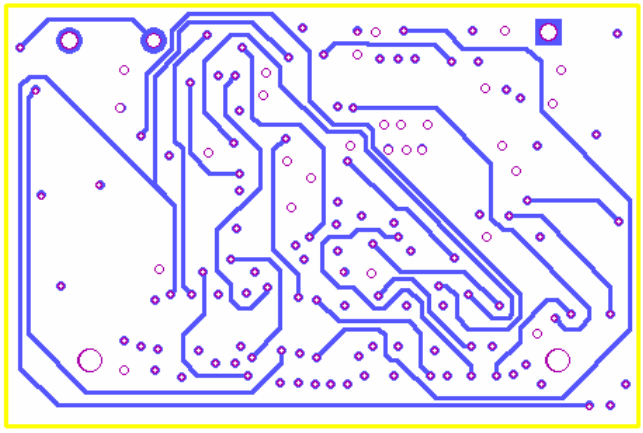

Figure A.1-4 First inner PCB layer of the Rene mote.

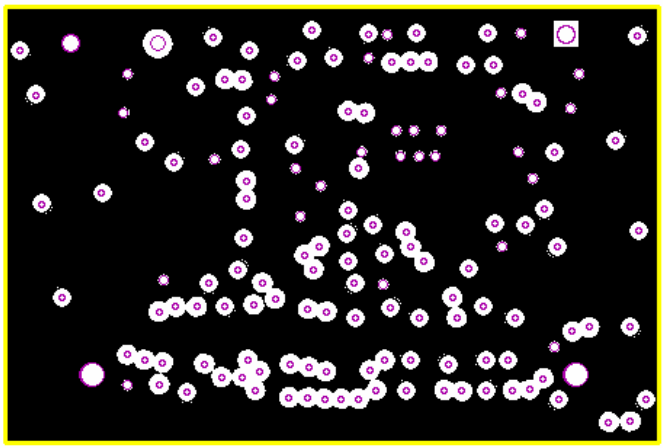

Figure A.1-5 Ground plane PCB layer of the Rene mote.

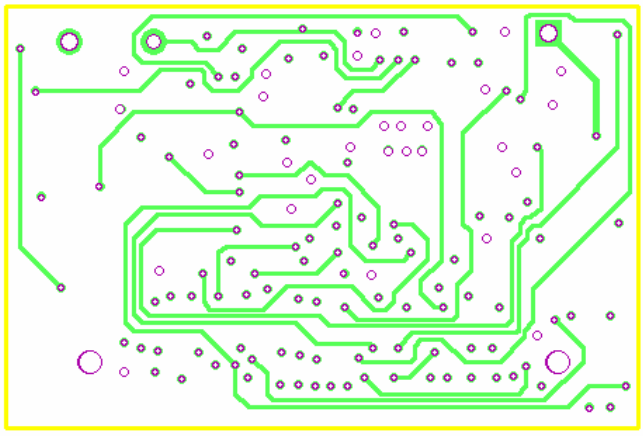

Figure A.1-6 Second inner PCB layer of the Rene mote.

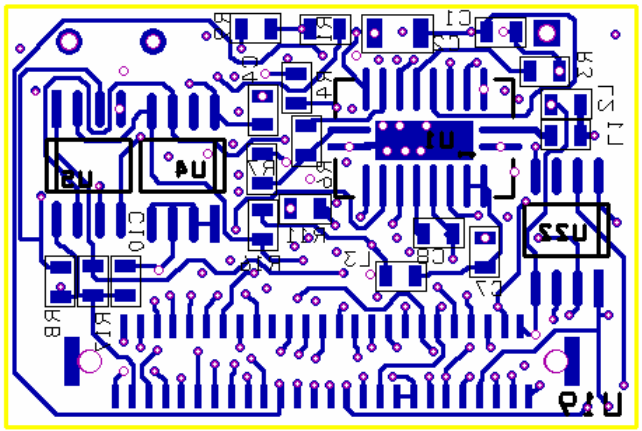

Figure A.1-7 Bottom PCB layer of the Rene mote.

A.1.3 Materials Listing and Related Datasheets

Table A.1-1 Materials listing for the Rene mote.

Part Specifier	Description	Distributor	Part Number
U4	EEPROM	Digikey	24LC256-I/SM
U19	51 Pin Connector	Digikey	H2163-ND
U16	51 Pin Connector	Digikey	H2175-ND
BT1	Battery Case for 2 AA	Digikey	SBH-321AS-ND
D2	Green Diff 0805 SMD	Digi-key	L62501CT-ND
D1	Hi EFF Red Diff 0805 SMD	Digi-key	L62505CT-ND
D3	Yellow Diff 0805 SMD	Digi-key	L62507CT-ND
R1, R9	100ohm 1/10W 5% 0805 SMD	Digi-key	P100ACT-ND
R7	100kohm 1/10W 5% 0805 SMD	Digi-key	P100KACT-ND
R8	10kohm 1/10W 5% 0805 SMD	Digi-key	P10KACT-ND
R16	2.2 kohm 1/10W 5% 0805 SMD	Digi-key	P2.2KACT-ND
R3	270kohm 1/10W 5% 0805 SMD	Digi-key	P270KACT-ND
R6	27kohm 1/10W 5% 0805 SMD	Digi-key	P27KACT-ND
R11	30kohm 1/10W 5% 0805 SMD	Digi-key	P30KACT-ND
R4	330kohm 1/10W 5% 0805 SMD	Digi-key	P330KACT-ND
R17	4.7 kohm 1/10W 5% 0805 SMD	Digi-key	P4.7KACT-ND
R12, R13, R14	470 ohm 1/10W 5% 0805 SMD	Digi-key	P470ACT-ND
C1	100pF 50V Ceramic Cap 0805 SMD	Digi-key	PCC101CGCT-ND
C4,C10	0.01uF 50V Ceramic CAP 0805 SMD	Digi-key	PCC103BNCT-ND
C5	0.1uF 50V Ceramic Chip CAP	Digi-key	PCC104BCT-ND
C8	0.015uF 50V Ceramic CAP 0805 SMD	Digi-key	PCC153BGCT-ND
C7	27pF 50V Ceramic CAP 0805 SMD	Digi-key	PCC270CGCT-ND
L1	10nH 10% Fixed SMD	Digi-key	PCD1160CT-ND
L2	100nH 5% Fixed SMD	Digi-key	PCD1172CT-ND
C2,C3	10uF 6.3V Tant TE Series	Digi-key	PCS1106CT-ND
X2	32.768kHz CYL XTAL C-002 RX Type	Digi-key	SE3202-ND
X1	4.000MHz 20pf SMD	Digi-key	XC587CT-ND
U5	IC MCU 2K FLSH 4MHZ LV SO8	Digi-key	AT90LS2343-4sc-ND
U22	IC POT TRIMMER NV 50K 8-SOIC	Digi-key	DS1804Z-050-ND
U2	IC MCU 8K 4MHZ A/D LV 44TQFP	Digi-key	AT90LS8535-4ac-ND
C6,C9	13pF 50V Ceramic 0402 SMD	Mouser	80-C0603C130J5G
L3	Ferrite Bead SMD 0805	Allied Electronics	2506033017YOD
U1	916.5MHz Transceiver	Insight/Memec	TR1000

Features

- AVR® – High-performance and Low-power RISC Architecture
  - 118 Powerful Instructions – Most Single Clock Cycle Execution
  - 32 x 8 General-purpose Working Registers
  - Up to 8 MIPS Throughput at 8 MHz
- Data and Nonvolatile Program Memories
  - 8K Bytes of In-System Programmable Flash
    SPI Serial Interface for In-System Programming
    Endurance: 1,000 Write/Erase Cycles
  - 512 Bytes EEPROM
    Endurance: 100,000 Write/Erase Cycles
  - 512 Bytes Internal SRAM
  - Programming Lock for Software Security
- Peripheral Features
  - 8-channel, 10-bit ADC
  - Programmable UART
  - Master/Slave SPI Serial Interface
  - Two 8-bit Timer/Counters with Separate Prescaler and Compare Mode
  - One 16-bit Timer/Counter with Separate Prescaler, Compare and Capture Modes and Dual 8-, 9-, or 10-bit PWM
  - Programmable Watchdog Timer with On-chip Oscillator
  - On-chip Analog Comparator
- Special Microcontroller Features
  - Power-on Reset Circuit
  - Real-time Clock (RTC) with Separate Oscillator and Counter Mode
  - External and Internal Interrupt Sources
  - Three Sleep Modes: Idle, Power Save and Power-down
- Power Consumption at 4 MHz, 3V, 20°C
  - Active: 6.4 mA
  - Idle Mode: 1.9 mA
  - Power-down Mode: <1 µA
- I/O and Packages
  - 32 Programmable I/O Lines
  - 40-lead PDIP, 44-lead PLCC, 44-lead TQFP, and 44-pad MLF
- Operating Voltages
  - V_{CC}: 4.0 - 6.0V AT90S8535
  - V_{CC}: 2.7 - 6.0V AT90LS8535
- Speed Grades:
  - 0 - 8 MHz for the AT90S8535
  - 0 - 4 MHz for the AT90LS8535

8-bit AVR® Microcontroller with 8K Bytes In-System Programmable Flash

AT90S8535
AT90LS8535

Summary

Rev. 1041HS–11/01

Note: This is a summary document. A complete document is available on our web site at *www.atmel.com*.

Features

- Utilizes the AVR® RISC Architecture
- AVR - High-performance and Low-power RISC Architecture
  - 118 Powerful Instructions - Most Single Clock Cycle Execution
  - 32 x 8 General Purpose Working Registers
  - Up to 10 MIPS Throughput at 10 MHz
- Data and Nonvolatile Program Memory
  - 2K Bytes of In-System Programmable Flash
    Endurance: 1,000 Write/Erase Cycles
  - 128 Bytes Internal RAM
  - 128 Bytes of In-System Programmable EEPROM
    Endurance: 100,000 Write/Erase Cycles
  - Programming Lock for Flash Program and EEPROM Data Security
- Peripheral Features
  - One 8-bit Timer/Counter with Separate Prescaler
  - Programmable Watchdog Timer with On-chip Oscillator
  - SPI Serial Interface for In-System Programming
- Special Microcontroller Features
  - Low-power Idle and Power Down Modes
  - External and Internal Interrupt Sources
  - Power-on Reset Circuit
  - Selectable On-chip RC Oscillator
- Specifications
  - Low-power, High-speed CMOS Process Technology
  - Fully Static Operation
- Power Consumption at 4 MHz, 3V, 25°C
  - Active: 2.4 mA
  - Idle Mode: 0.5 mA
  - Power Down Mode: <1 µA
- I/O and Packages
  - 3 Programmable I/O Lines (AT90S/LS2323)
  - 5 Programmable I/O Lines (AT90S/LS2343)
  - 8-pin PDIP and SOIC
- Operating Voltages
  - 4.0 - 6.0V (AT90S2323/AT90S2343)
  - 2.7 - 6.0V (AT90LS2323/AT90LS2343)
- Speed Grades
  - 0 - 10 MHz (AT90S2323/AT90S2343)
  - 0 - 4 MHz (AT90LS2323/AT90LS2343)

Description

The AT90S/LS2323 and AT90S/LS2343 are low-power CMOS 8-bit microcontrollers based on the AVR RISC architecture. By executing powerful instructions in a single clock cycle, the AT90S2323/2343 achieves throughputs approaching 1 MIPS per MHz allowing the system designer to optimize power consumption versus processing speed.

(continued)

Pin Configuration

PDIP/SOIC

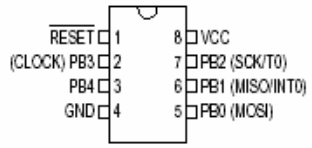

AT90S/LS2343

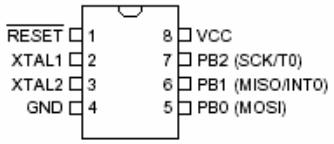

AT90S/LS2323

8-bit AVR® Microcontroller with 2K Bytes of In-System Programmable Flash

AT90S2323
AT90LS2323
AT90S2343
AT90LS2343

Rev. 1004B–04/99

MICROCHIP 24AA256/24LC256/24FC256

256K I²C™ CMOS Serial EEPROM

Features

- Low power CMOS technology
  - Maximum write current 3 mA at 5.5 V
  - Maximum read current 400 µA at 5.5 V
  - Standby current 100 nA typical at 5.5 V
- 2-wire serial interface bus, I²C compatible
- Cascadable for up to eight devices
- Self-timed ERASE/WRITE cycle
- 64-byte page-write mode available
- 5 ms max write-cycle time
- Hardware write protect for entire array
- Output slope control to eliminate ground bounce
- Schmitt trigger inputs for noise suppression
- 1,000,000 erase/write cycles
- Electrostatic discharge protection > 4000 V
- Data retention > 200 years
- 8-pin PDIP, SOIC, TSSOP, MSOP, and DFN packages
- 14-lead TSSOP package
- Temperature ranges:
  - Industrial (I): -40°C to +85°C
  - Automotive (E): -40°C to +125°C

Description

The Microchip Technology Inc. 24AA256/24LC256/24FC256 (24XX256*) is a 32K x 8 (256 Kbit) Serial Electrically Erasable PROM, capable of operation across a broad voltage range (1.8 V to 5.5 V). It has been developed for advanced, low power applications such as personal communications or data acquisition. This device also has a page-write capability of up to 64 bytes of data. This device is capable of both random and sequential reads up to the 256K boundary. Functional address lines allow up to eight devices on the same bus, for up to 2 Mbit address space. This device is available in the standard 8-pin plastic DIP, SOIC, TSSOP, MSOP, DFN and 14-lead TSSOP packages.

Device Selection Table

Part Number	Vcc Range	Max. Clock Frequency	Temp. Ranges
24AA256	1.8-5.5 V	400 kHz(1)	I
24LC256	2.5-5.5 V	400 kHz	I, E
24FC256	2.5-5.5 V	1 MHz	I

Note 1: 100 kHz for Vcc < 2.5 V.

Block Diagram

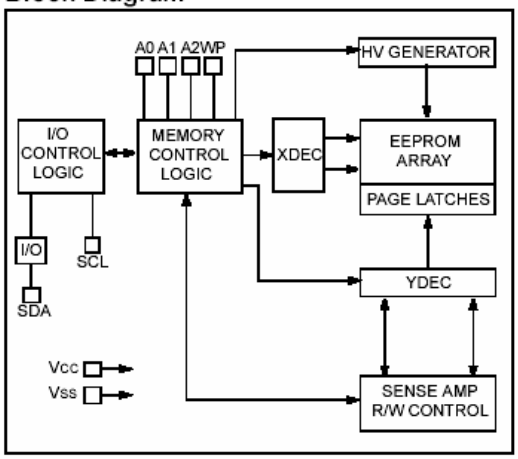

Package Types

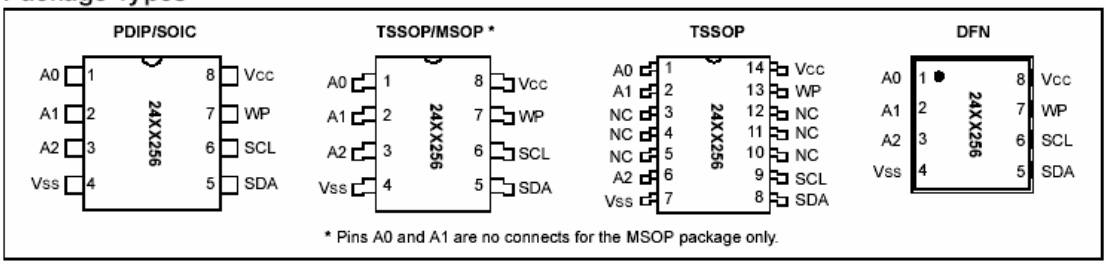

* Pins A0 and A1 are no connects for the MSOP package only.

*24XX256 is used in this document as a generic part number for the 24AA256/24LC256/24FC256 devices.

DALLAS SEMICONDUCTOR

DS1804
NV Trimmer Potentiometer

www.dalsemi.com

FEATURES

- Single 100-position taper potentiometer
- Nonvolatile "on-demand" wiper storage
- Operates from 3V or 5V supplies
- Up/down, increment-controlled interface
- Available in 8-pin (300-mil) DIP, 8-pin (150-mil) SOIC, 8-pin (118-mil) µSOP, and Flip Chip packages
- Operating Temperature:
  - Industrial: -40ºC to +85ºC
- Standard Resistance Values:
  - DS1804-010 10 kΩ
  - DS1804-050 50 kΩ
  - DS1804-100 100 kΩ

PIN ASSIGNMENT

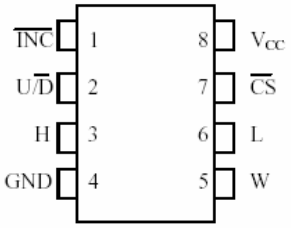

8-Pin DIP (300-mil)
8-Pin SOIC (150-mil)
8-Pin uSOP (118-mil)
8-Pin Flip Chip Package

See Mech. Drawings Section

PIN DESCIPTION

H	-	High-Terminal of Potentiometer
L	-	Low-Terminal of Potentiometer
W	-	Wiper of Potentiometer
V_{CC}	-	3V or 5V Power Supply
$\overline{CS}$	-	Chip Select
U/$\overline{D}$	-	Up/Down Control
$\overline{INC}$	-	Increment/Decrement Wiper Control
GND	-	Ground

DESCRIPTION

The DS1804 NV Trimmer Potentiometer is a nonvolatile digital potentiometer having 100 positions. The device provides an ideal method for low-cost trimming applications using a CPU or manual control input with minimal external circuitry. Wiper position of the DS1804 can be stored in EEPROM memory on demand. The device's wiper position is manipulated by a 3-terminal port that provides an increment/decrement counter controlled interface. This port consists of the control inputs $\overline{CS}$, $\overline{INC}$, and U/$\overline{D}$. The DS1804 is available in three resistor grades, which include a 10 kΩ, 50 kΩ, and 100 kΩ. The device is provided in an industrial temperature grade. Additionally, the DS1804 will operate from 3V or 5V supplies and is ideal for portable application requirements. Three packaging options are available and include the 8-pin (300-mil) DIP, 8-pin (150-mil) SOIC, 8-pin (118-mil) uSOP, and the Flip Chip Package.

RFM®

TR1000

916.50 MHz Hybrid Transceiver

- ***Designed for Short-Range Wireless Data Communications***
- ***Supports RF Data Transmission Rates Up to 115.2 kbps***
- ***3 V, Low Current Operation plus Sleep Mode***
- ***Stable, Easy to Use, Low External Parts Count***

The TR1000 hybrid transceiver is ideal for short-range wireless data applications where robust operation, small size, low power consumption and low cost are required. The TR1000 employs RFM's amplifier-sequenced hybrid (ASH) architecture to achieve this unique blend of characteristics. All critical RF functions are contained in the hybrid, simplifying and speeding design-in. The receiver section of the TR1000 is sensitive and stable. A wide dynamic range log detector, in combination with digital AGC and a compound data slicer, provide robust performance in the presence of on-channel interference or noise. Two stages of SAW filtering provide excellent receiver out-of-band rejection. The transmitter includes provisions for both on-off keyed (OOK) and amplitude-shift keyed (ASK) modulation. The transmitter employs SAW filtering to suppress output harmonics, facilitating compliance with FCC 15.249 and similar regulations.

Absolute Maximum Ratings

Rating	Value	Units
Power Supply and All Input/Output Pins	-0.3 to +4.0	V
Non-Operating Case Temperature	-50 to +100	°C
Soldering Temperature (10 seconds)	230	°C

Electrical Characteristics (typical values given for 3.0 Vdc power supply, 25 °C)

Characteristic	Sym	Notes	Minimum	Typical	Maximum	Units
Operating Frequency	f_O		916.30		916.70	MHz
Modulation Type				OOK/ASK		
OOK Data Rate					30	kbps
ASK Data Rate					115.2	kbps
Receiver Performance, High Sensitivity Mode						
Sensitivity, 2.4 kbps, 10-3 BER, AM Test Method		1		-106		dBm
Sensitivity, 2.4 kbps, 10-3 BER, Pulse Test Method		1		-100		dBm
Current, 2.4 kbps (R_{PR} = 330 K)		2		3.0		mA
Sensitivity, 19.2 kbps, 10-3 BER, AM Test Method		1		-101		dBm
Sensitivity, 19.2 kbps, 10-3 BER, Pulse Test Method		1		-95		dBm
Current, 19.2 kbps (R_{PR} = 330 K)		2		3.1		mA
Sensitivity, 115.2 kbps, 10-3 BER, AM Test Method		1		-97		dBm
Sensitivity, 115.2 kbps, 10-3 BER, Pulse Test Method		1		-91		dBm
Current, 115.2 kbps				3.8		mA
Receiver Performance, Low Current Mode						
Sensitivity, 2.4 kbps, 10-3 BER, AM Test Method		1		-104		dBm
Sensitivity, 2.4 kbps, 10-3 BER, Pulse Test Method		1		-98		dBm
Current, 2.4 kbps (R_{PR} = 1100 K)		2		1.8		mA
Receiver Out-of-Band Rejection, ±5% f_O	$R_{\pm 5\%}$	3		80		dB
Receiver Ultimate Rejection	R_{ULT}	3		100		dB

A.2 Mote Programming Board

A.2.1 Printed Circuit Board Layouts

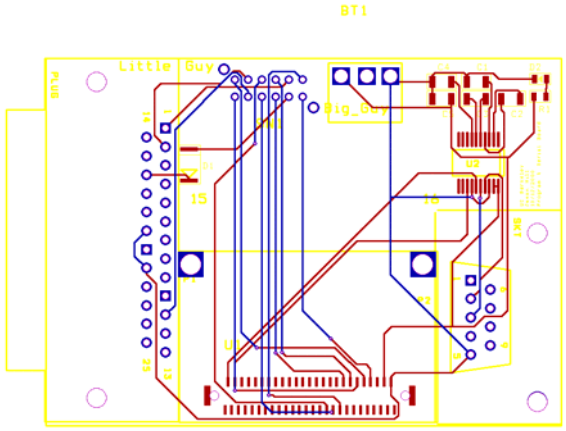

Figure A.2-1 Composite PCB layout for the Rene programming board.

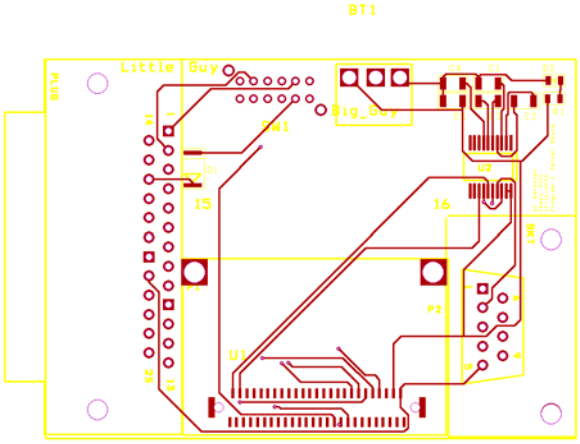

Figure A.2-2 Top layer PCB layout for the Rene programming board.

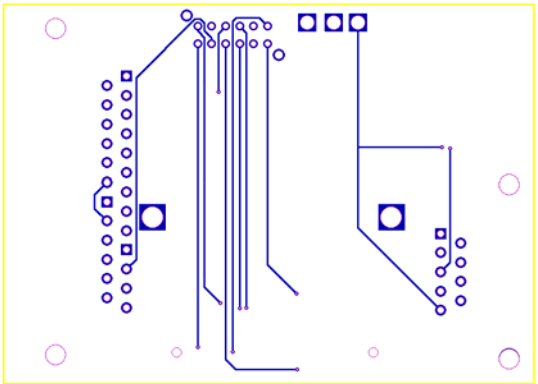

Figure A.2-3 Bottom layer PCB layout for the Rene programming board.

A.2.2 Materials Listing and Related Datasheets

Table A.2-1 Materials listing for the Rene programming board.

Part Specifier	Description	Distributor	Part Number
C1,C2,C3,C4,C5	0.01uF 50V Ceramic CAP 0805 SMD	Digi-key	PCC103BNCT-ND
R1	470 ohm 1/10W 5% 0805 SMD	Digi-key	P470ACT-ND
U1	51 Pin Connector	Digi-key	H2163-ND
U2	RS232	Maxim-ic	Max3224
D1	Schottky Diode	Digi-key	B120DICT-ND
D2	Hi EFF Red Diff 0805 SMD	Digi-key	L62505CT-ND
P1	DB25 Connector	Digi-key	425F-ND
P2	DB9 Connector	Digi-key	409F-ND
SW1	4PDT Switch	Digi-key	EG1949-ND

19-1289; Rev 1; 3/98

MAXIM

1µA Supply Current, 1Mbps, 3.0V to 5.5V, RS-232 Transceivers with AutoShutdown Plus

General Description

The MAX3224–MAX3227/MAX3244/MAX3245 are 3V-powered EIA/TIA-232 and V.28/V.24 communications interfaces with automatic shutdown/wakeup features and high data-rate capabilities.

All devices achieve a 1µA supply current using Maxim's revolutionary AutoShutdown Plus™ feature. These devices automatically enter a low-power shutdown mode when the RS-232 cable is disconnected or the transmitters of the connected peripherals are inactive, and the UART driving the transmitter inputs is inactive for more than 30 seconds. They turn on again when they sense a valid transition at any transmitter or receiver input. AutoShutdown Plus saves power without changes to the existing BIOS or operating system.

The MAX3225/MAX3227/MAX3245 also feature MegaBaud™ operation, guaranteeing 1Mbps for high-speed applications such as communicating with ISDN modems. The MAX3224/MAX3226/MAX3244 guarantee 250kbps operation. The transceivers have a proprietary low-dropout transmitter output stage enabling true RS-232 performance from a +3.0V to +5.5V supply with a dual charge pump. The charge pump requires only four small 0.1µF capacitors for operation from a 3.3V supply. The MAX3224–MAX3227 feature a logic-level output (READY) that asserts when the charge pump is regulating and the device is ready to begin transmitting.

All devices are available in a space-saving SSOP package.

Applications

Notebook, Subnotebook, and Palmtop Computers

Cellular Phones

Battery-Powered Equipment

Hand-Held Equipment

Peripherals

Printers

Features

- ♦ 1µA Supply Current
- ♦ AutoShutdown Plus—EDN Innovation of the Year
- ♦ Guaranteed Data Rate:
  250kbps (MAX3224/3226/3244)
  1Mbps (MAX3225/3227/3245)
- ♦ Guaranteed Slew Rate:
  6V/µs (MAX3224/3226/3244)
  24V/µs (MAX3225/3227/3245)
- ♦ Meets EIA/TIA-232 Specifications Down to 3.0V
- ♦ Guaranteed Mouse Driveability (MAX3244/3245)
- ♦ Ready-to-Transmit Logic-Level Output

Ordering Information

PART	TEMP. RANGE	PIN-PACKAGE
MAX3224CPP	0°C to +70°C	20 Plastic DIP
MAX3224CAP	0°C to +70°C	20 SSOP
MAX3224EPP	-40°C to +85°C	20 Plastic DIP
MAX3224EAP	-40°C to +85°C	20 SSOP
MAX3225CPP	0°C to +70°C	20 Plastic DIP
MAX3225CAP	0°C to +70°C	20 SSOP
MAX3225EPP	-40°C to +85°C	20 Plastic DIP
MAX3225EAP	-40°C to +85°C	20 SSOP

Ordering Information continued at end of data sheet.

Selector Guide

PART	NO. OF DRIVERS/ RECEIVERS	GUARANTEED DATA RATE (bps)	READY OUTPUT	AUTO-SHUTDOWN PLUS
MAX3224	2/2	250k	✔	✔
MAX3225	2/2	1M	✔	✔
MAX3226	1/1	250k	✔	✔
MAX3227	1/1	1M	✔	✔
MAX3244	3/5	250k	—	✔
MAX3245	3/5	1M	—	✔

AutoShutdownPlus and MegaBaud are trademarks of Maxim Integrated Products.

†Covered by U.S. Patent numbers 4,636,930; 4,679,134; 4,777,577; 4,797,899; 4,809,152; 4,897,774; 4,999,761; 5,649,210; and other patents pending.

A.3 Mote Serial Communications Board

A.3.1 Printed Circuit Board Layouts

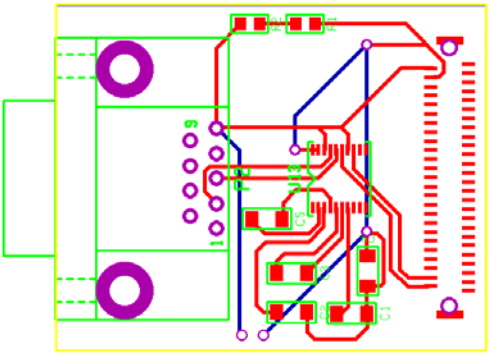

Figure A.3-1 Composite PCB layout of the serial communications board.

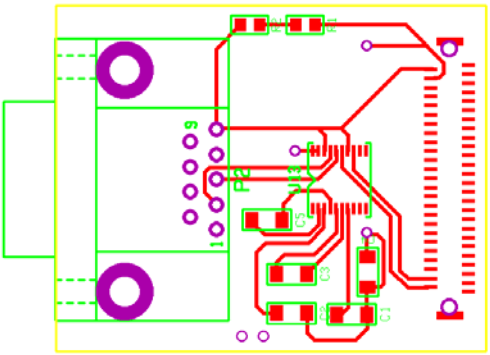

Figure A.3-2 Top PCB layer of the serial communications board.

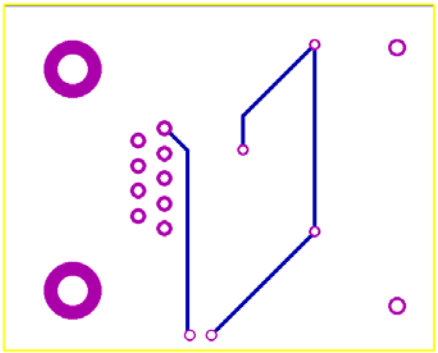

Figure A.3-3 Bottom PCB layer of the serial communications board.

A.3.2 Materials Listing

Table A.3-1 Materials listing for the mote serial communications board.

Part Specifier	Description	Distributor	Part Number
C1,C2,C3,C4,C5	0.01uF 50V Ceramic CAP 0805 SMD	Digi-key	PCC103BNCT-ND
R1	470 ohm 1/10W 5% 0805 SMD	Digi-key	P470ACT-ND
U1	51 Pin Connector	Digi-key	H2163-ND
U2	RS232	Maxim-ic	Max3224
D2	Hi EFF Red Diff 0805 SMD	Digi-key	L62505CT-ND
P2	DB9 Connector	Digi-key	409F-ND

A.4 Flexible Data Acquisition Circuit

A.4.1 Circuit Schematic

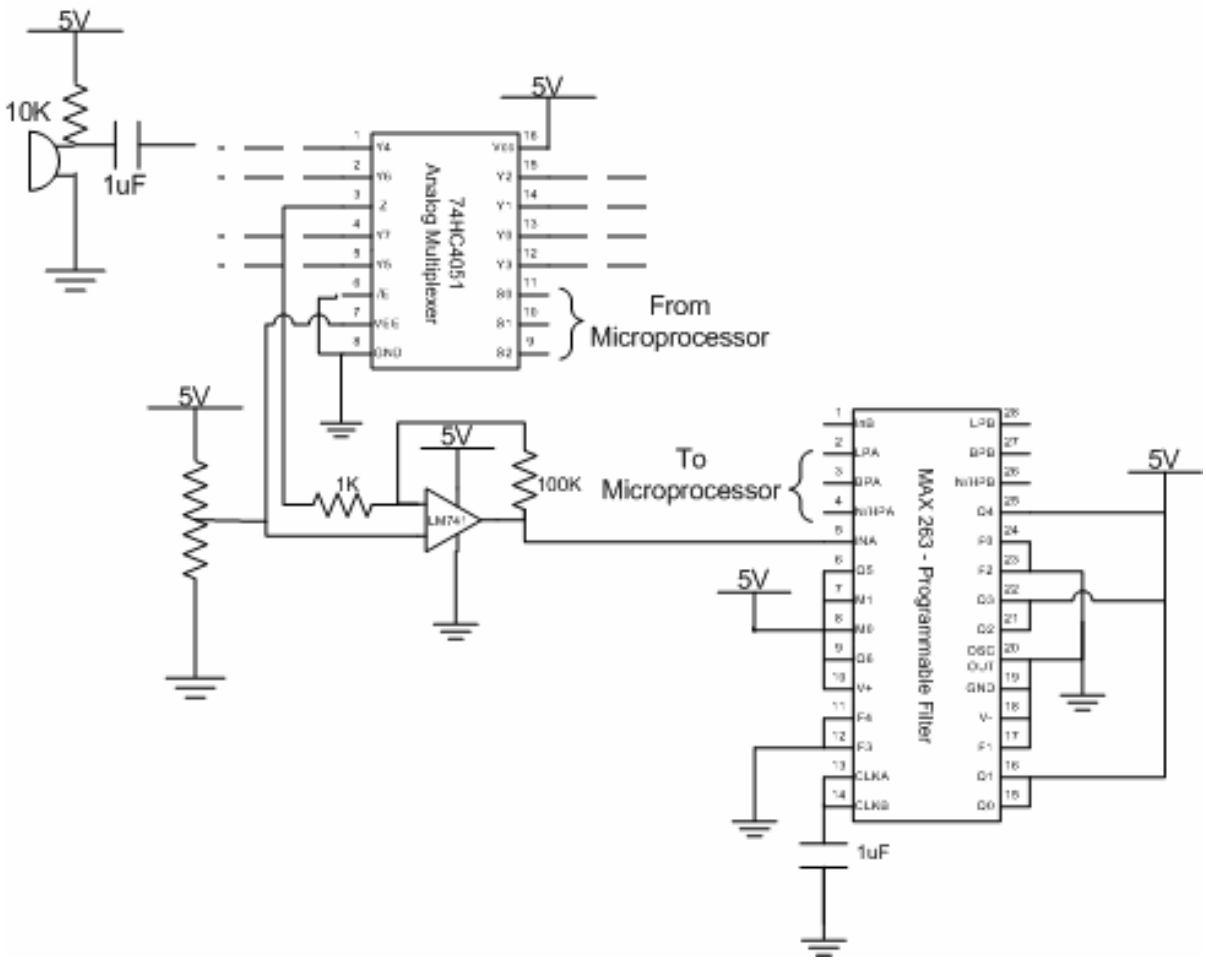

Figure A.4-1 Schematic for the flexible data acquisition circuit.

A.4.2 Printed Circuit Board Layout

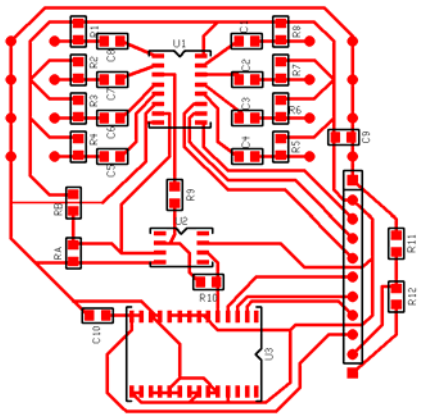

Figure A.4-2 PCB layout for the flexible data acquisition circuit.

A.4.3 Materials Listing

Table A.4-1 Materials listing for the flexible data acquisition circuit.

Part Specifier	Description	Vendor	Part Number
U1	8 channel analog multiplexer	Digi-key	MM74HC4051M-ND
U2	Single 741 Op-Amp SO-8	Mouser	511-UA741CD
U3	Pin-Programmable Universal and Bandpass Filters	Maxim-ic	MAX263
C1-C9, CM1-CM8	CAP 1uF 16V CERAMIC X5R 0805	Digi-key	PCC2314CT-ND
R1-R8	100kohm 1/10W 5% 0805 SMD	Digi-key	P100KACT-ND
R9-R16	1kohm 1/10W 5% 0805 SMD	Digi-key	P1.0KACT-ND
R9-R16	10kohm 1/10W 5% 0805 SMD	Digi-key	P10KACT-ND
RA, RB	1.0Mohm 1/8W 5% 0805 SMD	Digi-key	P1.0MACT-ND

National Semiconductor

August 2000

LM741
Operational Amplifier

General Description

The LM741 series are general purpose operational amplifiers which feature improved performance over industry standards like the LM709. They are direct, plug-in replacements for the 709C, LM201, MC1439 and 748 in most applications.

The amplifiers offer many features which make their application nearly foolproof: overload protection on the input and output, no latch-up when the common mode range is exceeded, as well as freedom from oscillations.

The LM741C is identical to the LM741/LM741A except that the LM741C has their performance guaranteed over a 0°C to +70°C temperature range, instead of −55°C to +125°C.

Connection Diagrams

Metal Can Package

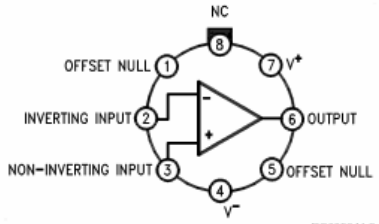

Note 1: LM741H is available per JM38510/10101

Order Number LM741H, LM741H/883 (Note 1), **LM741AH/883 or LM741CH**
See NS Package Number H08C

Dual-In-Line or S.O. Package

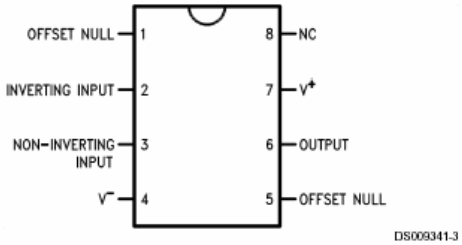

Order Number LM741J, LM741J/883, LM741CN
See NS Package Number J08A, M08A or N08E

Ceramic Flatpak

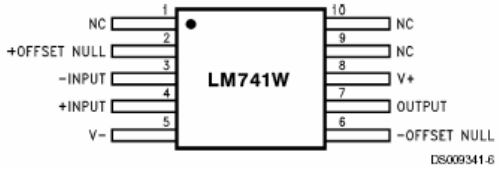

Order Number LM741W/883
See NS Package Number W10A

Typical Application

Offset Nulling Circuit

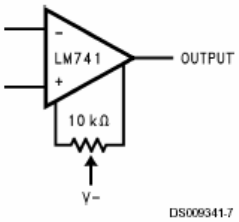

19-0597; Rev 3; 7/98

MAXIM

Pin Programmable Universal and Bandpass Filters

General Description

The MAX263/264 and MAX267/268 CMOS switched-capacitor active filters are designed for precision filtering applications. Center frequency, Q, and operating mode are all selected via pin-strapped inputs. The MAX263/264 uses no external components for a variety of bandpass, lowpass, highpass, notch and allpass filters. The MAX267/268 is dedicated to bandpass applications and includes an uncommitted op-amp. Two second-order filter sections are included in both devices.

An input clock and a 5-bit programming input precisely set the filter center/corner frequency. Q is also programmed from 0.5 to 64. Separate clock inputs for each filter half operate with either an external clock or a crystal.

The MAX263 and 267 operate with center frequencies up to 57kHz while the MAX264 and 268 extend the f_0 range to 140kHz by employing lower f_{CLK}/f_0 ratios. The MAX263/264 is supplied in 28 pin wide DIP and small outline packages while the MAX267/268 is supplied in 24 pin narrow DIP and wide SO packages. All devices are available in commercial, extended, and military temperature ranges.

Applications

Sonar and Avionics Instruments

Anti-Aliasing Filters

Digital Signal Processing

Vibration and Audio Analysis

Matched Tracking Filters

Features

- **Filter Design Software Available**
- **32-Step Center Frequency Control**
- **128-Step Q Control**
- **Independent Q and f_0 Programming**
- **Guaranteed Clock to f_0 Ratio—1% (A grade)**
- **75kHz f_0 Range (MAX264/268)**
- **Single +5V and ±5V Operation**

Ordering Information

PART	TEMP. RANGE	PACKAGE*	ACCURACY
MAX263ACPI	0°C to +70°C	Plastic DIP	1%
MAX263BCPI	0°C to +70°C	Plastic DIP	2%
MAX263AEPI	-40°C to +85°C	Plastic DIP	1%
MAX263BEPI	-40°C to +85°C	Plastic DIP	2%
MAX263ACWI	0°C to +70°C	Wide SO	1%
MAX263BCWI	0°C to +70°C	Wide SO	2%
MAX263AMJI	-55°C to +125°C	CERDIP	1%
MAX263BMJI	-55°C to +125°C	CERDIP	2%
MAX264ACPI	0°C to +70°C	Plastic DIP	1%
MAX264BCPI	0°C to +70°C	Plastic DIP	2%

(Ordering Information continued at end of data sheet.)

* *MAX263/264 packages are 28-pin 0.6" wide DIP and 28-pin 0.3" wide SO (Small Outline).*

MAX267/268 packages are 24-pin 0.3" narrow DIP and 24-pin 0.3" wide SO (Small Outline).

Typical Application

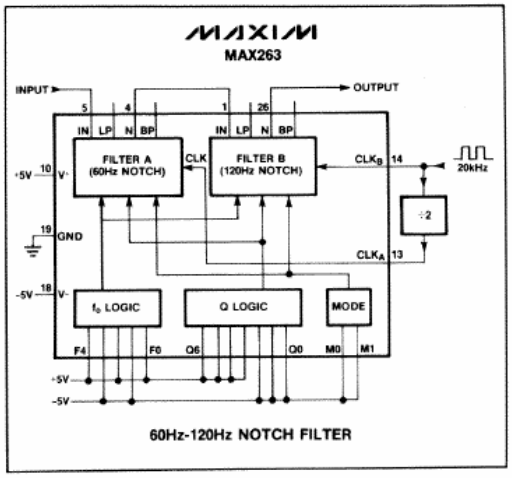

60Hz-120Hz NOTCH FILTER

Pin Configuration

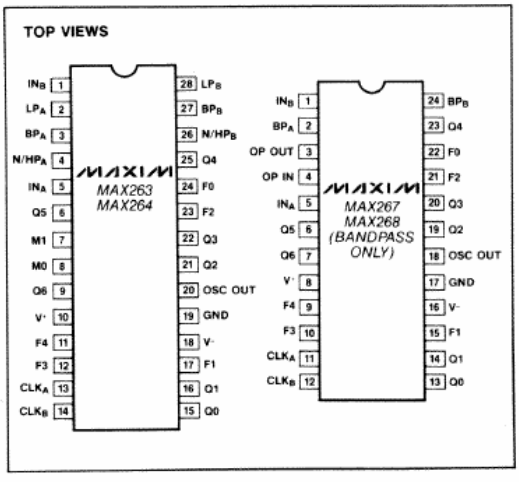

FAIRCHILD SEMICONDUCTOR™

August 1984
Revised May 1999

MM74HC4051 • MM74HC4052 • MM74HC4053
8-Channel Analog Multiplexer • Dual 4-Channel Analog Multiplexer • Triple 2-Channel Analog Multiplexer

General Description

The MM74HC4051, MM74HC4052 and MM74HC4053 multiplexers are digitally controlled analog switches implemented in advanced silicon-gate CMOS technology. These switches have low "on" resistance and low "off" leakages. They are bidirectional switches, thus any analog input may be used as an output and vice-versa. Also these switches contain linearization circuitry which lowers the on resistance and increases switch linearity. These devices allow control of up to ±6V (peak) analog signals with digital control signals of 0 to 6V. Three supply pins are provided for V_{CC}, ground, and V_{EE}. This enables the connection of 0–5V logic signals when $V_{CC} = 5V$ and an analog input range of ±5V when $V_{EE} = 5V$. All three devices also have an inhibit control which when HIGH will disable all switches to their off state. All analog inputs and outputs and digital inputs are protected from electrostatic damage by diodes to V_{CC} and ground.

MM74HC4051: This device connects together the outputs of 8 switches, thus achieving an 8 channel Multiplexer. The binary code placed on the A, B, and C select lines determines which one of the eight switches is "on", and connects one of the eight inputs to the common output.

MM74HC4052: This device connects together the outputs of 4 switches in two sets, thus achieving a pair of 4-channel multiplexers. The binary code placed on the A, and B select lines determine which switch in each 4 channel section is "on", connecting one of the four inputs in each section to its common output. This enables the implementation of a 4-channel differential multiplexer.

MM74HC4053: This device contains 6 switches whose outputs are connected together in pairs, thus implementing a triple 2 channel multiplexer, or the equivalent of 3 single-pole-double throw configurations. Each of the A, B, or C select lines independently controls one pair of switches, selecting one of the two switches to be "on".

Features

- Wide analog input voltage range: ±6V
- Low "on" resistance:
  - 50 typ. ($V_{CC}–V_{EE} = 4.5V$)
  - 30 typ. ($V_{CC}–V_{EE} = 9V$)
- Logic level translation to enable 5V logic with ±5V analog signals
- Low quiescent current: 80 µA maximum (74HC)
- Matched Switch characteristic

Ordering Code:

Order Number	Package Number	Package Description
MM74HC4051M	M16A	16-Lead Small Outline Integrated Circuit (SOIC), JEDEC MS-012, 0.150" Narrow
MM74HC4051WM	M16B	16-Lead Small Outline Integrated Circuit (SOIC), JEDEC MS-013, 0.300" Wide
MM74HC4051SJ	M16D	16-Lead Small Outline Package (SOP), EIAJ TYPE II, 5.3mm Wide
MM74HC4051MTC	MTC16	16-Lead Thin Shrink Small Outline Package (TSSOP), JEDEC MO-153, 4.4mm Wide
MM74HC4051N	N16E	16-Lead Plastic Dual-In-Line Package (PDIP), JEDEC MS-001 0.300" Wide
MM74HC4052M	M16A	16-Lead Small Outline Integrated Circuit (SOIC), JEDEC MS-012, 0.150" Narrow
MM74HC4052WM	M16B	16-Lead Small Outline Integrated Circuit (SOIC), JEDEC MS-013, 0.300" Wide
MM74HC4052SJ	M16D	16-Lead Small Outline Package (SOP), EIAJ TYPE II, 5.3mm Wide
MM74HC4052MTC	MTC16	16-Lead Thin Shrink Small Outline Package (TSSOP), JEDEC MO-153, 4.4mm Wide
MM74HC4052N	N16E	16-Lead Plastic Dual-In-Line Package (PDIP), JEDEC MS-001 0.300" Wide
MM74HC4053M	M16A	16-Lead Small Outline Integrated Circuit (SOIC), JEDEC MS-012, 0.150" Narrow
MM74HC4053WM	M16B	16-Lead Small Outline Integrated Circuit (SOIC), JEDEC MS-013, 0.300" Wide
MM74HC4053SJ	M16D	16-Lead Small Outline Package (SOP), EIAJ TYPE II, 5.3mm Wide
MM74HC4053MTC	MTC16	16-Lead Thin Shrink Small Outline Package (TSSOP), JEDEC MO-153, 4.4mm Wide
MM74HC4053N	N16E	16-Lead Plastic Dual-In-Line Package (PDIP), JEDEC MS-001 0.300" Wide

Devices also available in Tape and Reel. Specify by appending the suffix letter "X" to the ordering code.

Connection Diagrams

Pin Assignments for DIP, SOIC, SOP and TSSOP

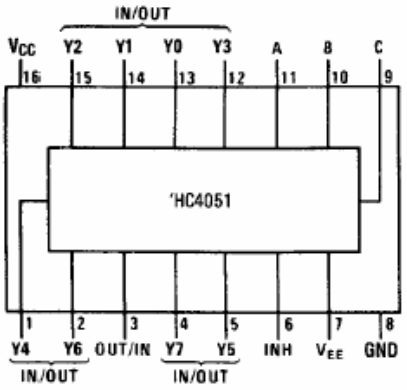

Top View

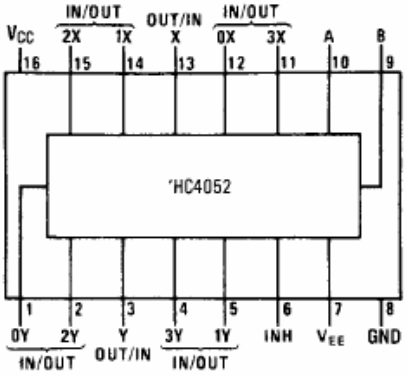

Top View

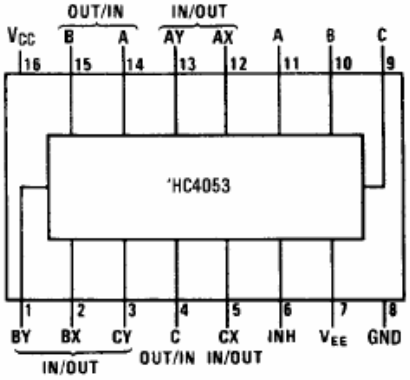

Top View

Truth Tables

MM744051

Input				"ON"
Inh	C	B	A	Channel
H	X	X	X	None
L	L	L	L	Y0
L	L	L	H	Y1
L	L	H	L	Y2
L	L	H	H	Y3
L	H	L	L	Y4
L	H	L	H	Y5
L	H	H	L	Y6
L	H	H	H	Y7

MM744052

Inputs			"ON" Channels	
Inh	B	A	X	Y
H	X	X	None	None
L	L	L	0X	0Y
L	L	H	1X	1Y
L	H	L	2X	2Y
L	H	H	3X	3Y

MM744053

Input				"ON" Channels		
Inh	C	B	A	C	b	a
H	X	X	X	None	None	None
L	L	L	L	CX	BX	AX
L	L	L	H	CX	BX	AY
L	L	H	L	CX	BY	AX
L	L	H	H	CX	BY	AY
L	H	L	L	CY	BX	AX
L	H	L	H	CY	BX	AY
L	H	H	L	CY	BY	AX
L	H	H	H	CY	BY	AY

A.5 Variable Gain Data Acquisition Circuit

A.5.1 Circuit Schematic

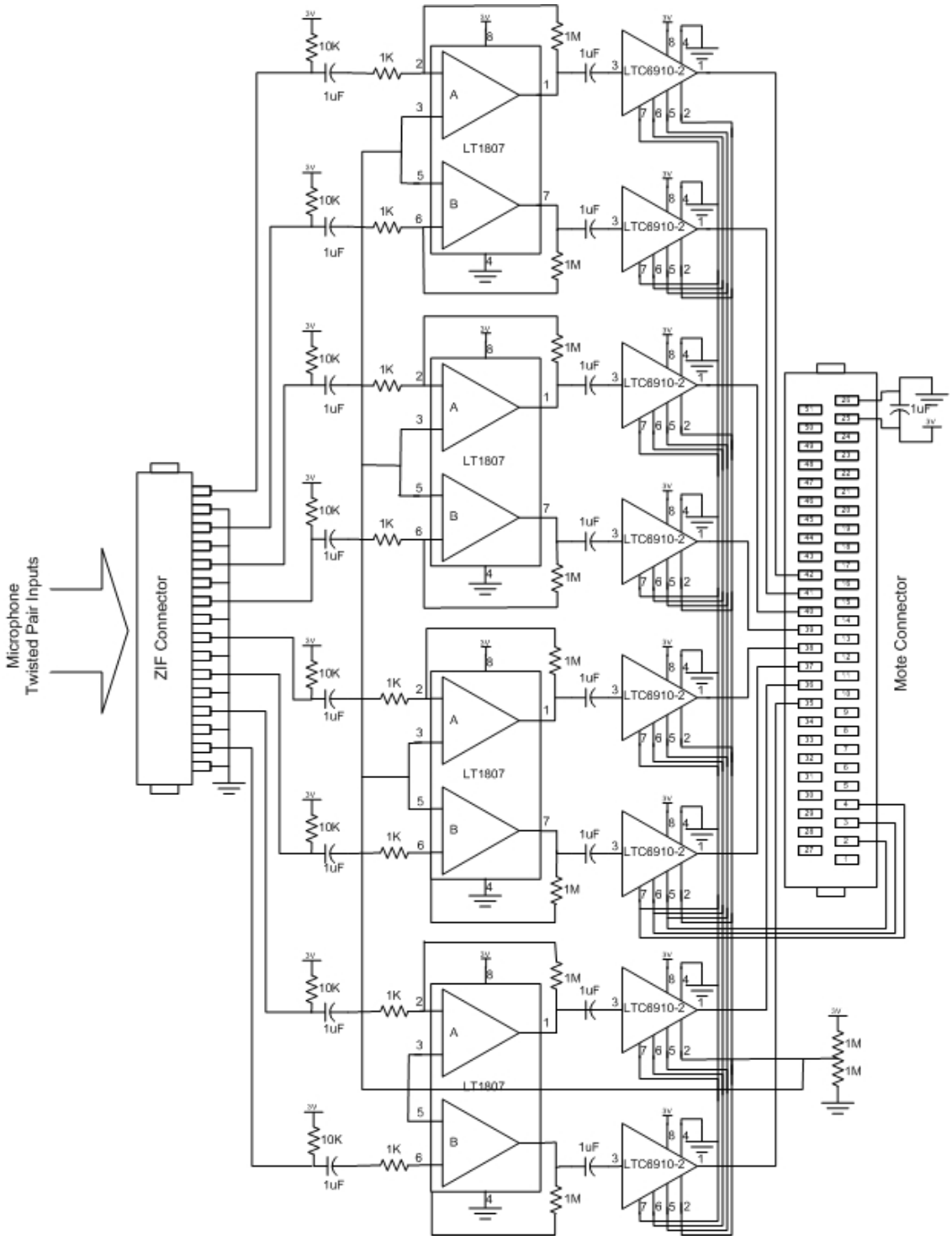

Figure A.5-1 Circuit schematic for the variable gain data acquisition system

A.5.2 PCB Layout

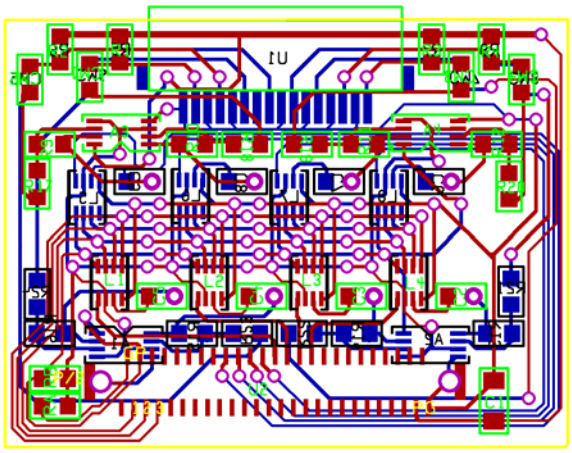

Figure A.5-2 Composite PCB layout of the variable gain data acquisition system.

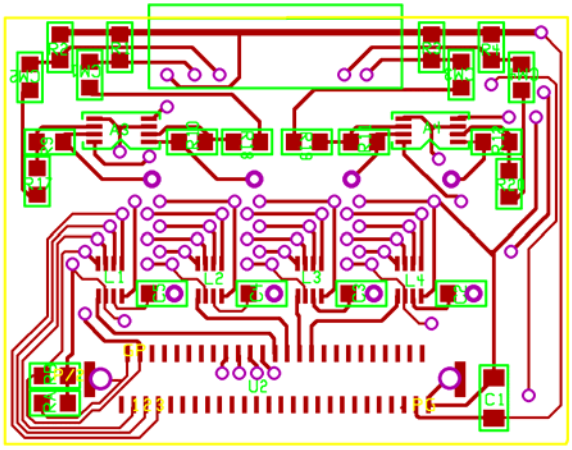

Figure A.5-3 Top PCB layer copper and silk from figure 2

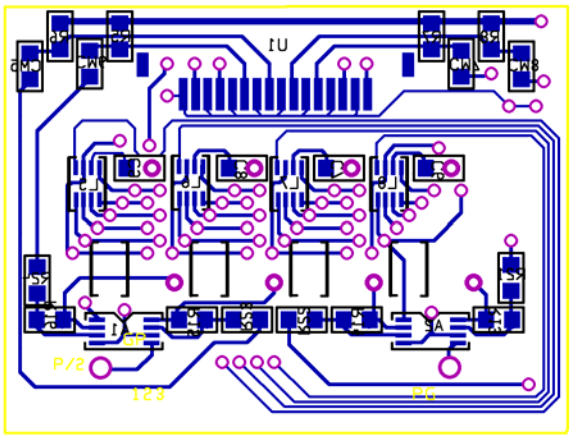

Figure A.5-4 Bottom PCB layer copper and silk from figure 2

A.5.3 Materials Listing and Related Datasheets

Table A.5-1 Materials listing for the variable gain data acquisition board.

Part Specifier	Description	Vendor	Part Number
R1-R8	100kohm 1/10W 5% 0805 SMD	Digi-key	P100KACT-ND
RA, RB	1.0Mohm 1/8W 5% 0805 SMD	Digi-key	P1.0MACT-ND
R9-R16	1kohm 1/10W 5% 0805 SMD	Digi-key	P1.0KACT-ND
C1-C9, CM1-CM8	CAP 1uF 16V CERAMIC X5R 0805	Digi-key	PCC2314CT-ND
U1	Conn 16 POS 1MM FLEX SMD	Digi-key	HFE16F
A1-A4	Dual rail-to-rail operational amplifier	Linear Technologies	LT1807
L1-L8	Variable gain operational amplifier	Linear Technologies	LTC6910-2

LINEAR TECHNOLOGY

LT1806/LT1807

325MHz, Single/Dual, Rail-to-Rail Input and Output, Low Distortion, Low Noise Precision Op Amps

FEATURES

- **Gain Bandwidth Product: 325MHz**
- **Slew Rate: 140V/µs**
- **Wide Supply Range: 2.5V to 12.6V**
- **Large Output Current: 85mA**
- **Low Distortion, 5MHz: –80dBc**
- **Low Voltage Noise: 3.5nV/√Hz**
- Input Common Mode Range Includes Both Rails
- Output Swings Rail-to-Rail
- Input Offset Voltage (Rail-to-Rail): 550µV Max
- Common Mode Rejection: 106dB Typ
- Power Supply Rejection: 105dB Typ
- Unity-Gain Stable
- Power Down Pin (LT1806)
- Single in SO-8 and 6-Pin SOT-23 Packages
- Dual in SO-8 and 8-Pin MSOP Packages
- Operating Temperature Range: –40°C to 85°C

APPLICATIONS

- Low Voltage, High Frequency Signal Processing
- Driving A/D Converters
- Rail-to-Rail Buffer Amplifiers
- Active Filters
- Video Line Driver

DESCRIPTION

The LT®1806/LT1807 are single/dual low noise rail-to-rail input and output unity-gain stable op amps that feature a 325MHz gain-bandwidth product, a 140V/µs slew rate and a 85mA output current. They are optimized for low voltage, high performance signal conditioning systems.

The LT1806/LT1807 have a very low distortion of –80dBc at 5MHz, a low input referred noise voltage of 3.5nV/√Hz and a maximum offset voltage of 550µV that allows them to be used in high performance data acquisition systems.

The LT1806/LT1807 have an input range that includes both supply rails and an output that swings within 20mV of either supply rail to maximize the signal dynamic range in low supply applications.

The LT1806/LT1807 maintain their performance for supplies from 2.5V to 12.6V and are specified at 3V, 5V and ±5V supplies. The inputs can be driven beyond the supplies without damage or phase reversal of the output.

The LT1806 is available in an 8-pin SO package with the standard op amp pinout and a 6-pin SOT-23 package. The LT1807 features the standard dual op amp pinout and is available in 8-pin SO and MSOP packages.These devices can be used as plug-in replacements for many op amps to improve input/output range and performance.

INITIAL RELEASE
Final Electrical Specifications

LTC6910-2

Digitally Controlled Programmable Gain Amplifier in SOT-23

April 2003

FEATURES

- **3-Bit Digital Gain Control (0, 1, 2, 4, 8, 16, 32 and 64V/V)**
- **8-Pin TSOT-23 Package**
- **Rail-to-Rail Input Range**
- **Rail-to-Rail Output Swing**
- **Single or Dual Supply: 2.7V to 10.5V Total**
- 13MHz Gain Bandwidth Product
- 9nV/√Hz Input Noise at Gain of 64
- 120dB Total System Dynamic Range
- Input Offset Voltage: 3mV (Gain = 1)
- Input Offset Voltage: 2mV (Gain = 8)

APPLICATIONS

- Data Acquisition Systems
- Dynamic Gain Changing
- Automatic Ranging Circuits
- Automatic Gain Control

DESCRIPTION

The LTC®6910-2 is a low noise digitally programmable gain amplifier (PGA) that is easy to use and occupies very little PC board space. The gain is adjustable using a 3-bit digital input to select inverting gains of 0, 1, 2, 4, 8, 16, 32 and 64V/V.

The LTC6910-2 is an inverting amplifier with a rail-to-rail output. When operated with unity gain, the LTC6910-2 will also process rail-to-rail input signals. A half-supply reference generated internally at the AGND pin supports single power supply applications. Operating from single or split supplies from 2.7V to 10.5V, the LTC6910-2 is offered in an 8-lead TSOT-23 package.

For other gain options, see the LTC6910-1 and LTC6910-3.

TYPICAL APPLICATION

Single Supply Programmable Amplifier

GAIN	G2	G1	G0
0	0	0	0
–1	0	0	1
–2	0	1	0
–4	0	1	1
–8	1	0	0
–16	1	0	1
–32	1	1	0
–64	1	1	1

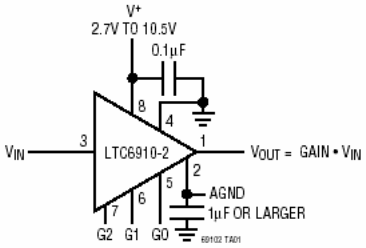

PIN 2 (AGND) PROVIDES BUILT-IN HALF-SUPPLY REFERENCE WITH INTERNAL RESISTANCE OF 5k. AGND CAN ALSO BE DRIVEN BY A SYSTEM ANALOG GROUND REFERENCE NEAR HALF SUPPLY

Frequency Response

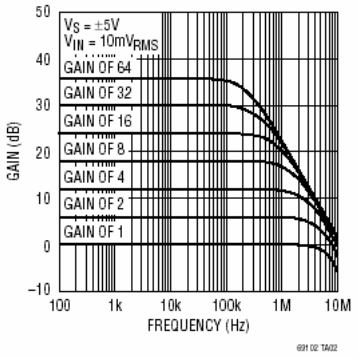

Appendix B
Programs

B.1 Mote Data Acquisition Software

```
.include "8535def.inc"

.def    temp            =r16    ;general purpose variable
.def    count           =r17    ;microphone counter
.def    high_byte       =r18    ;High byte ADC
.def    low_byte        =r19    ;Low byte ADC
.def    count2          =r20    ;Memory Count
.def    clow            =r21    ;Low byte of SRAM
.def    chigh           =r22    ;High byte of SRAM
.def    start           =r23    ;Start flag
.def    full            =r24    ;Memory full flag

.equ    sram_data = 0x0060

.CSEG
.org    $0000
        rjmp    BEGIN

.org OC2addr
        rjmp OC2_interrupt

.org URXCaddr                           ;definition in the
        rjmp UART_RX_interrupt;8535 include file

.org ADCCaddr
        rjmp ADC_complete_interrupt

;########## INTERRUPT ROUTINES ##########

;***** UART receive interrupt *****
;receive complete interrupt- cannot interrupt this routine
UART_RX_interrupt:
        cli                             ;disable global interrupt
        in temp,UDR
        rcall transmit      ;transmits what is received
        cpi temp, 'a'       ;sets start flag is a recieve (for "A"DC)
        brne nex
   ldi start, 1
nex:
        reti                        ;returns and reenables the gloabl interrupt

;***** Timer2 Compare interrupt *****
OC2_interrupt:
        cli
        push temp

        ldi temp, 0b00000000    ;reinitialize the counter
        out TCNT2, temp
        inc count2                              ;increment memory counter

        cpi count2, 0b00111111  ;when memory counter is full
        breq final                              ;disable interrupts
```

```
   ldi temp, 0b11101000    ;restart ADC interrupt
        out ADCSR, temp
        pop temp
        reti

final:
        ldi temp, 0b00000000      ;disables all interrupts
        out TIMSK, temp
        out ADCSR, temp
        ldi full, 1                             ;indicates full SRAM
        pop temp
        reti

;***** ADC Conversion Complete Interrupt*****
ADC_complete_interrupt:
        cli

        cpi count, 0b00001000     ;checks to see if all
        breq pause_ADC                  ;8 mics have been scanned

        in low_byte, ADCL               ;reads the low byte
        nop
        in high_byte, ADCH              ;reads the high byte
        ror high_byte                   ;left aligns the 10-bit result
        ror low_byte
        ror high_byte
        ror low_byte
        st Z+, low_byte                 ;stores the value in SRAM

        inc count                               ;increments the ADC Mux
        out ADMUX, count
        reti

pause_ADC:
        ldi count, 0b00000000     ;disable the ADC when all
        ldi temp, 0b01101000      ;8 have been read
        out ADCSR, temp
        reti

;########## Initialization ##########

;***** UART Initialization *****
init_UART:
        ldi temp, 12
        out UBRR, temp  ;init baudrate 19,200@4MHz
        ldi temp, (1<<RXEN)|(1<<TXEN)|(1<<RXCIE)        ;enable receiver, transmitter and RXint
        out UCR, temp
        ret

;***** ADC Initialization *****
init_ADC:

        ldi temp, 0b00000000
        out ADMUX, temp
   ldi temp, 0b01101000
```

```
        out ADCSR, temp
        ret

;***** TCCR2 Initialization *****
init_TCCR2:

        ldi temp, 0b00000000    ;clear the TCNT2 register
        out TCNT2, temp
        ldi temp, 0b00011001    ;0b00001010~12500Hz;0b00011001~5000Hz
        out OCR2, temp                  ;0b01111101~1000Hz;0b11000011~641Hz

        ldi temp, 0b00000011    ;set TCCR2 clock factor to 32
        out TCCR2, temp
        ldi temp, 0b10000000    ;enable TOV2 interrupt
        out TIMSK, temp
        ret

;########## SUBROUTINES ##########

;***** UART Transmit *****
transmit:
        sbis USR,UDRE  ;ready to send
        rjmp transmit
        out UDR, temp
        ret

;***** Transmit SRAM *****
;transmits collected data through the serial port
trans_SRAM:
        mov chigh, r31
        mov clow, r30
        ldi r31, high(sram_data)
        ldi r30, low (sram_data)
repeat:
        ld temp, Z+
        rcall transmit
        cp chigh, r31
        brne cont
        cp clow, r30
        breq donep
cont:
        rjmp repeat
donep:
        ret

;########## MAIN PROGRAM ##########
BEGIN:
;***** Stack Initialization *****
        ldi     Temp,high(RAMEND)  ; initialize stack
        out     SPH,Temp
        ldi     Temp,low(RAMEND)
        out     SPL,Temp
;*******************************

        rcall init_UART
        ldi start, 0
```

```
        sei                             ;global interrupt enable

con:
        cpi start, 1        ;loop until 'A' received
        brne con

        ldi full, 0                 ;initialization of variables
        ldi chigh, 0

        ldi r31, high(sram_data)
        ldi r30, low (sram_data)
        ldi count, 0b00000000
        ldi count2, 0b00000000
        ldi clow, 0b00000000
        ldi chigh, 0b00000000


        rcall init_ADC    ;initialize interrupt routines
        rcall init_TCCR2


con2:
        cpi full, 1                 ;don't do anything until SRAM is full
        brne con2

        rcall trans_SRAM            ;send SRAM through serial port

        ldi start, 0                ;loop back to beginning
        rjmp con

loop:
        rjmp loop
```

B.2 JAVA Serial Data Collection Software

```
//This program accepts data from the mote data acqusition software
//through the serial portand parses it into the appropriate channel files.

import java.awt.*;
import java.awt.event.*;
import javax.swing.*;
import java.io.*;
import java.util.*;
import javax.comm.*;

public class Combo extends JFrame
 {
  JTextArea console = new JTextArea();
  JScrollPane scroll = new JScrollPane(console);
  InputStream in;
  SerialPort serial;
  CommPortIdentifier port;
  OutputStream out;
  Vector v = new Vector();
  static CommPortIdentifier portId;
  static Enumeration portList;
  int total = 0;

  //Constructor
  //initializes the data window, opens the port, gets the appropriate data streams,
  //and adds the serial port listener
  public Combo()
   {
    console.addKeyListener(new SerKey());
    console.setLineWrap(true);
    console.setText("a = Start AD Conversion\nc = Clear Screen\nw = Write Contents to data.txt\n");
    console.setCaretPosition(console.getText().length());
    setSize(500,300);
    scroll.setHorizontalScrollBarPolicy(JScrollPane.HORIZONTAL_SCROLLBAR_NEVER);
    this.getContentPane().add(scroll);
    this.setDefaultCloseOperation(JFrame.EXIT_ON_CLOSE);
    this.show();

    portList = CommPortIdentifier.getPortIdentifiers();

    while (portList.hasMoreElements())
     {
      portId = (CommPortIdentifier) portList.nextElement();
      if (portId.getPortType() == CommPortIdentifier.PORT_SERIAL)
       {
        if (portId.getName().equals("COM1"))
              {
               try
                {
                 serial = (SerialPort)portId.open("Seravr", 100);
```

```
serial.setSerialPortParams(19200,SerialPort.DATABITS_8,SerialPort.STOPBITS_1,SerialPort.PARITY_NON
E);
                out = serial.getOutputStream();
                in = serial.getInputStream();
                serial.addEventListener(new serialEv());
                serial.notifyOnDataAvailable(true);
                System.out.println ("serial = " + serial);
          }
              catch(Exception e)
               {
                e.printStackTrace();
          }
        }
      }
    }
  }

  //Sets the cursor position at the end of the text
  public void posCursor()
   {
    console.setCaretPosition(console.getText().length());
   }

  //simply starts the program
  public static void main (String[] args)
   {
    Combo a = new Combo();
   }

  //Keyboard listener
  //sends commands to the mote and writes the data to files
  public class SerKey implements KeyListener
   {
    public void keyPressed (KeyEvent e){}
            public void keyReleased (KeyEvent e){}
            public void keyTyped (KeyEvent e)
             {
              try
               {
                System.out.println ("key typed");
                out.write(e.getKeyChar());
                System.out.println("e = " + e.getKeyChar());
                if (e.getKeyChar() == 'c')
           console.replaceRange("",0,console.getText().length());
                if (e.getKeyChar() == 'w')
                 {
            int c = 0;
            FileWriter out0 = new FileWriter("data0.txt");
            FileWriter out1 = new FileWriter("data1.txt");
            FileWriter out2 = new FileWriter("data2.txt");
            FileWriter out3 = new FileWriter("data3.txt");
            FileWriter out4 = new FileWriter("data4.txt");
            FileWriter out5 = new FileWriter("data5.txt");
            FileWriter out6 = new FileWriter("data6.txt");
            FileWriter out7 = new FileWriter("data7.txt");
```

```
            StringTokenizer s = new StringTokenizer(console.getText());
          s.nextToken();
          s.nextToken();
              while ((s.hasMoreTokens()) && (c < 62))
               {
           c++;
           out0.write(s.nextToken()+"\n");
           out1.write(s.nextToken()+"\n");
           out2.write(s.nextToken()+"\n");
           out3.write(s.nextToken()+"\n");
           out4.write(s.nextToken()+"\n");
           out5.write(s.nextToken()+"\n");
           out6.write(s.nextToken()+"\n");
           out7.write(s.nextToken()+"\n");
               }
          out0.close();
              out1.close();
              out2.close();
              out3.close();
              out4.close();
              out5.close();
              out6.close();
              out7.close();
             }
            }
            catch (Exception ex)
             {
              ex.printStackTrace();
             }
            }
}

//Serial Port listener
//Receives information from the mote, manages the buffer
public class serialEv implements SerialPortEventListener
 {
  byte[] readBuffer = new byte[512];


  public void serialEvent(SerialPortEvent event)
   {
    switch(event.getEventType())
          {
      case SerialPortEvent.BI:
      case SerialPortEvent.OE:
      case SerialPortEvent.FE:
      case SerialPortEvent.PE:
      case SerialPortEvent.CD:
      case SerialPortEvent.CTS:
      case SerialPortEvent.DSR:
      case SerialPortEvent.RI:
      case SerialPortEvent.OUTPUT_BUFFER_EMPTY:
       break;
      case SerialPortEvent.DATA_AVAILABLE:
            readBuffer = new byte[512];
```

```
        try
              {
          int numBytes = in.read(readBuffer);
          total+=numBytes;
          for (int j = 0; j < numBytes; j++)
                {
                 console.append(""+adjustUnsigned(readBuffer[j])+"\n");
                 v.add(new Byte(readBuffer[j]));
                }
               console.setCaretPosition(console.getText().length());
          System.out.println("total = " + total);
         }
             catch (IOException e)
              {
               e.printStackTrace();
              }
             v.removeAllElements();
      }
    }
  }

}
```